

INFORMATION TO USERS

This manuscript has been reproduced from the microfilm master. UMI films the text directly from the original or copy submitted. Thus, some thesis and dissertation copies are in typewriter face, while others may be from any type of computer printer.

The quality of this reproduction is dependent upon the quality of the copy submitted. Broken or indistinct print, colored or poor quality illustrations and photographs, print bleedthrough, substandard margins, and improper alignment can adversely affect reproduction.

In the unlikely event that the author did not send UMI a complete manuscript and there are missing pages, these will be noted. Also, if unauthorized copyright material had to be removed, a note will indicate the deletion.

Oversize materials (e.g., maps, drawings, charts) are reproduced by sectioning the original, beginning at the upper left-hand corner and continuing from left to right in equal sections with small overlaps.

Photographs included in the original manuscript have been reproduced xerographically in this copy. Higher quality 6" x 9" black and white photographic prints are available for any photographs or illustrations appearing in this copy for an additional charge. Contact UMI directly to order.

Bell & Howell Information and Learning
300 North Zeeb Road, Ann Arbor, MI 48106-1346 USA
800-521-0600

UMI[®]

The Neuronal Response to Injury

by

Michael Adrian Colicos, M.Sc,
Department of Neurology and Neurosurgery
McGill University, Montreal

September 1999

A Thesis

Submitted to the Faculty of Graduate Studies and Research
In Partial Fulfillment of the Requirements
of the degree of
Doctor of Philosophy

Copyright© Michael A. Colicos, 1999



National Library
of Canada

Acquisitions and
Bibliographic Services

395 Wellington Street
Ottawa ON K1A 0N4
Canada

Bibliothèque nationale
du Canada

Acquisitions et
services bibliographiques

395, rue Wellington
Ottawa ON K1A 0N4
Canada

Your file *Votre référence*

Our file *Notre référence*

The author has granted a non-exclusive licence allowing the National Library of Canada to reproduce, loan, distribute or sell copies of this thesis in microform, paper or electronic formats.

The author retains ownership of the copyright in this thesis. Neither the thesis nor substantial extracts from it may be printed or otherwise reproduced without the author's permission.

L'auteur a accordé une licence non exclusive permettant à la Bibliothèque nationale du Canada de reproduire, prêter, distribuer ou vendre des copies de cette thèse sous la forme de microfiche/film, de reproduction sur papier ou sur format électronique.

L'auteur conserve la propriété du droit d'auteur qui protège cette thèse. Ni la thèse ni des extraits substantiels de celle-ci ne doivent être imprimés ou autrement reproduits sans son autorisation.

0-612-55314-0

Canada

Table of contents	Page
Abstract	v
Résumé	vii
Acknowledgments	ix
Contributions of Authors	x
Publications from Graduate Research	xi
1) Introduction	
1.1) Rationale and Objectives	i
1.2) Mammalian brain injury	4
1.2.1) Traumatic Brain Injury	5
1.2.2) Seizure-induced brain injury	5
1.2.3) Hippocampal dysfunction following injury	7
1.3) Neuronal cell death	9
1.4) Reactive synaptogenesis and neuronal regeneration	14
1.5) Axonal guidance factors	17
2) Characterization of dystrophic neuronal regions following traumatic brain injury.	
2.0) Foreword	21
2.1) Summary	21
2.2) Introduction	22
2.3) Methods	
2.3.1) Production of cortical impact brain injury	25
2.3.2) Acute neurological assessments	25
2.3.3) Tissue preparation	26
2.3.4) Cresyl violet staining	27
2.3.5) Silver staining	27
2.3.6) Semi-thin sections	28
2.4) Results	
2.41) Neurologic responses	28
2.42) Time course of appearance of dystrophic dentate gyrus granule cells	29
2.43) Morphological examination of dystrophic dentate gyrus granule cells	29
2.44) Dystrophic cells in other brain regions 24 hours post injury	30
2.45) Regional distribution of dystrophic cells	31
2.46) Post injury hippocampal cell loss	31
2.5) Discussion	31

3) Apoptotic characteristics of hippocampal cell death following traumatic brain injury.

3.0) Foreword	41
3.1) Summary	41
3.2) Introduction	42
3.3) Methods	
3.3.1) Production of cortical impact brain injury	45
3.3.2) Tissue preparation	46
3.3.3) Cresyl violet staining	46
3.3.4) Silver staining	47
3.3.5) Hoechst staining	47
3.3.6) Semi-thin sectioning	47
3.3.7) DNA extraction and gel electrophoresis	48
3.3.8) TUNEL staining	49
3.3.9) Electron microscopy	49
3.4) Results	
3.4.1) Light microscope analysis of regions of cell death	50
3.4.2) Electron microscope study of chromatin condensation and vacuole formation in dentate gyrus granule cells	52
3.4.3) Mitochondrial and rough endoplasmic reticulum (RER) morphology	52
3.4.4) <i>In situ</i> analysis of DNA fragmentation	53
3.5) Discussion	54

4) Regulated expression of netrin in the adult mammalian brain following seizure.

4.0) Foreword	64
4.1) Summary	64
4.2) Introduction	65
4.3) Methods	
4.3.1) <i>In situ</i> hybridization	67
4.3.2) Immunohistochemistry	72
4.3.3) Pilocarpine induction of seizure	73
4.4) Results	
4.4.1) Netrin expression in the normal adult rat brain	74
4.4.2) Netrin induction following seizure	75
4.4.3) Netrin-1 expression in the netrin-1 ^{βgeo/+} mouse brain	77
4.4.4) Netrin receptor DCC induction following seizure in rats	78
4.4.5) Subcellular localization of netrin protein	79
4.5) Discussion	
4.5.1) Netrin expression in basal ganglia	79

4.52) Netrin expression in dopamine related structures	80
4.53) Netrin expression in cortical structures	82
4.54) Conclusions	83
5) Conclusions	
5.1) Delayed apoptotic cell death following TBI	
5.1.1) TBI	96
5.1.2) Cell death	98
5.1.3) Apoptosis	101
5.2) Netrin expression and induction in the adult mammalian brain	
5.2.1) Potential mechanisms of regeneration in the CNS	105
5.2.2) Netrin expression in the normal adult brain	106
5.2.3) Netrin induction following pilocarpine induced seizure	107
5.2.4) Physiological function of netrin in the adult	109
6) Bibliography	112

Abstract

This work is a study of *in vivo* neuronal injury of the central nervous system (CNS). It investigates the neuropathological sequelae and mechanisms involved in both the response to and recovery from CNS injury. Two animal models are used: traumatic brain injury (TBI) and seizure, both performed in the rat. Using the cortical impact injury model of TBI in the rat, the pathophysiological results of injury and the induction of protracted apoptotic cell death in specific brain regions of traumatically injured animals are addressed. Following TBI, silver stain histological analysis detected the appearance of dystrophic neurons in the hippocampus, cortex, amygdala, thalamus, and hypothalamus. Dystrophic cells were detected for at least 2 weeks following injury, and their location correlated with regions of cell loss. These regions have been shown to be functionally related to the post-injury behavioural deficits observed in this paradigm. These dystrophic cells were demonstrated to be apoptotic by morphological examination using electron microscopy, gel electrophoresis and *in situ* detection of DNA fragmentation, and nuclear condensation detected using Hoechst stain. Recovery from the behavioural deficits caused by the injury is accompanied by biochemical changes that suggest that regeneration of the affected neuronal systems is occurring. To address this aspect of the neuronal response to injury and to investigate a possible biochemical mechanism, netrin induction following pilocarpine-induced seizure (a model of human temporal lobe epilepsy) was investigated. First, netrin, an embryonically-expressed axonal guidance molecule was shown to be expressed in the adult rat brain, and the distribution of netrin protein and mRNA was mapped. Then, by sampling tissue at successive time points

following pilocarpine-induced seizure in rats, netrin and the axon-attracting netrin receptor DCC were demonstrated to be induced in brain regions associated with neuronal cell damage and loss, and subsequent axonal sprouting. Together these data demonstrate a role for the activation of apoptotic mechanisms in the neuronal cell loss that occurs following injury and suggest a role for the upregulation of netrin protein in the subsequent regeneration and recovery of the central nervous system following injury.

Résumé

Ce travail est une étude des dommages neuronaux *in vivo* du système nerveux central (CNS). Il étudie les séquelles et les mécanismes neuropathologiques impliqués dans la réponse à et la reprise des dommages de CNS. Deux modèles animales sont utilisés: les dommages traumatiques de cerveau (TBI) et la saisie, toutes les deux sont exécutés dans le rat. En utilisant le modèle cortical de dommages d'impact de TBI dans le rat, les résultats pathophysiologiques des dommages et l'induction de la mort apoptotique prolongée de cellules dans des régions spécifiques du cerveau d'animaux ayant subi un traumatisme sont adressés. Après TBI, l'analyse histologique de taches argentées a détecté l'aspect des neurones dystrophiques dans le hippocampe, le cortex, l'amygdala, le thalamus, et l'hypothalamus. Des cellules dystrophiques ont été détectées pour au moins 2 semaines suivant des dommages, et leur emplacement a corrélé avec des régions de perte cellulaire. Ces régions ont été montrées pour être fonctionnellement liées aux déficits comportementaux observés post-dommages dans ce paradigme. Ces cellules dystrophiques ont été démontrées pour être apoptotiques par l'examen morphologique en utilisant la microscopie électronique, l'électrophorèse de gel et la détection *in situ* de la fragmentation d'ADN, et la condensation nucléaire détectée utilisant la tache de Hoechst. La reprise des déficits comportementaux provoqués par les dommages est accompagnée des changements biochimiques qui suggèrent que la régénération des systèmes neuronaux atteints se produit. Pour adresser cet aspect de la réponse neuronale aux dommages et pour étudier un mécanisme biochimique possible, l'induction de netrin suivant la saisie pilocarpine-induite (un modèle de l'épilepsie temporelle humaine de lobe) a été étudiée.

D'abord, le netrin, une molécule exprimée embryologiquement qui a pour fonction de guider des axones durant le développement du CNS a été montré pour être exprimé dans le cerveau adulte du rat. La distribution de la protéine de netrin et du mRNA a été tracée. Ensuite, suivant la saisie induite par la pilocarpine, les cerveaux ont été examinés à certains temps successifs. Netrin et le récepteur de netrin attractant pour axones, DCC ont été démontrés pour être induits dans des régions de cerveau associées aux dommages et à la perte neuronale de cellules, et la germination ultérieure d'axonal. Ensemble ces données démontrent un rôle pour le lancement des mécanismes apoptotique dans la perte neuronale de cellules qui se produit suivant des dommages et suggèrent un rôle pour la hausse d'induction de la protéine de netrin dans la régénération et la reprise ultérieures du système nerveux central après des dommages.

Acknowledgements

Research performed at the Montreal Neurological Institute was funded in part by a Savoy Foundation Studentship, and by MRC Grant #MT-13725. Research performed at the University of Texas was funded by an ARP grant from the Texas Higher Education Board, a fellowship from the Klingenstein Foundation and MH49962. I'd like to thank Ed Dixon for his help with the injury work; Neal Waxham for his support throughout my studies in Texas; Phil Barker for his support on my academic advisory committee at McGill; Jack Snipes for his belief and support in the pursuit of creative thought; Colleen Manitt, my partner in the work on netrin; Tim Kennedy for making all of this possible; and Robyn Flynn, who stuck this out with me to the end.

Contributions of Authors

All work reported in the included manuscripts was performed by Michael A. Colicos with the following exceptions. In **Colicos, M.A., Dixon, C.E., Dash, P.K. (1996)** Selective neuronal death following cortical impact injury in rats: A silver impregnation study. *Brain Research* 739:120-131, the majority of the injuries were performed by Dr. S. Lui and Dr. J. Bao of the University of Texas, Department of Neurosurgery, Dr. C.E. Dixon supervising. In **Colicos, M.A., Dash, P.K. (1996)** Apoptotic morphology of dentate gyrus granule cells following cortical impact injury: Possible role in spatial memory deficits. *Brain Research* 739:111-119, the gel in Figure 5a was run by Dr. Pramod Dash, Department of Neurobiology and Anatomy, University of Texas.

Publications during Graduate Research

The following list includes publications not included in the thesis body, but that are based on research done during my Ph.D. studies.

1) Roux, P.P., **Colicos, M.A.**, Barker, P.A., Kennedy, T.E. (1999) p75 Neurotrophin Receptor Expression Is Induced in Apoptotic Neurons After Seizure. *Journal of Neuroscience* 19: 6887-6896

2) **Colicos, M.A.**, Kelly, M.A., Lowenstein, D.H., Tessier-Lavigne, M., Kennedy, T.E. (1999) Regulated Expression of Netrin in the Adult Mammalian Brain Following Seizure. *Journal of Neuroscience* (in preparation)

3) Manitt, C., **Colicos, M.A.**, Peterson, A.C., Kennedy T.E. (1999) Netrin Expression by Neurons and Oligodendrocytes in the Developing and Adult Mammalian Spinal Cord. *Journal of Neuroscience* (in preparation)

4) Li, H., Alonso-Vanegas, M., **Colicos, M.A.**, Jung, S.A., Lochmuller, H., Sadikot, A.F., Snipes, G.J., Seth, P., Karpati, G., Nalbantoglu, J. (1999) Intracerebral adenovirus-mediated p53 tumour suppressor gene therapy for experimental human glioma. *Clin Cancer Res.*5(3):637-42.

5) **Colicos, M.A., Dash, P.K.** (1996) Apoptotic morphology of dentate gyrus granule cells following cortical impact injury: Possible role in spatial memory deficits. *Brain Research* 739:111-119.

6) **Colicos, M.A., Dixon, C.E., Dash, P.K.** (1996) Selective neuronal death following cortical impact injury in rats: A silver impregnation study. *Brain Research* 739:120-131.

7) Noel, F., Frost, W.N., Tain, L-M., **Colicos, M.A., Dash, P.K.** (1995) Recovery of tail-elicited siphon-withdrawal reflex following unilateral axonal injury is associated with ipsi- and contralateral changes in gene expression in *Aplysia californica*. *Journal of Neuroscience* 15(10):6926-38.

1) Introduction

1.1) Rationale and Objectives

Cellular architecture, biochemical state and synaptic connectivity are the key features that dictate how a neuron transmits its information, and consequently determine how the single neuron becomes integrated into the larger neuronal systems of the brain. Neuro-pathological conditions can disrupt these characteristics, and lead to functional deficits in brain function. However, behavioural recovery from these deficits can also be observed. The processes of neuronal injury and regeneration are of crucial interest, not only in terms of their clinical relevance, but also with respect to our understanding of basic brain function. While *in vitro* systems have provided a large body of knowledge regarding these phenomena, no such system can duplicate the complex global parameters of the mammalian brain. The study of experimental brain injury provides an effective method to assess the processes of neuronal degeneration and regrowth in the intact animal.

The study of neuronal degeneration is primarily motivated by a desire to understand the dynamics of neurodegenerative diseases and conditions, in the hope of developing a clinical treatment for the ensuing behavioural deficits. Two phenomena are frequently targeted to achieve this goal: the prevention of neuronal cell loss due to the injury and the enhancement of the ability of the mammalian CNS to regenerate. This study first addresses the issue of neuronal cell death following traumatic brain injury (TBI). Evidence from other injury paradigms such as ischemic brain injury (Charriaut-Marlangue et al., 1996; Charriaut-Marlangue et al., 1995; Li et al., 1995) suggests that protracted neuronal cell death can occur following injury, and extend into brain regions

not immediately associated with the initial insult. My study of TBI addressed two main questions. The first question was *does neuronal cell death expand spatially and temporally from the initial insult?* To answer this, I demonstrated that cortical impact injury results in pathophysiological alterations in CNS neurons, and importantly, that these changes can occur beyond the primary site of injury. This is of relevance on a systems level, since the brain regions in which neuropathological changes were observed include regions that play a role in subsequent behavioural deficits. For example, several experimental brain injury paradigms in the rat have been demonstrated to produce deficits in spatial learning and memory (Smith et al., 1991; Lyeth et al., 1990; Dixon et al., 1991), Spatial learning and memory is a function associated with the hippocampus (Squire 1992). However the cause of hippocampal dysfunction in any of these injury paradigms has not yet been determined. Evidence presented here shows that traumatic brain injury can lead to cell death and consequent alterations in neuritic and synaptic structure in the major input pathway to the hippocampus. This cell death could well be expected to play a role in the hippocampal functional deficits observed.

In addition to the presence of cell death, the time course of the appearance of regions of cell death extended far beyond the initial insult. This observation led to the second question, *what is the mechanism of the delayed neuronal cell death observed following TBI?* Determining the mechanism of the spread of neuropathological effects is critical, as it offers a potential point of clinical intervention in attempts to limit the expanse of the effect of the insult. This question was addressed by characterization of the nature of neuronal cell death following injury. The mechanism of this cell death was

demonstrated as apoptosis, a physiological form of cell death (Kerr et al., 1972; Wyllie 1980). The induction of apoptosis is becoming well understood, and this knowledge can now provide insight into the biochemical mechanisms underlying the expansion of the neuronal death observed following TBI.

The second phenomenon investigated in this study was the ability of the mammalian CNS to regenerate following injury. To examine this I addressed the question *are biochemical markers of axonal growth processes present and are they invoked following injury?* The specific candidate for this function was the chemotropic factor netrin, an embryonically expressed molecule with the ability to direct axonal outgrowth. This study required two facts to be established: whether netrin is expressed in the adult in functionally relevant brain regions, and whether netrin gene expression is regulated following injury. Two studies examined these issues: first, an analysis of netrin expression in the normal adult rat brain, and second, the determination of the induction profile of netrin following seizure. Netrin expression in the adult was investigated by use of three main techniques: anti-netrin immunohistochemistry in the rat, *in situ* hybridization of a rat netrin-1 probe with normal rat tissue, and analysis of a transgenic mouse in which the netrin-1 promoter drives expression of β -galactosidase, netrin-1 ^{β geo/+} (Serafini et al., 1996; Skarnes et al., 1995). This work established the expression profile of netrin in the adult brain, demonstrating an association with basal ganglia, cerebellar and cortical brain structures.

To study the dynamics of netrin expression following neuronal injury, I used pilocarpine-induced seizure in rats, a well established animal model of human temporal

lobe epilepsy (Rice et al., 1998; Hamani and Mello, 1997). The model produces initial status epilepticus followed by recurrent seizures which occur for months to follow, paralleling the behavioural pathology of the human condition (for review see Turski et al., 1989). Histological analysis of tissue from seized animals revealed damage in the entorhinal cortex, a presumed focal point of the seizure. This study demonstrates the regulation of netrin and its chemoattractant receptor DCC (deleted in colorectal carcinoma) in several brain regions, including the regions of tissue damage and altered electrophysiological response, such as the entorhinal cortex, and regions of axonal sprouting, such as the dentate gyrus of the hippocampus. By characterizing the expression of the axonal growth factor netrin and its reactivity in regions of injured tissue in the adult, an excellent candidate for an effector of regenerative processes in the CNS has been established.

1.2) Mammalian Brain Injury

Neuropathological insult to the mammalian brain can occur two ways: as a result of physical or chemical damage, such as occurs following traumatic injury, stroke or seizure; or brain injury can result as a consequence of a disease state, such as in Alzheimer's or Parkinson's disease. While the cause of the injury may vary, many of the biochemical mechanisms that function on a cellular level may be held in common. This study focuses on the effects of and response to two types of pathophysiological damage; due to an impact, in the TBI model, and electrochemical insult, by induced hyper-excitation during seizure. The result of either perturbation is a decrease in the structural

integrity of the system and consequential loss of function of the affected pathways.

1.2.1) Traumatic Brain Injury

Traumatic brain injury (TBI) in humans has been shown to cause pathophysiological changes in brain function (Rudelli et al., 1982). The neuropathological consequences of brain injury are many, including cortical necrosis of the contusion site (Sutton et al., 1994, Sutton et al., 1993), cortical axonal degeneration (Povlishock 1992), degeneration of hippocampal hilar neurons (Lowenstein et al., 1992). In addition, the occurrence of seizure (Nilsson et al., 1994) and ischemia (Bryan et al., 1995) as a consequence of TBI also contribute to pathophysiological changes. To investigate the biochemical mechanisms involved in TBI, several animal model systems have been developed (Hamm et al., 1992; Dixon et al., 1991). As in human TBI, experimental brain injury in rats has been shown to produce both short term deficits in motor function, and deficits in long term spatial memory performance (Smith et al., 1991; Lyeth et al., 1990; Dixon et al., 1991). The spatial memory deficits are distinguishable from motor or sensory dysfunction and can persist for weeks following injury (Dixon et al., 1991).

1.2.2) Seizure induced brain injury

Pilocarpine induced seizure activity in rats (Turski et al., 1983) is widely accepted as a model for human temporal lobe epilepsy (Rice et al., 1998; Hamani and Mello, 1997), and produces long term behavioural, histological and biochemical changes.

Pilocarpine is a muscarinic agonist, producing status epilepticus (SE) as well as subsequent spontaneous recurrent limbic seizures for several months following treatment. The post-injury electrographic and behavioural profile is one of the features of pilocarpine-induced seizure that parallels the human condition (for review see Turski et al., 1989). The recurrent spontaneous seizures proceed through several defined stages, and resemble the effects caused by repeated electrical stimulation of specific brain regions, a procedure known as kindling (Cavalheiro et al., 1991).

In terms of the neurohistological changes that occur following seizure, three main phenomena have been observed: cell death, axonal sprouting and neurogenesis. Both short and long term neuronal cell death occurs throughout the brain (Represa et al., 1994; Fujikawa 1996). This cell death, depending on location and severity of the seizure, can be either apoptotic or necrotic in nature. Low level damage appears to primarily affect interneurons and produce apoptosis, whereas more dramatic seizure activity results in more widespread necrosis (Mello and Covolan 1995; Bengzon et al., 1997; Represa et al., 1994). In concert with this, axonal sprouting can subsequently be detected in some of these regions. These include the projections of cholinergic forebrain neurons of the basal forebrain (Holtzman and Lowenstein, 1995), and both sprouting of the granule cell mossy fibers themselves (Mello et al., 1993) and increased neurogenesis in the hippocampus (Parent et al., 1997). It has been suggested that the denervation of the inner molecular layer following the hilar cell loss constitutes the initial stimulus for hippocampal sprouting (Tauck and Nadler, 1985), and this sprouting can be both supra- and intragranular (Mello et al., 1993).

Both glutaminergic and dopaminergic systems play a role in the long term sequelae of pilocarpine induced seizures. Dopaminergic agonists and antagonists can modulate the SE phase (George and Kulkarni, 1997) while the NMDA receptor antagonists MK-801 has been shown to block the spontaneous recurrent seizures and limit the cell death in the CA1 hippocampal field (Rice et al., 1998). Biochemical changes include upregulation of neurotrophins as well as furin and other prohormone convertases enzymes (Schmidt-Kastner et al., 1996; Marcinkiewicz et al., 1997). In addition to changes in gene induction, dopamine utilization increases in the nucleus accumbens, olfactory tubercle and cingulate cortex, and decreases in the hippocampus (Alam and Starr, 1996).

1.2.3) Hippocampal dysfunction following injury

While the role of the hippocampus in some forms of human memory has been long proposed (Squire and Zola-Morgan, 1991; Squire 1992; Scoville and Milner, 1957), its study has been mostly by way of lesions, from which behavioral recovery is limited (reviewed in Jarrard 1993; Moser et al., 1993). In the cortical impact model of traumatic brain injury used in this study, the ability to learn is compromised (Hamm et al., 1992; Dixon et al., 1991), and so by study of the damage and the restoration of function, insight into this critical aspect of brain function can be addressed. A consistent observation following TBI is the production of hippocampal spatial learning and memory deficits (Hamm et al., 1992; Dixon et al., 1991). The physiological causes of these deficits are still unclear. At mild injury levels, hippocampal memory deficits have been shown to

occur in the absence of overt hippocampal tissue loss (Lyeth et al., 1990). Under these conditions, neural dysfunction due to neurotransmitter imbalance has been hypothesized as a contributing factor to the deficits seen (Yamamoto et al., 1988). However, at moderate to severe levels of injury, some hippocampal neuronal cell death has been observed (Lowenstein et al., 1992, Goodman et al., 1994). This cell death would be expected to directly contribute to behavioral deficits.

The hippocampal structure provides a well characterized brain region in which to study the neuropathological effects of TBI. Not only has a behavioral assay for dysfunction been documented, but also the intrinsic circuitry has been well characterized. The hippocampus is classed as supramodal association cortex, and receives and integrates information from all sensory modalities (Swanson, 1983). The basic information pathway in the hippocampus can be summarized by the tri-synaptic circuit. Simplistically described, this begins with the major input from the entorhinal cortex, through the perforant path, into the dentate gyrus. The second part of the circuit is defined by the axons of these granule cells, the mossy fibers, which extend and synapse on the CA3 pyramidal cells. The final synapse is onto the CA1 pyramidal cells, where the axons of the CA3 neurons (the Schaffer collaterals) terminate (Shepherd, 1990a). The evidence presented here focuses on the dentate-mossy fiber synaptic system. The response of this system to perturbation has been investigated in other neuropathological paradigms. For example, the mossy fibers have been reported to suffer retrograde degeneration following the loss of their target cells, the pyramidal CA3 neurons. This has been documented following both kainic acid induced seizure lesions (Pollard et al., 1994) and

dexamethasone treatment (Uno et al., 1990). In addition, axonal sprouting and reactive synaptogenesis has been well documented in the mossy fibers following lesion, injury and seizure (described in detail below).

Spatial learning and memory ability can be directly assayed in a Morris water maze test (Morris et al., 1982; Smith et al., 1991). Briefly, this test requires the subject to find a fixed, hidden, underwater platform while swimming, relying on spatially fixed visual cues in its environment. Repeated training in the maze over a 5 day period produces an increase in performance, as indicated by a decrease in the length of time required to find the platform. This increase is believed to be due to the fact that the subject has remembered the position of the platform relative to the spatial cues, and is therefore able to get there faster (Morris et al., 1982). The cortical impact injury paradigm used in this work has been demonstrated to produce deficits in this ability, in comparison to sham injured animals (Hamm et al., 1992). This deficit can be expressed in terms of the percentage of the control performance. If the spatial learning and memory test is given 10 days after injury, the deficit seen is high (~40% of sham performance). If the test is initiated at later time point following injury, the deficit is less (approaching 80% of sham performance by 5 weeks post injury). The recovery of the injured brain structures has been proposed to contribute to the reduction in deficit (Dixon et al., 1991).

1.3) Neuronal cell death

Cells die by one of two mechanisms, necrosis or apoptosis. Necrotic cell death is a degenerative increase in cellular disorder, often caused by mechanical damage,

complement-mediated cell lysis, hypoxia or highly toxic agents (Alnemri and Litwack, 1993). Such insults result in loss of membrane homeostasis leading to swelling of all cytoplasmic compartments. Subsequent release of lysosomal enzymes and dissolution of organelles due to membrane rupture results in a homogeneous nuclear morphology and a predominance of intracellular debris (for review see Kerr, 1993). In contrast to this, apoptosis is a physiological cellular function that is triggered by extracellular signals (Kerr et al., 1972). Apoptosis is a morphologically defined term, characterized in part by chromatin condensation, vacuole formation, and DNA cleavage by an endonuclease (Wyllie et al., 1984). Apoptotic cell death can serve a homeostatic function for the organism and is ubiquitously employed during development, including maturation of the nervous system. It is a physiological process of cell elimination, during which, in contrast to necrosis, there is no induction of an inflammatory response (Duvall et al., 1985; Fadok et al., 1992).

While this study focuses on the identification of the morphological determinates of apoptotic cell death, the elucidation of the pathways involved in the signaling and biomechanical processes involved in apoptotic cell death has made great progress over the past several years. The biochemical phenomena under investigation that make up the complex regulatory and effector systems controlling apoptosis can be divided into three general classes. The first of these focuses on the mechanisms of induction from chemotoxic or DNA damaging agents, and involves oncoprotein function and cell cycle control molecules. The second line of study concentrates on the receptor/ligand complexes and the intracellular signalling cascade which trigger apoptosis as a response

to extracellular signals such as growth factor withdrawal. The third objective is a delineation of the effector molecules which are the actual machinery which produce the morphological phenotype observed. All of these phenomena are inseparably linked, however their distinction facilitates their study. As a general framework, it can be hypothesized that oncoprotein regulation serves to prime the cell for apoptosis, which can then be either continued or halted, as determined by survival signals. Once committed, the effector systems function to complete the process (Evan and Littlewood, 1998; Harrington et al., 1994).

Efforts to elucidate the biochemical mechanisms involved in apoptosis began with the oncoprotein and tumour suppressor pathways, and indeed represent the biochemical foundation of the phenomena itself. One of the first oncogenes demonstrated to have pro-apoptotic properties was *c-myc*. Deregulation of *myc* proteins is often associated with cancer, and it appears that this is also the case with apoptosis (for review see Amati et al., 1998). However there has generally been a co-requirement associated with *myc* and its role in apoptosis, and in fact the specific targets are still elusive. The search for the co-required molecules led to the tumour suppressor p53 and the apoptosis suppressor *bcl-2* and later the Ras oncoproteins (for review see Evan and Littlewood, 1998). This line of investigation ushered cell biology into a new age of understanding of the dynamics of the cell cycle, how it is so tightly regulated, and how it can go wrong. In brief, a balance is held between growth arrest and proliferation, and another between cell survival and apoptosis. The regulatory molecules controlling these choices are tightly interlocked. For example, Ras expression can determine both the arrest/proliferation state, as well as

survival/apoptosis. However, which is affected is tied to the state of Myc and Bcl-2. Ras and Myc expression together promote proliferation whereas Ras and Bcl-2 together promote cell survival. Conversely Ras and Myc also regulate apoptosis, and Ras and Bcl-2 regulate growth arrest. This interdependency sets the stage for a dynamic regulatory system which is both self checking and sensitive to the many other cell signals that contribute to the determination of the final fate of the cell (for review see Evan and Littlewood, 1998).

With the cell cycle responding to this dynamic regulatory system, the cell is poised to receive information from its environment as to the correct course of action. The so called death receptors have been demonstrated to be trigger points for the apoptotic signalling cascade. These include receptors of the tumour necrosis factor (TNF) receptor gene superfamily (Smith et al., 1994; Gruss and Dower, 1995). The TNF superfamily is defined by a cytosine rich extracellular domain, and the death receptor subfamily is defined by an intracellular death domain (Nagata 1997; Tartaglia et al 1993). A major environmental signal for neuronal cell survival are the neurotrophins, including neuronal growth factor (NGF), and brain derived growth factor (BDNF), NT3, and NT4/5 (for review see Barker, 1998). The TNF superfamily receptor critical in this regulatory pathway is the p75 neurotrophin receptor (for reviews see Barker, 1998; Miller and Kaplan, 1998). Once the extracellular signals are processed, the downstream intracellular signalling cascade is activated through transcription factors (for review see Ashkenazi and Dixit, 1998). This sets the stage for the induction of the actual machinery to carry out the process of apoptotic cell death.

The key apoptotic effector molecules are a family of proteases known as caspases. For example, the protein inhibitor of the endonuclease responsible for DNA cleavage is itself inactivated by caspases, leaving the nuclease free to degrade the chromosome (Enari et al., 1998; Liu et al., 1997). Caspases directly disassemble cellular structures, such as the nuclear lamina (Takahashi et al., 1996; Orth et al., 1996), and in this way play a direct physical role in cellular breakdown. Caspases also act by deregulating other proteins, usually by separating the catalytic and regulatory domains (Thornberry and Lazebnik, 1998). It is this final cascade that results in the destruction of the cell, and the production of the morphological changes observed (for review see Thornberry and Lazebnik, 1998). In the case of the development of the neural system, this is usually the desired conclusion. In the case of injury, the removal of a specific neuron may be either desired or detrimental.

In vitro studies have shown that neurons can be induced to undergo apoptosis by treatment with the β -amyloid peptide as well as with intracellular calcium altering treatments such as glutamate (Bonfoco et al., 1995; Deckwerth et al., 1993; Loo et al., 1993). Biochemical conditions such as these are often components of neuropathological conditions, and consequently the potential contribution of apoptosis in several paradigms has been investigated. For example, both in models of ischemia and of epilepsy, DNA fragmentation has been reported to accompany neuronal death (Charriaut-Marlangue et al., 1996; Charriaut-Marlangue et al., 1995; Li et al., 1995; MacManus et al., 1993; Nitatori et al., 1995; Pollard et al., 1994). This implied the presence of apoptosis in these injury paradigms. However, following ischemia it was noted that the fragments of DNA

produced were of different sizes than those normally seen during apoptotic cell death, suggesting that an alternate DNA degrading enzyme was functioning following stroke injury (MacManus et al., 1995). The case for the presence of apoptotic mechanisms was further supported by evidence that key players in the apoptotic cascade are indeed at work. The activation of caspase-3, critical in apoptosis, is induced by experimental cerebral ischemia (Namura et al., 1998). It is currently believed that the form of cell death seen during ischemic injury does not fit the stereotypical criteria of either apoptosis or necrosis (Barinaga, 1998). The contribution of apoptosis to ischemia is perhaps best substantiated by models of therapeutic treatments that target the process. For example, both MK-801, an NMDA receptor antagonist, or peptide inhibitors of the caspase family (z-VAD.FMK and z-DEVD.FMK) can protect mouse brain from ischemic cell damage (Ma et al., 1998). Evidence such as this also suggests that in fact, in terms of necrosis and apoptosis, the *in vivo* situation is not quite as delineated as can be observed in cell culture.

1.4) Reactive synaptogenesis and neuronal regeneration

An obvious consequence of neuronal cell death is the loss of the synaptic connections that were contributed by the neurons that have died. The connectivity defined by the synapses is a significant factor in determining the output of the neural system. Consequently, synaptic loss is a point at which neuropathological insult can become translated into altered behaviour. Synapses can also be altered even if the neuron does not die, but is injured or compromised in function. Events such as axon shearing, retraction of synapses, and altered electrophysiological response have all been observed

following traumatic injury (Povlishock et al., 1992; Povlishock et al., 1983).

The ability of axons to sprout new synapses following injury has been well documented. This has been shown to occur following the death of the hippocampal hilar neurons (Okazaki et al., 1995), which is a reported consequence of fluid percussion injury (Lowenstein et al., 1992). The mossy fibers, the axons of the dentate gyrus granule cells of the hippocampus, normally extend and connect to the pyramidal cell dendrites in the CA3 hippocampal region and to interneurons in the dentate hilus and the dentate granule cell layer. Under normal circumstances (with the exception of aged humans), mossy fibers are never seen to undergo recurrent growth, back into their own granule cell layer (for review see Sloviter 1994a). However, seizure has been shown to induce not only recurrent growth back through the granule cell layer, but also the penetration of fibers through to the molecular, dendritic layer that then synapse on the granule cells themselves (Okazaki et al., 1995). This reorganization is one of the best characterized examples of axon collateral sprouting and synaptogenesis in the adult mammalian CNS (for review see Sloviter, 1994a). Several seizure paradigms can elicit mossy fiber sprouting and synaptogenesis, such as induction both pharmacologically and electrically (Tauck and Nadler, 1980; Sutula et al., 1988; Babb et al., 1991), in spontaneously epileptic mouse strains such as tottering (Stanfield, 1989) and stargazer (Qiao and Nobeles, 1993), and in human temporal lobe epilepsy (TLE) (for review see Sloviter, 1994b). The mechanism of the induction of events such as these have yet to be determined. In both human TLE and in animal seizure models, many changes to the local circuitry occur, such as the selective loss of hilar interneurons with the survival of granule cell layer GABAergic interneurons

(Robbins et al., 1991; Sloviter et al., 1991; deLanerolle et al., 1989; Babb et al., 1989), as well as the loss of the main CA3 targets themselves (Pollard et al., 1994). Networks of feedforward and feedback inhibition are normally formed between the granule cells and these interneurons (Amaral, 1978). The loss of these post-synaptic targets of the granule cells may contribute to the induction of mossy fiber sprouting. However, the specific contribution of cell death, denervation and activity to this process, as well as the nature of the molecules involved, is not well understood.

The study of the biochemistry of the activity-dependent response of the synapse has also often utilized hyperactivation through the induction of seizure activity. Seizure has been demonstrated to induce many immediate early genes including transcription factors (for review see Morgan and Curran, 1991), as well as early effector genes such as ornithine decarboxylase (Baudry et al., 1986) and tissue-plasminogen activator, tPA (Qian et al., 1993). Trophic factors such as NGF, BDNF, and EGF (Gall and Isakson, 1989; Isakson et al., 1991; Ernfors et al., 1991; Gall, 1993) have also been observed to be induced subsequent to the early events. These and other studies have paved the way for an understanding of the biochemical mechanisms underlying the synaptic response to injury, as well as of basic synaptic plasticity.

The dynamic behaviour of the synapse can be seen both in the normal animal during development and plasticity, as well as following injury. While much has been learned about the induction of basic growth mechanisms in neurons post injury, less is known about the mechanisms of post-injury axonal guidance and synapse formation. Integration of information gained from the study of guidance mechanisms in development

with data concerning activity-dependent biochemical mechanisms of the synapse will hopefully contribute to the investigation of their potential role following injury in the adult CNS.

1.5) Axonal guidance factors

During the development of the nervous system, axons must be guided to their appropriate target, and once there, form appropriate synaptic connections. Two classes of molecules have been suggested to account for the guidance of the axon during this process. The first class consists of pathway-derived cues: cell surface and extracellular matrix molecules which are expressed by cells which lie along the axon's trajectory. The second class are diffusible chemotropic cues, which are molecules secreted by the actual target cell towards which the axon is heading (for review see Tessier-Lavigne and Goodman, 1996). Evidence for the existence of the pathway-derived cues has come primarily from embryological experiments (Lance-Jones and Landmesser, 1980, 1981; Harris, 1989). Many of the molecules have been isolated and described, and consist of cell adhesion and extracellular matrix molecules such as laminin, NCAM, and N-cadherin (Riggott and Moody, 1987; Reichardt et al., 1989; Jessell, 1988; Takeichi, 1988; Hynes and Lander, 1992). Molecules of this class have been functionally demonstrated to direct axonal outgrowth during vertebrate CNS development (Stoeckli et al., 1995, 1997)

Chemotropism is the guidance of an axon by a gradient of molecular cues, and is an idea that has been proposed since early investigations of the nervous system (Ramon y Cajal, 1902). Current evidence suggests the existence of both target derived

chemoattractants (Lumsden and Davies, 1983; 1986; Tessier-Lavigne et al., 1988) and target derived chemorepellents (Pini 1993; Colimarino and Tessier-Lavigne, 1995a). One of the first isolated and best characterized of these chemotropic molecules is netrin. Experiments both *in vitro* and *in vivo* demonstrated that the embryonic spinal floor plate secretes a chemoattractant for the axons of developing spinal commissural neurons (for review see Colimarino and Tessier-Lavigne, 1995b). The netrins were subsequently purified and cloned based on their ability to promote the outgrowth of spinal commissural axons *in vitro* (Kennedy et al., 1994; Serafini et al., 1994).

Several lines of evidence have demonstrated that netrin plays a functional role in axonal guidance. During the initial isolation, *in vitro* assays using recombinant vertebrate protein demonstrated that netrin could reproduce the outgrowth and turning effects of the floor plate on embryonic spinal commissural axons (Kennedy et al., 1994). When the protein sequence of netrin was determined, it was shown to be a homologue of the *C. elegans* gene *unc-6* (Serafini et al., 1994) in which mutations produce misdirected axonal trajectories in the worm (Ishii et al., 1992; Hedgecock et al., 1990). Additional evidence comes from a netrin loss of function mutation in the mouse, which disrupts the formation of the ventral spinal commissure, the hippocampal commissure, and corpus callosum (Serafini et al., 1996). These data strongly support the hypothesis that netrins function as axon guidance cues during vertebrate neural development.

Netrin has been demonstrated to be able to act as both a chemoattractant in the case of spinal commissural axons (Kennedy et al., 1994), and as a chemorepellent for trochlear motor neurons (Colimarino and Tessier-Lavigne, 1995a). The division between

these two functions has been proposed to be regulated by the nature of the netrin receptor present on the axonal growth cone. The isolation and characterization of the receptor molecules for netrin has been facilitated by inference from genetic analysis in *C. elegans*. In the *C. elegans* *unc-6* (netrin) mutant phenotype, both dorsal-ventrally and ventral-dorsally directed axon trajectories are disrupted (Hedgecock et al., 1990). Another mutant phenotype, *unc-5*, showed only the disruption of ventral-dorsally directed trajectories, whereas *unc-40* mutants showed only the disruption of the dorsal-ventral trajectories (Hedgecock et al., 1990). This suggested that these two gene products could play a role in directing axon growth in response to a source of *unc-6*. *Unc-40* and *unc-5* encode transmembrane members of the IgG superfamily (Chan et al., 1996; Leung-Hagesteijn et al., 1992) and *unc40* was found to be homologous to mammalian DCC (Keino-Masu, 1996; Chan et al., 1996, Kolodziej et al., 1996). The classification of DCC as a functional netrin receptor was suggested by binding studies (Keino-Masu et al., 1996) and by the fact that a loss of DCC function in the mouse produces a phenotype similar to the netrin loss of function phenotype (Fazeli et al., 1997). The two *unc-5* rat homologues also interact directly with netrin in binding studies, suggesting they are also netrin receptors (Leonardo et al., 1997). An interesting feature of the *unc-5* receptors is the presence of a death domain in *unc-5H*, suggesting a possible link of netrin/*unc-5* to the cell survival signaling cascade (Hofmann and Tschopp, 1995).

While a role for netrin expression during development is becoming well characterized, evidence that netrin expression persists in the adult brain (Kennedy et al., 1994; Kennedy et al., 1996; Colicos et al, 1997; Livesey and Hunt, 1997) suggests a

continuing role for netrin in regulation of axonal structure throughout the life of the animal. The netrin receptor DCC has also been shown to be expressed in the adult mammalian brain (Volenec et al., 1997; Livesey and Hunt, 1997). In order to investigate a role for netrin in the adult, and determine if it is present and functional in regenerative post-injury processes, the spatial and temporal expression of the molecules involved must be determined. This study on the neuronal response to injury is completed by addressing this issue, with the characterization of netrin in the normal adult rat, and following seizure-induced injury.

2) Characterization of dystrophic neuronal regions following traumatic brain injury.

2.0) Foreword

The pathological changes that occur in systems of neurons following injury can be grossly classified as alterations in cellular biochemistry and/or alterations in cellular structure. In order to test the hypothesis that TBI affects neurons other than those at the primary site of injury, I used a sensitive silver staining technique to identify and localize dystrophic neurons and their processes. While physical damage at the cortical contusion site is obvious, certain previously observed behavioural deficits in spatial learning and memory tasks suggested the involvement of structures distal to the injury. Here, overt changes are not obvious; however, a detailed analysis of serial brain sections taken from animals over a time course following injury identified distinct regions of neuronal cell death distal to the site of injury. This work was summarized in the paper "*Delayed, selective neuronal death following experimental cortical impact injury in rats: Possible role in memory deficits.*" Colicos, M.A., Dixon, C.E., Dash, P.K. (1996) *Brain Research* 739:111-119, and is presented below as published.

2.1) Summary

Clinical and experimental studies show that loss of neurons in the hippocampus and/or the entorhinal cortex can impede formation and storage of spatial memory. Using a controlled cortical impact model of traumatic brain injury (TBI) in rats, we have examined the temporal and spatial pattern of neuronal death using silver impregnation and

cresyl violet staining. Dystrophic neurons can be detected in the dentate gyrus, and the CA1 and CA3 subfields of the hippocampus for up to 2 weeks following injury. These dystrophic cells appeared shrunken and possessed features of apoptosis. Areas containing the dystrophic cells suffer substantial cell loss as demonstrated by thinning of the neuronal layers. Dystrophic cells are also found in the amygdala, entorhinal and piriform cortices, thalamic and hypothalamic regions, and surrounding the contusion site. The loss of these cells may contribute to the memory deficits observed following TBI.

2.2) Introduction

Traumatic brain injury (TBI) causes abnormal information processing, motor dysfunction, attention deficits and impairments of memory (Levin, 1992). Memory deficits are some of the most persistent consequences of TBI in humans. The cellular and biochemical mechanisms underlying these memory dysfunctions are poorly understood. In order to investigate the mechanism(s) of memory deficits, rodent models have been developed that mimic various features of the pathophysiology associated with human TBI (Dixon and Hayes, 1996; Gennarelli, 1994). Similar to human TBI, rodent models produce persistent spatial memory (a form of declarative memory) deficits (Dash et al., 1995; Hamm et al., 1992; Smith et al., 1991; Long et al., 1996).

Two of the most widely employed brain trauma models in rodents are fluid percussion and controlled cortical impact (Dixon and Hayes, 1996; Gennarelli, 1994). Fluid percussion produces brain injury by rapid injection of fluid into the closed cranial cavity (Dixon et al., 1987; MacIntosh et al., 1989). The advantages of the fluid

percussion model primarily reside in its simplicity and its ability to produce significant disturbances in the brain including axonal injury and intraparenchymal hemorrhages (Povlishock et al., 1992). However, fluid percussion injury allows little control over injury parameters and often causes brain stem injury and death (Dixon and Hayes, 1996). The controlled cortical impact model for rodents is a recently introduced animal model of TBI. This model utilizes a pneumatic piston to deform a controllable volume of exposed cortex over a range of impact velocities (Dixon et al., 1991). The severity of the injury can be varied by altering the depth of excursion or the velocity of the impactor. Much of the pathophysiology of human TBI, including contusion and axonal injury, appear to be reproduced using this model (Dixon and Hayes, 1996; Meany et al., 1994). For example, cortical impact produces contusion and necrotic cell loss at the site of impact (Goodman et al., 1994; Sutton et al., 1993). Moreover, an overall decrease in CA1 and CA3 pyramidal cells of the of the hippocampus by two weeks postinjury has been reported (Goodman et al., 1994). However, neither the time course nor the morphological characteristics of these cell losses have been examined in this model. Furthermore, cell loss in other brain structures has not been investigated.

Both clinical and experimental studies have shown that the hippocampus and possibly the entorhinal, perirhinal and parahippocampal cortices are necessary for declarative memory storage (Meunier et al., 1993; Squire and Zola-Morgan, 1991; Squire 1992; Suzuki et al., 1993). For example, hippocampal lesions in rats cause poor performances in the Morris water maze and radial maze tasks, which are thought to assess spatial memory (Barnes, 1979; Morris, 1982). Recently, studies in monkeys indicate that

the perirhinal, parahippocampal and entorhinal cortices contribute substantially to recognition memory (Meunier et al., 1993; Suzuki et al., 1993). Thus, cell loss in these areas could have serious cognitive consequences. Hippocampal cells have been shown to be selectively vulnerable to many insults to the central nervous system which are associated with memory dysfunction (Auer and Siesjo, 1988). For example, stroke in humans and four-vessel occlusion models of ischemia in rodents cause substantial loss of CA1 pyramidal cells (Petito et al., 1987; Pulsinelli et al., 1982). CA3 pyramidal cells are vulnerable to temporal lobe epilepsy in humans, and chemically and electrically induced seizures in rats (Babb and Brown, 1991; Nevander et al, 1985; Olney et al., 1983). Furthermore, lateral fluid percussion causes the death of hippocampal hilar neurons in rodents (Lowenstein et al., 1992). Due to an essentially unidirectional information flow into and out of the hippocampus (Amaral and Witter., 1989), it has been suggested that loss of cells in any subfield would contribute to memory dysfunction.

In order to further understand the cause of spatial memory deficits following TBI, we have used a silver impregnation stain, in combination with cresyl violet staining, to examine the temporal and spatial pattern of cell death following controlled cortical impact injury in rats. These staining techniques revealed dystrophic cells in the hippocampus, entorhinal and piriform cortices, amygdala, thalamus and hypothalamus. Light microscope examination of semi-thin sections suggests that this cell death may be apoptotic in nature.

2.3) **Methods**

2.3.1) **Production of cortical impact brain injury**

A controlled cortical impact device was used to cause brain injury as previously described (Dash et al., 1995; Meany et al., 1994). All protocols were in compliance with NIH's *Guide for the Care and Use of Laboratory Animals* and approved by the Institutional Animal Care and Use Committee. Briefly, a total of 32 male Sprague-Dawley rats (Harlan Sprague Dawley, Indianapolis) were anesthetized with 4% isoflurane with a 2:1 N₂O/O₂ mixture. Following endotracheal intubation, rats were mechanically ventilated with a 2% isoflurane and 2:1 N₂O/O₂ mixture. Animals were mounted in a stereotaxic frame with their ventral surface facing down. Bilateral craniectomies (6.0 mm in diameter) were performed midway between the bregma and the lambda with the medial edges of the craniectomies 1 mm lateral to midline. Cortically impacted rats received a single, unilateral impact at 6 meters/sec, 2.5 mm deformation. Sham rats underwent identical surgical procedures but were not injured. Core body temperature was monitored continuously by a rectal thermistor probe and maintained at 37-38°C by use of an external probe-controlled heating pad. After injury, the scalp was sutured closed and the animal extubated to minimize the anesthetic effects on the acute neurological assessments.

2.3.2) **Acute neurological assessments**

A battery of tests that had been shown to be sensitive to varying magnitudes of brain injury in the rat were employed to confirm the injury magnitude (Dash et al., 1995; Hamm et al., 1992; Long et al., 1996). Assessments of simple nonpostural somatosensory

functions were conducted by recording the duration of suppression of a response to stimulation. The corneal reflex was evaluated by lightly touching the cornea with a cotton swab to elicit an eyeblink. The pinna reflex was measured by touching the ear canal with a wooden applicator. Assessments of simple postural somatomotor functions included measurements of the duration of suppression of flexion reflexes to stimulation. The assessment of the paw and tail flexion reflexes consisted of the gradual application of pressure on the contralateral hindpaw or tail until paw or tail withdrawal was noted. More complex, postural somatosensory function was assessed by recording the duration of suppression of the righting response. The righting response was defined as the animal's ability to right itself three times consecutively after being placed on its back. Statistical significance was determined using a Student's t-test and the mean duration of suppression for each reflex.

2.3.3) Tissue preparation

At the appropriate time points after injury, rats were anesthetized with sodium pentobarbital, and then transcardially perfused with 100 ml of 37°C saline with 1 unit/ml heparin followed by 150 ml of 37°C fixative [4% paraformaldehyde, 15% picric acid in phosphate-buffered saline (PBS)]. Brains from naive, sham injured and injured animals were removed and equilibrated in the fixative containing 30% sucrose at 4°C for 2 days. Fixed brains were then mounted in O.C.T. (Optimal cutting temperature, Miles Inc.) cryostat embedding medium. Approximately 100 coronal sections, 40-microns in thickness, spanning the entire hippocampus were cut from each brain on a cryostat.

Sections were placed in PBS in 24-well tissue culture plates, washed once with PBS, and stored at 4°C until use.

2.3.4) **Cresyl violet staining**

Visualization of the tissue sections was done by first mounting them on microscope slides, and then staining with a 2% cresyl violet solution (prepared in 0.1% acetic acid). Slices were rinsed in deionized water and destained in 1% acetic acid plus 10% ethanol. Slides were cover-slipped and photographed with a Nikon Axio-phot microscope using brightfield illumination, on Kodak 64T slide film.

2.3.5) **Silver staining**

Freely floating sections were stained by the silver impregnation protocol of Gallyas et al. with the modification described by Sloviter et al. (Gallyas et al., 1980; Gallyas and Zoltay., 1992; Sloviter et al., 1993). This staining protocol reliably stains only dystrophic neurons. Every eighth section was stained using this modified staining protocol. Briefly, sections were washed twice for 15 minutes in distilled H₂O in a 24-well plate. Slices were then incubated twice with 0.5 ml each of pretreatment solution (1:1 solution of 9% NaOH and 1.2% NH₄NO₃) for 10 minutes. Slices were incubated for 30 minutes in 0.5 ml of a silver impregnation solution (60 ml of a 9% w/v NaOH was combined with 40 ml of a 16% w/v NH₄NO₃, then 0.6 ml of a 50% AgNO₃ was added drop-wise while mixing). Following the incubation, the slices were washed two times in 1 ml of buffer (For 100 ml of wash solution, 0.1 ml of 1.2% NH₄NO₃, 0.5 gm anhydrous

NaCO₃ and 30 ml 95% ethanol was combined with water to 100 ml) for 10 minutes each wash. The signal was developed in 0.5 ml of buffer for one minute (for 100 ml of buffer, 0.1 ml of 1.2% NH₄NO₃, 0.05 gm citric acid, 1.5 ml 37% formalin, and 10 ml 95% ethanol was combined with H₂O to 100 ml). Stained sections were then transferred to PBS and soaked overnight at room temperature before mounting on glass slides. Argyrophilic neurons were visualized and photographed as described above.

2.3.6) **Semi-thin sections**

Semi-thin sections were prepared by first dehydrating mounted 40-micron slices stepwise in an ethanol series (10 min each step in 50%, 60%, 70%, 80%, 90%, 95%, 99% and 100%). Slices were then embedded in Epon 8-12, baked at 60°C overnight, then removed from the microscope slides. Epon embedded tissue was then further sectioned into 0.5 micron slices using a Beckman microtome. Cells were visualized by staining with a 1% solution of toluidine blue in 1% borax. Cells were photographed at a magnification of 100X as described above.

2.4) **Results**

2.4.1) **Neurologic responses**

A battery of acute neurological responses were measured immediately after the injury. The durations of suppression of both simple (corneal, pinna, paw flexion, tail pinch) and complex somatosensory (righting) functions were significantly different between sham and injured animals (Table 1). These injury related suppressions of

reflexes are consistent with previous reports using this injury paradigm (Dash et al 1995, Long et al 1996).

2.4.2) Time course of appearance of dystrophic dentate gyrus granule cells

Dystrophic cells are argyrophilic and therefore appear dark in comparison to normal cells when subjected to the silver impregnation staining method (Gallyas et al., 1980; Sloviter et al., 1993). In naive (n=4) and sham injured (n=4, at 24 hours) animals, a few random argyrophilic cells were observed throughout the entire brain (data not shown). However, these cells are probably vascular endothelial cells, which are normally argyrophilic. Figures 1A and 1B illustrate the presence of a large number of argyrophilic granule cells in the ipsilateral dentate gyrus, 6 hours postinjury (n=4). These dystrophic neurons appeared to be regionally localized in the dentate gyrus. The number of argyrophilic cells in the ipsilateral dentate gyrus appeared to be maximal by 24 hours postinjury (Fig 1C and 1D, n=8). Moreover, at two weeks postinjury (Fig 1E and 1F, n=8), we also detected the presence of a small number of argyrophilic neurons in five out of the eight animals examined. Dystrophic neurons were also detected, although less abundant, in the contralateral dentate gyrus of injured animals at the time points examined (data not shown).

2.4.3) Morphological examination of dystrophic dentate gyrus granule cells

In order to examine the morphologies of the argyrophilic cells in more detail, semi-thin sections (0.5 micron) from 24 hr postinjury animals were examined at 100X

magnification. Figure 2A shows the appearance of the granule cells distal to the dystrophic region. These cells have typical granule cell morphology including normal nuclei (Sloviter et al., 1993a). Normal granule cells (N) stain lightly with toluidine blue and have dispersed chromatin (Sloviter et al., 1993a). An occasional dystrophic cell (D) can be seen dispersed amongst the normal cells. In contrast to the normal cells, these cells appear shrunken with both the nucleus and the cytoplasm being darkly stained. Figure 2B shows the morphologies of the granule cells within the dystrophic area of the dentate gyrus as identified by the silver-impregnation staining. A large number of dystrophic cells can be seen in this region. The nucleus of these cells appears to have condensed chromatin. In addition, some cells were found to contain prominent spherical apoptotic bodies (A) as well as numerous vacuoles (V). These dystrophic cells are again intermingled with normal granule cells in this region.

2.4.4) Dystrophic cells in other brain regions 24 hours postinjury

Figure 3A shows the presence of dystrophic pyramidal cells in the CA3 and CA4 (hilar) subfields of the ipsilateral hippocampus. Some of these neurons possess dystrophic neurites which also appear darkly stained. Dystrophic cells were also observed in the CA1 region (data not shown). Figure 3B shows the presence of a large number of argyrophilic cells which are observed surrounding the site of contusion. The contusion site itself, which contains a large number of necrotic cells (appearing non-argyrophilic in this staining protocol) can be seen as the lighter stained region. Argyrophilic cells can also be seen in the thalamus (Fig 3C) and the hypothalamus (Fig 3D). A large group of

argyrophilic cells in the regions of the piriform and entorhinal cortices can be seen in figure 3E and 3F respectively.

2.4.5) Regional distribution of dystrophic cells

Figure 4 shows an illustration of the regional distribution of dystrophic cells compiled from eight animals at 24 hour postinjury. Dystrophic neurons are consistently seen in the CA1, CA3, dentate gyrus and hilar regions of the hippocampus (H) and were also found in the amygdala (A), thalamus (T), hypothalamus (HT), and piriform (P) and entorhinal (E) cortices. Dystrophic cells are observed both in the ipsilateral and contralateral brain regions.

2.4.6) Postinjury hippocampal cell loss

Several regions in the hippocampus were consistently identified as having dystrophic cells by the silver stain technique. To determine the extent of subsequent cell loss in these regions, cresyl violet staining of two-week postinjury brain sections was performed. Cell loss was observed as thinning of the neuronal cell layers of the hippocampus. Figures 5A and 5B show the CA3 regions from a two-week postoperative sham and injured animals. In injured animals, the CA3 region suffers from substantial loss of pyramidal cells. Figures 5C and 5D are representative photomicrographs of the CA1 regions from two-week sham and injured animals illustrating the thinning of this cell layer. Figures 5E and 5F show enlarged views of the dentate gyrus from sham and injured animals respectively. The region of the dentate gyrus shown corresponds to the area

containing the dystrophic neurons illustrated in Figures 1F-1J. Thinning of the granule cell layer can be seen in the injured animal.

2.5) Discussion

In this report, we present evidence to show that experimental TBI causes a delayed cell death in selective brain structures, secondary to the site of impact. This cell death appears to continue for at least two weeks resulting in a substantial cell loss from the affected regions. To our knowledge, this is the first description of such cell loss as a result of experimental cortical impact injury.

Using a modified silver staining technique, we show the presence of a large number of argyrophilic cells in the dentate gyrus, CA1 and CA3 subfields of the hippocampus of injured animals (Fig 4). Argyrophilic neurons were detected for up to two weeks postinjury. However, the argyrophilic neurons visualized at early time points following injury may persist for a week or two before being cleared and possibly contribute to the signal observed at later time points. Previous studies have shown that argyrophilic neurons are dystrophic and eventually die (Crain et al., 1988; Gruenthal et al., 1986; Sloviter et al., 1993a; Sloviter et al., 1993b; Warner et al., 1991). Consistent with this, we observed a marked cell loss in the dentate gyrus, CA1 and CA3 subfields of the hippocampus which contained dystrophic neurons (Fig 5). This study also shows the presence of dystrophic cells in the hilar region of the hippocampus, the amygdala, the entorhinal and piriform cortices, the thalamic and hypothalamic regions, and the cortex near the site of impact (Fig 4).

Neuronal loss following TBI can be broadly divided into three categories: 1) cell death due to physical damage as a result of trauma, 2) necrotic cell death by release of excessive excitatory neurotransmitters such as glutamate, and 3) the delayed cell death we are reporting in this study. The first two types of cell death happen soon after trauma and may not provide an adequate time window for clinical intervention. However, the third type of cell death can be potentially prevented by therapeutic intervention. Therefore, an understanding of the mechanism(s) underlying this delayed cell loss would be of great importance. Light microscope examination of these cells suggests that they possess the features of apoptosis (Fig 2B). For example, some of these cells contained apoptotic bodies and vacuoles. Other dystrophic cells appeared shrunken with condensed chromatin. These cells may represent different stages of apoptosis. In the accompanying article we present cellular and molecular evidence to support this observation. Several studies have shown that the apoptotic death of CNS neurons can result from the loss of target derived trophic factors or by prolonged exposure to low levels of excitatory neurotransmitters (Ankarcrona et al., 1995; Deckwerth and Johnson, 1993). The cell death we observed may be the result of similar mechanisms.

Two widely used rodent models of TBI, fluid percussion and cortical impact, each reproducing various aspects of human TBI including cell loss and axonal injury, have been developed (Dixon and Hayes, 1996; Gennarelli, 1994). For example, death of hilar neurons has been observed following a lateral fluid percussion model of TBI (Hicks et al., 1993; Lowenstein et al., 1992). Loss of CA1 and CA3 cells has been reported following a cortical impact injury with unilateral craniectomy (Goodman et al., 1994). Cortical

impact injury with bilateral craniectomies has been reported to cause diffuse axonal injury which is a hallmark of human TBI (Meany et al., 1994). This is thought to be caused by lateral movement of the brain in response to the impact. The wide distribution of dystrophic cells we detect following cortical impact injury may be accounted for by the use of the bilateral craniectomy we employed in this study. Moreover, the spatial distribution of these cells with respect to the direction of the impact (Fig 4) suggests that impact angle may contribute to the observed localized distribution. Future experiments utilizing different impact angles may help verify this hypothesis.

Previously, we have reported that cortical impact injury with bilateral craniectomy causes deficits in spatial learning and memory using a Morris water maze task (Dash et al., 1995; Long et al., 1996). The performance in this task is thought to require both hippocampal and entorhinal cortical function (Morris et al., 1982). Marked cell loss was detected in the dentate gyrus, CA1 and CA3 regions. It is possible that the cell loss in these regions could alter neuronal signalling and may contribute to the observed spatial memory deficits. It is difficult to ascertain from this study whether dentate granule cells, CA3 or CA1 cells are more important with respect to posttraumatic memory dysfunction. It has been suggested that loss of cells in any subfields of the hippocampus would contribute to spatial memory dysfunction (Amaral and Witter, 1989). Moreover, since the hippocampus receives inputs from various parts of brain and is involved in integration of information, loss of these cells also could contribute to other cognitive impairments. Furthermore, cell loss in the amygdala, piriform cortex, thalamus and hypothalamus following cortical impact injury suggests other behavioral deficits might occur following

TBI. We are currently performing behavioral experiments to evaluate the functions of the dystrophic regions presented in this report following cortical impact injury in rats.

Figure 1) Temporal pattern of silver staining of hippocampal dentate gyrus granule cells. Representative photomicrographs showing 5X magnification overview of the ipsilateral hippocampal region, as well as an enlargement (40X) of each dentate gyrus inner blade cell layer. Dystrophic neurons appear dark in the silver impregnation staining. A-B: 6 hours postinjury, C-D: 24 hours postinjury, E-F: 2 weeks postinjury.

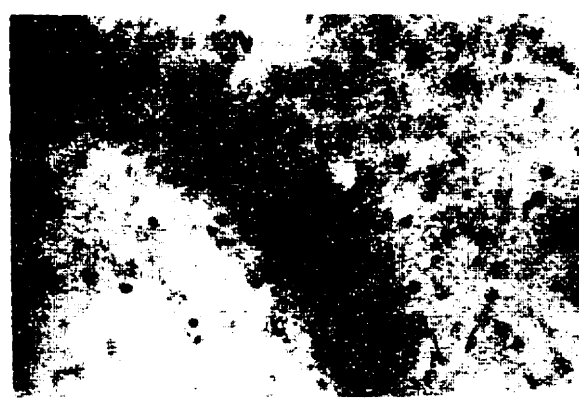
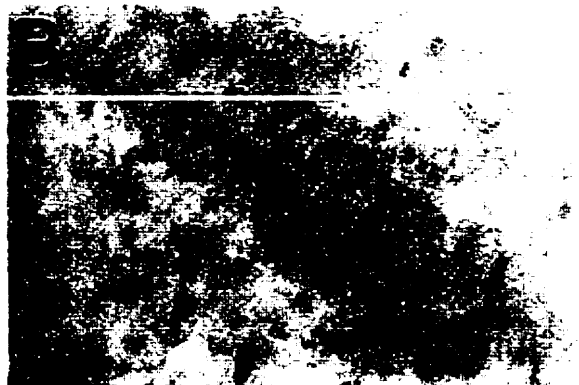


Figure 2) Morphology of dentate gyrus granule cells. 0.5-micron thick sections were prepared from the dentate gyrus ipsilateral to the site of impact from 24-hour injured animals . Slices were stained with toluidine blue and the inner blade of the dentate gyrus was photographed at 100X magnification as described in the Materials and Methods section. A: Photomicrograph of a section showing the morphology of the granule cells distal to the dystrophic region. Normal (N) and dystrophic (D) cells are shown. B: Photomicrograph taken from the core of the dystrophic region. Apoptotic bodies (A) and vacuoles (V) can be seen. Other dystrophic cells (D) appear shrunken with condensed chromatin.



Figure 3) Presence of dystrophic cells in selected brain regions. Representative pictures showing the location of dystrophic neurons in 24 hr postinjury animals. A: CA3 region of the ipsilateral hippocampus. Dystrophic pyramidal cells as well as dystrophic neurites can be seen. B: Cortex, below the contusion site. The necrotic cells at the site of impact, seen at the top of this photograph, stain lightly with this protocol. C: Thalamic region, possibly the ventral posterolateral thalamic nucleus. D: Hypothalamus. E: Piriform cortex region. F: Entorhinal cortex region. Arrows indicate argyrophilic cells.

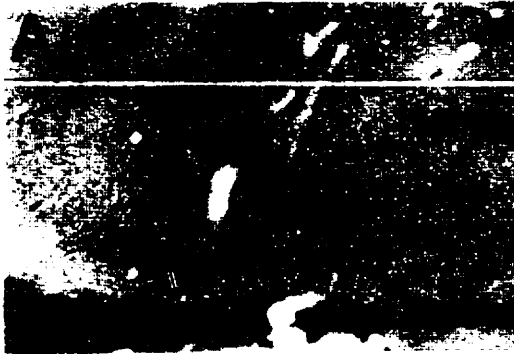
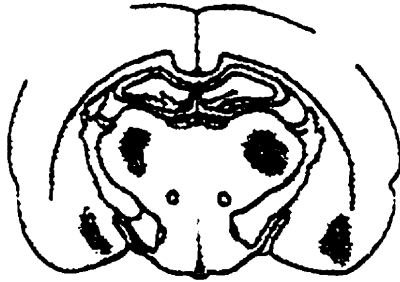
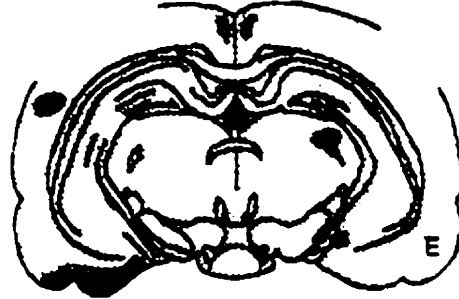


Figure 4) Summary figures showing the spatial distribution of the dystrophic cells. Illustration of five representative coronal sections indicating dystrophic neurons in different brain regions. The data used to map the distribution of dystrophic cells were obtained from a total of eight animals at 24 hour postinjury. Color coding represents the number of animals which showed dystrophic cells in that region. Abbreviations: A - amygdala, E - entorhinal cortex; H - Hippocampus; HT - hypothalamus; P - piriform cortex; T - Thalamus. Sections correspond to A: Bregma -2.56 mm, B: Bregma -3.30 mm, C: Bregma -3.60 mm, D: Bregma -4.80 mm, E: Bregma -6.30 mm.

A Bregma -2.6



D Bregma -4.8



B Bregma -3.3



E Bregma -6.3



C Bregma -3.6

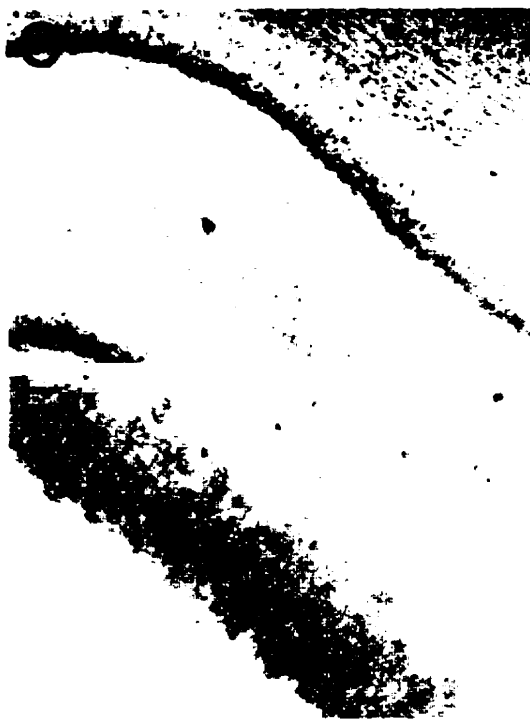
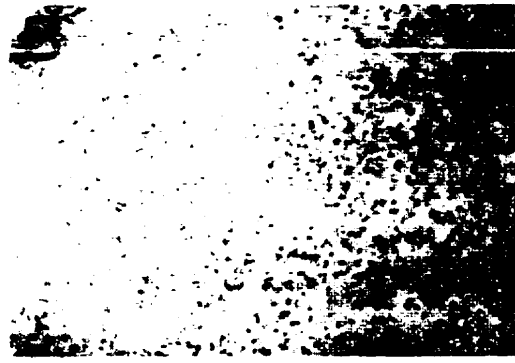


1 2 4 6 8



Figure 5) Cell loss in ipsilateral hippocampal subfields two weeks postinjury.

Photomicrographs of representative cresyl violet stained sections from sham and injured animals. Cell loss can be seen as thinning of the neuronal layers. A: CA3 subfield from a sham-operated animal. B: CA3 region from a 2-week postinjury animal. C: CA1 cell layer from a sham. D: CA1 subfield of an injured animal. The arrow indicates the region of pyramidal cell loss. E: Granule cell layer from the inner blade of the dentate gyrus from a sham animal. F: Inner blade of the ipsilateral dentate gyrus from a 2-week injured animal. This region corresponds to the region of the inner blade which contained dystrophic granule cells.



3) Apoptotic characteristics of hippocampal cell death following traumatic brain injury.

3.0) Foreword

Having identified neuropathological effects distal to the site of injury following TBI, the biochemical nature of this degeneration was investigated. Cells die by two mechanisms, necrosis and apoptosis. Necrosis is due to a degenerative increase in cellular disorder, whereas apoptosis is a distinct cellular function, often gene expression dependent, that is triggered by extracellular signals. Following cortical contusion, our silver stain analysis identified dystrophic neurons in the hippocampus. The cell death observed in dentate gyrus granule cells was then further characterized using several methods: light microscopic and electron microscopic analysis demonstrated the presence of chromatin condensation and vacuole formation; *in situ* labelling demonstrated the induction of DNA fragmentation; and DNA laddering was demonstrated using gel electrophoresis. In addition to these hallmarks of apoptotic cell death, necrotic characteristics were also present. This work was summarized in the paper "*Apoptotic morphologies of dentate gyrus granule cells following experimental cortical impact injury in rats: Possible role in spatial memory deficits.*" Colicos, M.A., Dash, P.K. (1996) Brain Research 739:120-131, and is presented below as published.

3.1) Summary

Loss of hippocampal neurons as a result of traumatic brain injury (TBI) is thought to contribute to the observed spatial memory deficits. Using a rodent model of

experimental brain injury, we have examined the nature of hippocampal cell death following TBI. Light microscope examination of stained sections showed the presence of a large number of hyperchromatic and dystrophic neurons in the dentate gyrus of the hippocampus. These cells appeared to be undergoing nuclear condensation. Electron microscope examination demonstrated the presence of cell shrinkage, condensed chromatin, nuclear segmentation, and cytoplasmic vacuolization. Detection of a DNA ladder and in situ labeling (TUNEL) were also consistent with the process of apoptosis. However, in some dystrophic neurons these morphologies were also accompanied by the presence of swollen mitochondria and a lack of distinctive rough endoplasmic reticulum which are typically associated with necrosis. These findings show that cortical impact injury produces cell death in the hippocampus which has both apoptotic and necrotic features.

3.2) Introduction

Traumatic brain injury (TBI) in humans produces both retrograde (memory of events preceding the trauma) and anterograde (memory of posttraumatic events) amnesia (Boll, 1982; Squire and Alvarez, 1995). Retrograde amnesia is graded such that recent memories are lost more easily than remote memories. Anterograde amnesia can sometimes be ungraded and extensive depending on the severity of the injury. Unfortunately, no effective therapies for human head injury are available. Animal models for TBI have been developed in an attempt to unravel the cellular and biochemical mechanisms underlying memory deficits in human head injury (Dixon and Hayes, 1996;

Gennarelli, 1994; McIntosh et al., 1989). Cortical impact injury, a widely employed model of TBI, produces spatial learning and memory deficits in rats, similar to those seen in human traumatic brain injury (TBI) (Dash et al., 1996; Dixon et al., 1991; Goodman et al., 1994; Hamm et al., 1992; Long et al., 1996; Meany et al., 1994; Sutton et al., 1993). It is thought that hippocampal cell death may contribute to these deficits (Goodman et al., 1994; Kotapka et al., 1991; Lowenstein et al., 1992). Neuronal loss following TBI can be broadly divided into three categories: 1) cell death due to physical damage as a result of trauma, 2) necrotic cell death by release of excessive excitatory neurotransmitter such as glutamate, and 3) delayed cell death. Using a modified silver impregnation technique, we have identified delayed cell loss in the dentate gyrus, CA1, CA3 and hilar regions of the hippocampus in injured animals (Colicos et al., 1996a). Preliminary light microscope examination suggested that these dystrophic cells may be dying by apoptosis.

Apoptosis is a form of active cell death process occurring during nervous system maturation (Hamburger and Oppenheim, 1982). It is a physiological process of cell elimination, during which, in contrast to necrosis, there is no induction of an inflammatory response (Duvall et al., 1985; Gerschenson and Rotello, 1992). The morphological determinants of apoptosis begin with cell shrinkage, condensation of the chromatin, segmentation of the nucleus, and fragmentation of the chromosomal DNA (Arends and Wyllie, 1991; Duvall and Wyllie, 1986; Earshaw, 1986; Kerr et al., 1972; Wyllie, 1980). The cell plasma membrane then becomes convoluted, cytoplasmic vacuolization occurs, and the cellular fragments are packaged into membrane enclosed vesicles. These vesicles, known as apoptotic bodies, express surface markers that cause

them to be phagocytosed by neighboring cells (Fadok et al., 1992; Wyllie, 1980). During apoptosis, intracellular organelles such as mitochondria and rough endoplasmic reticulum (RER) remain intact (Ankarcrona et al., 1995; Cossarizza et al., 1994; Newmeyer et al., 1994; Watt et al., 1994; Weis et al., 1995). In comparison to necrosis, apoptosis appears to be a slow process (Bonfoco et al., 1995) and often depends on gene expression and protein synthesis (Deckwerth and Johnson, 1993; Ratan et al., 1994). Recent *in vitro* studies have shown that neurons can be induced to undergo apoptosis by treatment with the β amyloid peptide as well as with intracellular calcium altering treatments such as glutamate (Bonfoco et al., 1995; Deckwerth and Johnson, 1993; Loo et al., 1993). Although controversial, the role of apoptosis in neuropathological conditions is beginning to emerge. For example, DNA fragmentation has been reported to accompany neuronal death in models of ischemia and epilepsy (Charriaut-Marlangue et al., 1996; Charriaut-Marlangue et al., 1995; Li et al., 1995; MacManus et al., 1993; Nitatori et al., 1995; Pollard et al., 1994). However, neither apoptotic cell death nor its role in memory dysfunction has been examined following TBI.

Apoptosis and necrosis appear to be a continuum of cell death processes (Ankarcrona et al., 1995; Choi, 1995). Many treatments that induce apoptosis at low levels can cause necrosis at higher concentrations (Bonfoco et al., 1995; Choi, 1995). For example, exposure of cortical neurons to low concentrations of NMDA induces apoptotic cell death (Ankarcrona et al., 1995; Choi, 1995). In contrast, intense exposure to high concentrations of NMDA induces necrotic cell damage (Bonfoco et al., 1995; Choi, 1995). This data suggests that the intensity and duration of insult may direct the ensuing

pathways towards either necrotic or apoptotic neuronal death (Choi, 1995). In addition, there are findings that suggest that intermediate levels of insults can produce both necrotic and apoptotic features (Charriaut-Marlangue et al., 1995; Gwag et al., 1994).

In this report, we have investigated the morphology of dentate gyrus granule cells following controlled cortical impact injury in rats. These neurons possess the morphological features of apoptosis. DNA laddering and *in situ* terminal deoxy transferase-mediated dUTP nick end labeling (TUNEL-staining) were also consistent with apoptosis. However, some of these dystrophic cells showed the presence of swollen mitochondria and a lack of well defined rough endoplasmic reticulum, morphological features usually associated with necrosis.

3.3) **Methods**

3.3.1) **Production of cortical impact brain injury**

Lateral controlled cortical impact injury in rats was produced essentially as described previously (Dash et al., 1995; Meaney et al., 1994). All protocols were in compliance with NIH's *Guide for the Care and Use of Laboratory Animals* and approved by the Institutional Animal Care and Use Committee. Cortically impacted rats received a single impact at 6 meters/sec, 2.5 mm deformation. Sham rats underwent identical surgical procedures but were not impacted. Core body temperature was monitored continuously by a rectal thermistor probe and maintained at 37-38°C using a heating pad. After injury, the scalp was sutured closed and the animal extubated.

3.3.2) Tissue preparation

24-hr postinjury rats were anesthetized with sodium pentobarbital. After animals failed to respond to tail and foot pinch, they were transcardially perfused with 100 ml of 37°C saline with 1 unit/ml heparin. This was followed by perfusion with 150 ml of 37°C freshly prepared fixative [4% paraformaldehyde, 15% picric acid in phosphate-buffered saline (PBS)]. Brains from naive, sham injured and injured animals were removed and equilibrated in the fixative containing 30% sucrose at 4°C for 2 days. Fixed brains were then mounted in O.C.T. (Optimal cutting temperature, Miles Inc., Elkhart, IN) cryostat embedding medium. 40-micron thick coronal sections, spanning the entire hippocampus were cut from each brain on a cryostat. Sections were placed in PBS in 24-well tissue culture plates, washed once with PBS, and stored at 4°C until use.

3.3.3) Cresyl violet staining

Sections to be stained by cresyl violet were first mounted on microscope slides, and then stained with a 2% cresyl violet solution (prepared in 0.1% acetic acid). Slices were rinsed in deionized water and destained in 1% acetic acid plus 10% ethanol. Some slices were counter-stained using an antibody raised against the 200 kDa neurofilament protein (Sigma, St. Louis, MO) and an ABC kit (Vector, Burlingame, CA) as recommended by the vendor. Slides were cover-slipped and photographed with a Nikon Axio-phot microscope using brightfield illumination, on Kodak 64T slide film.

3.3.4) **Silver staining**

Freely floating sections were stained by the silver impregnation protocol of Gallyas et al. with the modification described by Sloviter et al. (Gallyas et al., 1980; Sloviter et al., 1993). Slices were mounted on microscope slides, visualized, and photographed as described above.

3.3.5) **Hoechst staining**

Slices were briefly rinsed in PBS and incubated in a 2 µg/ml solution of Hoechst stain (# 33342 prepared in PBS) for 10 min at room temperature. Slices were then washed twice for 5 min each in PBS, mounted on microscope slides and cover-slipped for visualization. Fluorescence was detected using an Axio-phot microscope with a broad range UV filter.

3.3.6) **Semi-thin sectioning**

Semi-thin sections were prepared from Epon-embedded slices. Slices were first dehydrated stepwise in an ethanol series (10 min each in 50%, 60%, 70%, 80%, 90%, 95%, 99% and 100% ethanol) and then embedded in Epon 8-12. Semi-thin sections (0.5 micron) were prepared using a Beckman microtome. Cells were visualized by staining with a 1% solution of toluidine blue in 1% borax. Cells were photographed at a magnification of 100X as described above.

3.3.7) DNA extraction and gel electrophoresis

At the appropriate time points, brains from injured and control animals were quickly removed and hippocampi were dissected in oxygenated ice-cold artificial cerebrospinal fluid (CSF: 10 mM HEPES pH 7.2, 1.3 mM NaH_2PO_4 , 3 mM KCl, 124 mM NaCl, 10 mM dextrose, 26 mM NaHCO_3 , 2 mM CaCl_2 and 2 mM MgCl_2). Sample preparation was carried out at 4°C. The tissues were separately homogenized (10 strokes) in five volumes of a buffer containing 15 mM HEPES pH 7.2, 0.25 M sucrose, 60 mM KCl, 10 mM NaCl, plus protease inhibitors (1 mM EGTA, 5 mM EDTA, and 1 mM PMSF) in a dounce homogenizer using a loose pestle. The cells were then pelleted at 2000 x g for 10 minutes. To lyse the cells, the pelleted material was suspended in 1.0 ml of 5 mM Tris pH 8.0, 10 mM EDTA, 0.5% Triton X-100. The resuspended cells were left on ice for 15 min followed by centrifugation at 13,000 x g for 20 min at 4°C. The supernatant solution was treated with 100 µg/ml of RNase A for 1 hr at 37°C. This was followed by the addition of freshly prepared proteinase K and SDS to final concentrations of 200 µg/ml and 1% respectively. The resulting solution was incubated at 50°C for 1 hr. The cytoplasmic DNA was extracted with equal volumes of Tris saturated phenol, followed by phenol/chloroform and chloroform. The DNA was precipitated with 2.5 volumes of ethanol. The DNA samples were suspended in 10 µl of TE (10 mM Tris pH 8.0, 1 mM EDTA) buffer, incubated at 75°C for 5 min and loaded on a 1.5% agarose gel. At the completion of electrophoresis, the gels were stained with ethidium bromide and photographed.

3.3.8) TUNEL staining

Apoptosis is associated with fragmentation of chromatin into a characteristic 180-200 base pair DNA ladder (Brown et al., 1993; Wyllie, 1980). The DNA fragments can be detected by reaction with terminal deoxy transferase which incorporates nucleotides into the free 3'-ends of DNA molecules (Wood et al., 1993). Since cells undergoing apoptosis have large numbers of DNA fragments, the transferase incorporates more nucleotides into these cells. TUNEL detection of DNA fragmentation utilizes digoxigenin-11-DUTP (Boehringer Mannheim) in a terminal transferase extension reaction. Forty-micron thick slices, adjacent to those used for silver impregnation staining, were placed in 200 μ l of tailing solution (40 μ l 5X buffer (supplied with enzyme), 10 μ l dUTP DIG, 10 μ l 10mM dATP, 10 μ l TdT, 130 μ l H₂O), and incubated at room temperature for 30 minutes. Slices were then washed twice in PBS for one hour each at room temperature. The slices were then incubated with an anti-digoxigenin-horseradish peroxidase conjugated secondary antibody (Boehringer Mannheim) as recommended by the vendor. The binding was detected by use of a DAB kit (Vector). The slices were counter-stained lightly with hematoxylin (Sigma). Sections were mounted on glass slides, and photographed at low (5X and 40X) magnifications. For semi-thin sections, slices were embedded in epon as described above and further sliced to 0.5 microns, mounted and photographed at 100X.

3.3.9) Electron microscopy

Animals were perfused for electron microscope analysis by the same protocol as

described under *Tissue preparation*, with the exception of the fixative (2.5% glutaraldehyde, 2% paraformaldehyde in PBS). Fixed brains were removed and cut into approximately 1 mm coronal sections using a Jacobowitz brain slicer. Tissue sections spatially equivalent to those identified as containing hyperchromatic dystrophic cells as detected by cell staining were used. This tissue was then postfixed in 2% OsO₄ overnight. The sections were dehydrated in ethanol series. The sections were then mounted in Epon 8-12, cut into 60-90 nm sections using a Beckman microtome, and mounted on grids. The slices were stained for 30 min in 2% uranyl acetate, and examined with a JOEL 100CX EM using an accelerating voltage of 80 kV and a magnification of 10,000X.

3.4) Results

3.41) Light microscope analysis of regions of cell death

To look for delayed cell death in the hippocampus, tissue from 24 hour (n=6) postinjury animals, as well as from naive (n=4) and sham (n=4) injured animals, were first examined using several staining techniques. Tissue sections 40 microns thick were examined spanning the entire hippocampus. Figure 1A shows a cresyl violet stained section obtained from a sham animal and figure 1B from an injured animal. At this 24 hr time point, no overt loss of hippocampal neuronal cells can be detected. Moreover, no differences were detected between naive and sham hippocampi (data not shown). To assist in the identification of dystrophic cells, silver impregnation staining was performed. Dystrophic neurons stain dark using this silver impregnation technique. Figure 1C shows a section of the ipsilateral hippocampus adjacent to the section shown in figure 1B. As

observed previously, dystrophic neurons can be seen in the dentate gyrus, CA1, CA3 and hilar subfields (Colicos et al., 1996a). A high magnification photomicrograph of the inner blade of the dentate gyrus (box in figure 1C) is shown in figure 1D. Darkly stained granule cells can be identified intermingled with normal cells. Figure 1E shows an equivalent cresyl violet stained section, counterstained with an antibody to the neurofilament 200 kDa protein. With this technique, small, dense, hyperchromatic cells can be seen. To better visualize the nucleus, Hoechst 33342 stain was also employed. The appearance of both normal and the hyperchromatic nuclei can be seen in figure 1F.

In order to examine the morphology of the hyperchromatic cells in more detail, semi-thin sections (0.5 micron) of epon embedded tissue from injured animals were examined at 100X magnification. Figure 2 illustrates the cellular morphology of the inner blade dentate gyrus granule cell layer as visualized by toluidine blue stain. The region shown in figure 2A corresponds to the dystrophic region shown in the box in Fig 1C. Dystrophic cells located in this region appear shrunken with both the nucleus and cytoplasm being darkly stained. The nuclei of these cells contain multiple clumps of chromatin. In contrast, the normal granule cells in this region stain lightly with toluidine blue and have dispersed chromatin. Figure 2B shows a region of the dentate gyrus immediately adjacent to the boxed area of figure 1C. This region contained predominately normal granule cells. A few cells, however, contain prominent spherical apoptotic bodies, and numerous vacuoles. The morphology of the hyperchromatic cells was further investigated by electron microscopy.

3.42) Electron microscope study of chromatin condensation and vacuole formation in dentate gyrus granule cells

Figure 3A is an electronmicrograph illustrating a morphologically normal granule cell taken from a 24 hr postinjury animal. Normal granule cell nuclei possess diffuse, flocculent chromatin, with some minor clumping (Sloviter et al., 1993). Figure 3B and 3C show electronmicrographs of dystrophic granule cells from 24 hour postinjury tissue. Figure 3B illustrates a granule cell undergoing the early stages of nuclear condensation, with chromatin clumping occurring at the nuclear membrane. At this early stage of nuclear condensation, axio-somatic synapses can still be seen in some cells (Figure 3B-insert). The synapses were identified by the presence of postsynaptic densities. Morphologically normal cells are found immediately adjacent to the dying neurons. Figure 3C shows the nucleus of a granule cell undergoing segmentation. At this stage, formation of vacuoles (V) can be seen.

3.43) Mitochondrial and rough endoplasmic reticulum (RER) morphology

Apoptosis is an active process which often requires gene expression and protein synthesis (Deckwerth and Johnson, 1993; Ratan et al., 1994; Wyllie et al., 1984). Consistent with this, cells undergoing the early stages of apoptosis have been reported to have morphologically normal mitochondria and rough endoplasmic reticulum and maintain mitochondrial membrane potential (Ankarcona et al., 1995; Newmeyer et al., 1994). However, at late stages of degeneration, the function of these structures has been reported to be impaired (Cossarizza et al., 1994; Gerschenson et al., 1992; McIntosh et al.,

1989; Sloviter et al., 1993; Weis et al., 1995). Using the electron microscope, we examined the morphology of the mitochondria and RER in normal and in dystrophic granule cells. Figure 4A shows the mitochondria (M) and RER in a normal granule cell (also shown in Fig 3A). The mitochondria appear normal with discernable cristae while the RER contain numerous polyribosomes. A dystrophic granule cell which appears to be at an early stage of nuclear segmentation is shown in figure 4B. The condensed chromatin in this cell is localized to the nuclear membrane. The presence of morphologically normal mitochondria and RER can still be seen in this neuron. Figure 4C shows the morphology of a dystrophic granule cell with condensed chromatin, which, rather than being localized at the nuclear membrane appears to be distributed. In this cell, the mitochondria are swollen and the RER structure is not clearly visible.

3.44) *In situ* analysis of DNA fragmentation

In order to investigate the biochemical correlates of apoptotic cell death, DNA fragmentation analyses were performed (Batistatou and Greene, 1991; Brown et al., 1993; Wyllie et al., 1981). Figure 4A shows a photograph of an ethidium bromide-stained agarose gel. Hippocampal cytoplasmic DNA extracts were prepared and electrophoresed as described in the Materials and Methods Section. The hippocampal extract from a control animal did not show any detectable laddering (lane 1). Lanes 2 and 3 show the cytoplasmic DNA extracted from the contralateral and ipsilateral hippocampi respectively, from a 24 hr postinjury animal. A characteristic ladder can be clearly seen in the ipsilateral sample (lane 3). Although much less intense, a ladder is present in the

contralateral sample. By 72 hrs postinjury, the ladder in the ipsilateral hippocampal sample was much less intense than the 24 hr samples.

Figure 4B shows TUNEL staining of a slice from the region of the dentate gyrus containing the hyperchromatic cells. This stain most intensely labels cells which contain a large number of free 3'-OH DNA ends. Figure 4C shows a high magnification picture of a semi-thin section taken from the tissue shown in figure 4B. The presence of dark brown DAB stain can be seen in the cytoplasm and collected around the nuclear membrane.

3.5) Discussion

In this study, we have examined the morphological features of dentate gyrus granule cells following controlled cortical impact brain injury. The dystrophic cells, as identified by silver impregnation, cresyl violet, and Hoechst staining, appear shrunken, and have condensed nuclei and chromatin. EM microscope examination showed apoptotic morphology including the association of condensed chromatin to the nuclear membrane and segmentation of nuclei. DNA fragmentation was demonstrated by the presence of a characteristic ladder and was corroborated by positive TUNEL staining.

Light microscope examination of cresyl violet, silver impregnated, and Hoechst stained sections revealed the presence of a number of dystrophic neurons in the inner blade of the dentate gyrus of injured animals. When semi-thin sections of this region were examined, the dystrophic cells were found to be hyperchromatic and shrunken. Flanking the dystrophic region, a few distinctly apoptotic cells were observed. These

cells contained visible apoptotic bodies and vacuoles.

The nuclear events of apoptosis begin with the chromatin condensing into large clumps (Duvall and Wyllie, 1986; Earnshaw, 1986; Kerr et al., 1972; Wyllie et al., 1981). These clumps are localized to the nuclear envelope (Earnshaw, 1986). The nuclear pores redistribute by sliding away from the surface of the condensed chromatin and accumulate between them (Lazebnik et al., 1993). Subsequently, the nuclear segmentation occurs. In order to determine if the hyperchromatic neurons we observed were dying by apoptotic processes, we investigated some of the key morphological events. Granule cells undergoing apoptosis following TBI had their condensed chromatin appended to the nuclear periphery and show nuclear segmentation (Fig 4B). In some cells, discontinuities in the nuclear membrane can be seen (data not shown) which could be due to accumulation of nuclear pores. Other characteristic features of apoptosis such as vacuole formation, intact rough endoplasmic reticulum, and normal mitochondria were detected in these apoptotic granule cells. However, the number of mitochondria appeared to be less than in normal cells. This could be due to our inability to unequivocally identify mitochondria in these electron dense, shrunken cells.

DNA laddering and TUNEL staining were utilized to examine a biochemical correlate of apoptosis (Batistaton and Greene, 1991; Wyllie et al., 1984). Using the hippocampal cytoplasmic DNA extracts, we detected a characteristic DNA ladder in samples obtained from injured animals. The intensity of this ladder was maximal at 24 hr postinjury in the ipsilateral hippocampal sample. This observation is consistent with our previous finding that dystrophic neurons are more abundant in the ipsilateral as compared

to the contralateral hippocampus at this time point (Colicos et al., 1996a). It has been recently reported that there is more than one endonuclease functioning during apoptosis, one producing 50 and 300 kb fragments (Walker et al., 1994), and a second producing the 180-200 bp internucleosomal fragments (Cain et al., 1994). Although no direct activity measurements were made, the presence of a 180 bp ladder suggests that both nuclease activities are present (Brown et al., 1993; Earnshaw, 1986). Consistent with this, the labelling of DNA in the cytoplasm (Figure 5C) using TUNEL staining suggests that the nucleosome fragments generated are small enough to leak out of the nucleus. TUNEL staining can also potentially label necrotic nuclei, in that the non-specific degradation of the chromatin would produce a similar increase in 3'-OH groups. However, degradation of the DNA during necrosis is rapid and is not likely to contribute to the labelling reactions at the delayed time points we examined (Bonfoco et al., 1995; Gerschenson and Rotello, 1992). Moreover, in our hands, necrotic cells at the site of injury in the cortex did not show strong positive TUNEL staining.

Apoptosis occurs in two physiological stages. Following a signal, which may be either intrinsic or extrinsic to the cell, the cell enters a committed phase (Earnshaw, 1986). This is followed by an execution phase which is autonomously carried out by the cell. The known morphological features of apoptosis arise during this phase. Depending on the cell type and the surrounding environment, the durations of the committed and execution phases may vary. This can be further complicated by the coexistence of cells, some with necrotic, others with apoptotic features, making it difficult to determine the prominent mechanism of cell death. The EM photomicrograph of the granule cell shown

in Figure 4C appears to have condensed chromatin, an apoptotic morphology, and swollen mitochondria, a morphology typical to necrosis. Several possible mechanisms could explain this combination of morphologies. First, it has been reported that the same insult can elicit either necrosis or apoptosis (Ankarcrona et al., 1995; Choi, 1995). This phenomenon has been observed in several cell types including neurons. For example, cultured neurons exposed to glutamate or NMDA can show the morphological features of both apoptosis and necrosis (Ankarcrona et al., 1995; Bonfoco et al., 1995). Therefore, it is possible that a single insult, depending on the intensity and duration, may trigger apoptosis and necrosis simultaneously. Second, it is possible that following TBI some cells receive a signal (either intrinsic or extrinsic) to enter the committed phase of apoptosis and begin the execution phase as observed by cell shrinkage and condensed chromatin. However, subsequent to this, a secondary insult results in the necrotic morphologies we observed. This is consistent with the reports that following TBI calcium continues to accumulate for up to 48 hrs after the injury (Fineman et al., 1993). Thus, cells may initially begin an apoptotic process, but as calcium continues to accumulate, become necrotic. Finally, it is possible that the duration of the execution phase was too long allowing secondary necrosis to eliminate the cell (Catchpoole and Stewart, 1993). Future experiments may help to distinguish between these possibilities.

The injury paradigm utilized in this study has been shown to produce deficits in spatial learning and memory (Dash et al., 1995; Long et al., 1996). It is thought that hippocampal cell death may contribute to these deficits (Goodman et al., 1994; Kotapka et al., 1991). Our previous results showed that the protracted, delayed cell death results in a

significant cell loss from the hippocampus (Colicos et al., 1996a). The data presented in this study indicate that the dystrophic neurons in the dentate gyrus die in part by the process of apoptosis. The morphologies of the dystrophic cells identified in other brain regions have not yet been examined. Identification of the mechanisms of this delayed apoptotic cell death will allow us to develop strategies for therapeutic intervention to protect against the cell death and potentially the spatial memory deficits seen following brain injury.

Figure 1) Histological examination of 24 hr postinjury ipsilateral dentate gyrus granule cells. A: Representative photomicrograph of a cresyl violet stained hippocampal section taken from a sham-operated animal. B: Representative cresyl violet stained section of the hippocampus from a 24 hr injured animal. No overt differences in the neuronal cell layers were seen between the sham and injured animals. C: Silver impregnation stained section of an adjacent slice to that shown in figure 1 B. Dystrophic cells can be seen as darkly stained using this technique. Box indicates dystrophic region shown in D-F. D: High magnification photomicrograph of the inner blade of the dentate gyrus from a silver stained section. Dystrophic cells can be seen intermingled with normal granule cells. E: High magnification photomicrograph of a cresyl violet stained section counterstained with an antibody to the 200 kDa neurofilament protein. Using this protocol, hyperchromatic cells are distinguishable from normal cells. F: Photomicrograph of a Hoechst stained slice showing the nuclear condensation occurring in the dystrophic cells.

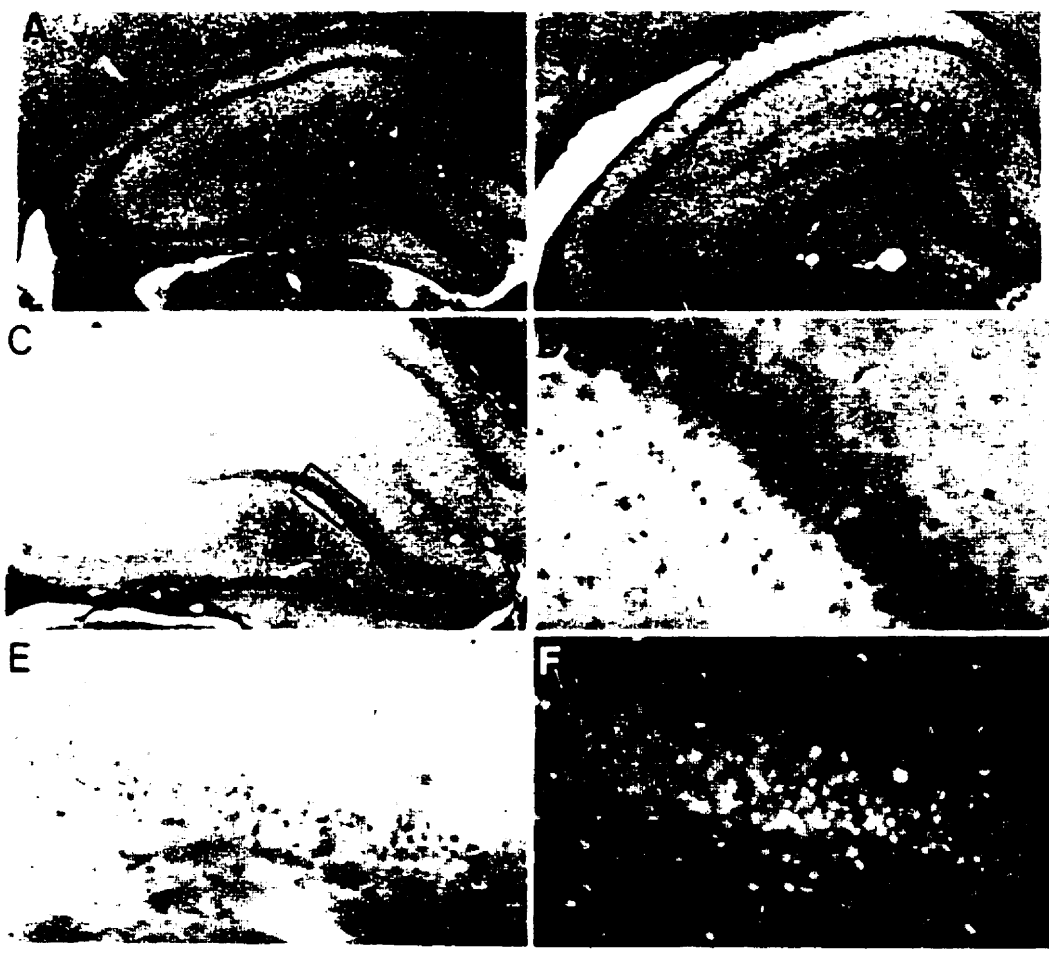


Figure 2) High magnification light microscope analysis of dentate gyrus neuronal cell layer. Semi-thin slices (0.5 microns in thickness) were stained with toluidine blue and photographed at 100X magnification. A: Photomicrograph of a section taken from within the boxed region illustrated in figure 1C. The figure shows the morphology of the granule cells within this dystrophic region. Normal (N) and dystrophic (D) cells are shown. B: Photomicrograph taken of a section of the inner blade flanking the boxed area shown in figure 1C. The cells in this region are predominately normal. A few cells containing apoptotic bodies (A) and vacuoles (V) can be seen.

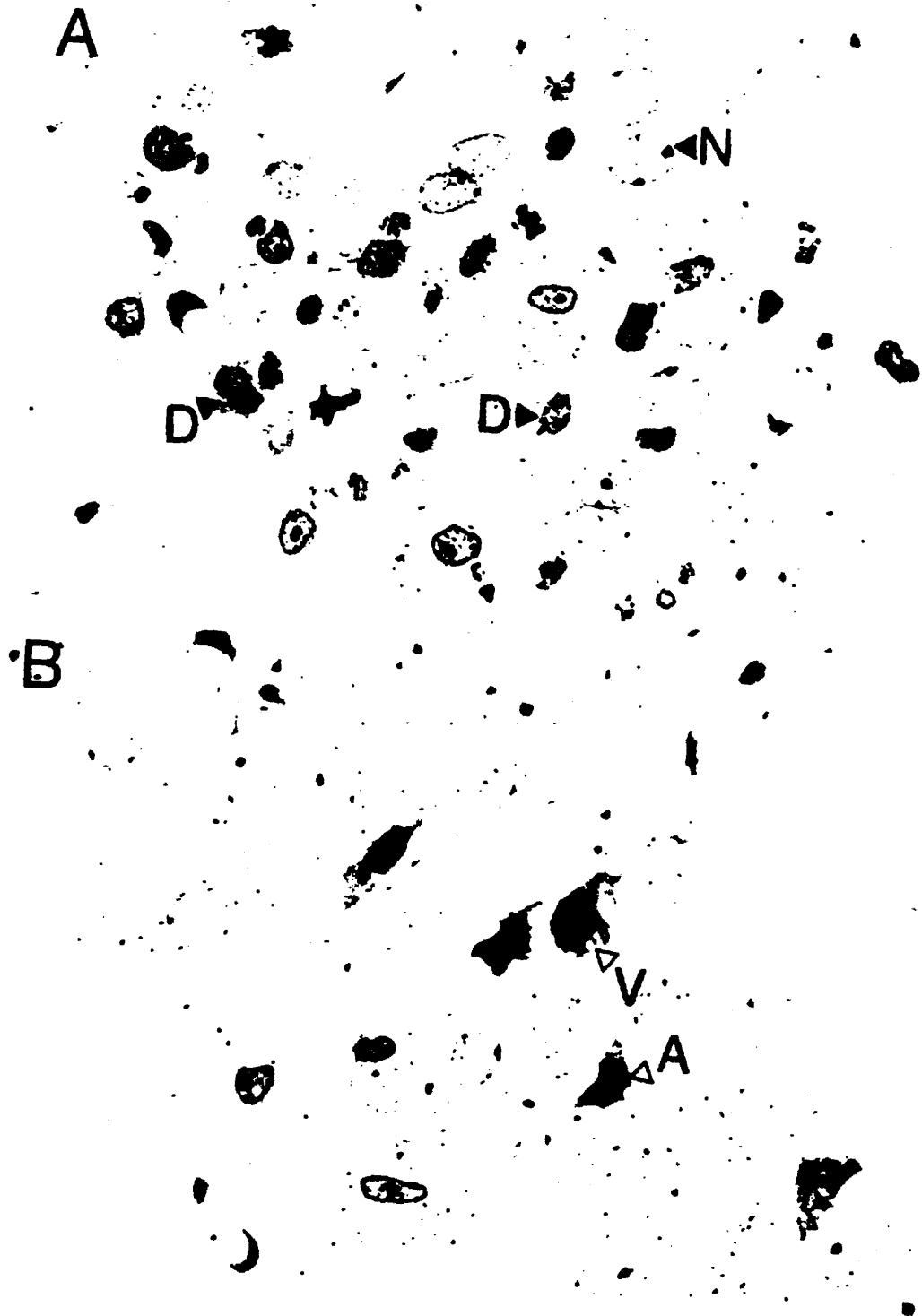


Figure 3) Electron microscopy of dystrophic dentate gyrus granule cells. A: Electronmicrograph of a normal granule cell. B: Morphology of a granule cell at the early stage of apoptosis showing chromatin condensation. The chromatin is predominately localized to the nuclear membrane. Insert shows an axio-somatic synapse, from the dystrophic cell (box). C: Apoptotic granule cell illustrating segmentation of the nucleus. Cytoplasmic vacuoles are beginning to form (V), and the cell has become degenerate. Bar represents 1 micron, the same magnification was used for all micrographs.

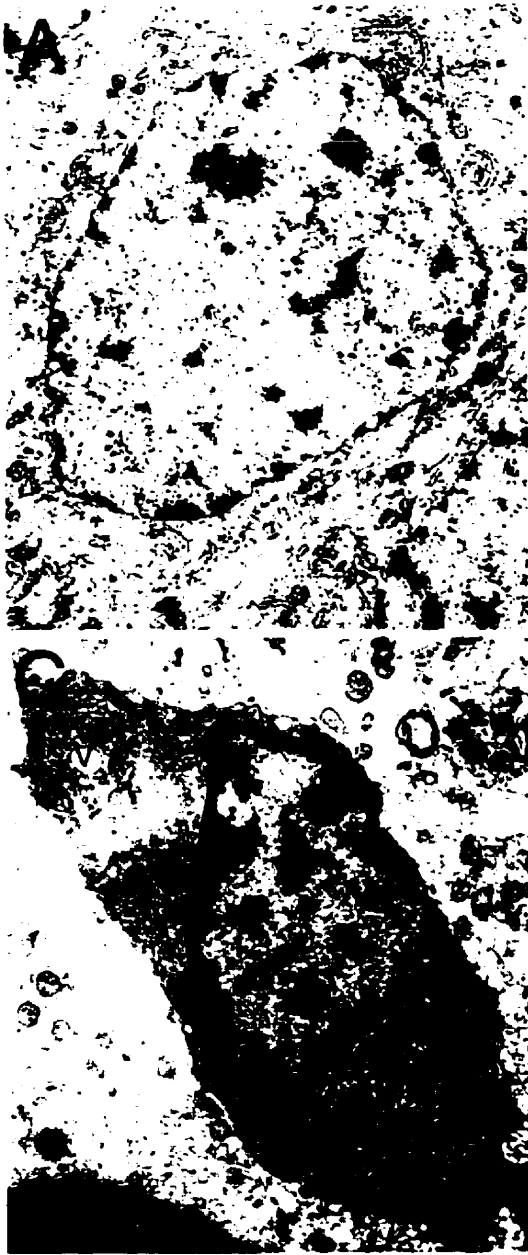


Figure 4) Morphology of rough endoplasmic reticulum (RER) and mitochondria (M).

A: Photomicrograph of a normal granule cell containing clearly visible RER and mitochondria. The mitochondria contain discernable cristernae. B: Picture of a granule cell undergoing the early stages of nuclear segmentation. The chromatin is condensed and localized to the nuclear membrane which is invaginated. The RER is still visible and the mitochondria appear morphologically normal. C: Representative photomicrograph showing both apoptotic and necrotic features. The chromatin is condensed but dispersed. The mitochondria appear swollen and no distinguishable RER is present. Bar in C represents 1 micron. The same magnification was used for all micrographs.

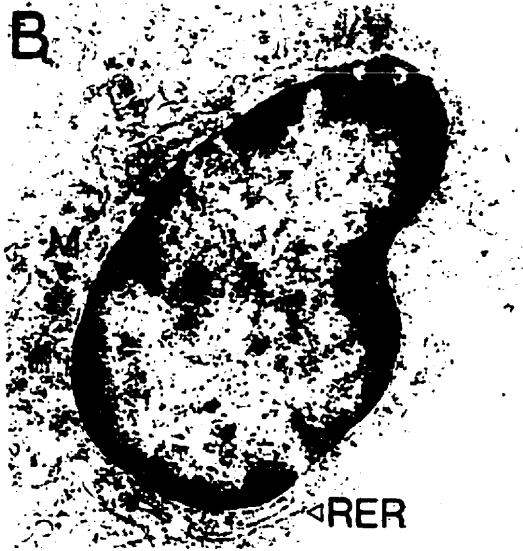
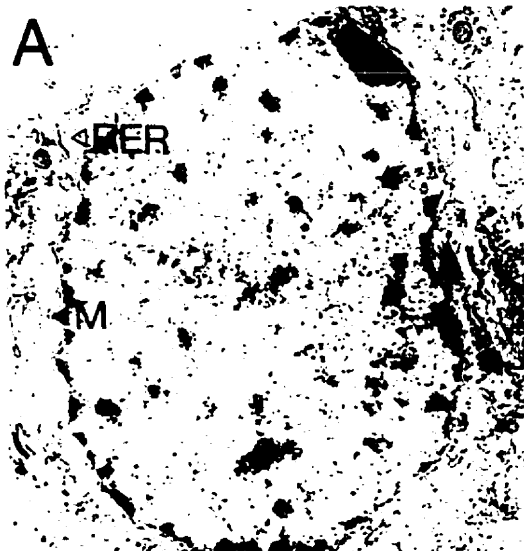
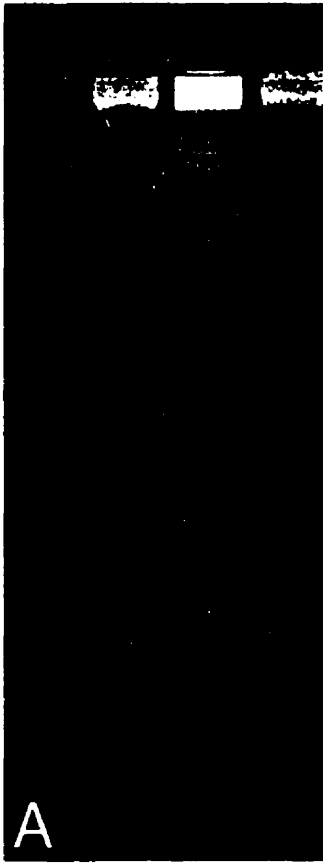


Figure 5) DNA Fragmentation. A: Representative photograph of an ethidium bromide stained gel. Hippocampal cytoplasmic DNA was extracted and electrophoresed as described in the Materials and Methods section. Lane 1. Control, Lane 2. 24-hr postinjury (contralateral), Lane 3. 24 hr postinjury (ipsilateral), Lane 4. 3-day postinjury (ipsilateral). DNA fragmentation is identified by the presence of a characteristic ladder.

B: *In situ* labelling (TUNEL staining) for DNA fragmentation. The photomicrograph was taken from the hyperchromatic region (box in figure 1C) of the dentate gyrus, 24 hours postinjury. C: 0.5 micron epon section taken from the same slice shown in B. The stain appears to be primarily associated with the nuclear membrane, with some of the labeled DNA being detected in the cytoplasm.

1 2 3 4 B



C



4). Regulated expression of netrin in the adult mammalian brain following seizure.

4.0) Foreword

After demonstrating the presence and the apoptotic nature of delayed cell death following traumatic head injury, a mechanism that may contribute to the recovery of the injured neuronal system was then investigated. As a candidate mechanism for post-injury neuronal remodelling, the embryonic chemotropic factor netrin was demonstrated to be expressed in the adult mammalian brain. The regulation of netrin and one of its receptors (deleted in colorectal carcinoma, DCC) was investigated following seizure induced injury, and the expression of both shown to be enhanced in several brain regions. The subcellular localization of these two proteins was analysed and related to the injury paradigm. The following findings comprise the majority of data contained in a paper currently being prepared for submission to the Journal of Neuroscience. This will constitute the first report of constitutive expression of netrin in adult mammalian cortical structures, the first report of the distribution of netrin protein in the adult mammalian brain, and the first reported demonstration of the induction of netrin expression following experimentally induced seizure.

4.1) Summary

The chemotropic factor netrin has been demonstrated to be expressed during neural development, and has been shown to be capable of promoting and altering the trajectory of extending axons. In this report we define the pattern of netrin expression and the

distribution of netrin protein in the adult rat and mouse brain. This was done using antibodies against netrin, *in situ* hybridization analysis, and by analysis of a transgenic mouse in which the netrin-1 promoter drives the expression of lacZ. In the normal animal, netrin expression was observed in basal ganglia structures, amygdaloid, hypothalamic, limbic, cortical and cerebellar regions, and appears to be associated with areas of the brain containing dopaminergic neurons and dopaminergic innervation. It was observed that following pilocarpine induced seizure in rats, there was an initial decrease, followed by a long term increase in both the expression level and abundance of netrin positive cells. This increase occurs in regions associated with the seizure activity and the resulting neuronal damage. We hypothesize a role for netrin in neurite sprouting and regeneration that might occur in these regions following injury.

4.2) Introduction

During the development of the nervous system, axons navigate along defined pathways to reach their specific targets. This is accomplished by the growth cones response to guidance cues in the environment (for review see Tessier-Lavigne and Goodman, 1996). These cues include chemorepulsive and chemoattractant factors such as netrin. Netrin-1 has been demonstrated to function as a floor-plate expressed chemoattractant for dorsal commissural neurons during spinal cord development (Kennedy et al., 1994; Serafini et al., 1994), and can also repel dorsally projecting trochlear motor neurons (Colamarino and Tessier-Lavigne, 1995a). Netrin has also been implicated in the orientation of axons in the dorsal hindbrain and cerebellum (Shirasaki et

al., 1985; Tamanda et al., 1995; Ackerman et al., 1997) and of retinal ganglia cell growth cones (Deiner et al., 1997; Delatorre et al., 1997). While a role for netrin expression during development is becoming clear, evidence that netrin expression persists in the adult brain (Kennedy et al., 1994; Kennedy et al., 1996; Colicos et al., 1997; Livesey and Hunt, 1997) suggests a continuing role for netrin in regulation of axonal structure throughout the life of the animal.

Pilocarpine induced seizure activity in rats is a widely utilized model of human temporal lobe epilepsy (Rice and Delorenzo, 1998; Hamani and Mello, 1997), and produces long term behavioral, histological and biochemical changes. Pilocarpine is a muscarinic agonist, producing status epilepticus (SE) as well as subsequent spontaneous recurrent limbic seizures for months following treatment (for review see Turski et al., 1989). Neurotransmitter systems also play a role in the long term sequela of pilocarpine induced seizures. NMDA receptor agonist MK-801 has been shown to block the spontaneous recurrent seizures, and limit the cell death in the CA1 hippocampal field (Rice and Delorenzo, 1998), while dopaminergic agonists and antagonists can modulate the SE phase (George and Kulkarni, 1997). Neurohistological changes include both short and long term neuronal cell death (Fujikawa, 1996), as well as subsequent axonal sprouting in cholinergic forebrain neurons and in the dentate gyrus of the hippocampus (Holtzman and Lowenstein, 1995). Biochemical changes include upregulation of neurotrophins, as well as furin and other prohormone convertases enzymes (Schmidt-Kastner et al., 1996; Marcinkiewicz et al., 1997; Isackson et al., 1993).

In this report we document the baseline level of netrin expression in the rodent,

utilizing netrin immunohistochemistry on rat tissue and *in situ* hybridization of rat tissue with a netrin-1 anti-sense probe. In addition, we have analyzed the distribution of netrin-1 in the adult mouse brain by using a transgenic mouse in which the netrin-1 promoter drives the expression of β -galactosidase (Serafini et al., 1996, Skarnes et al., 1995). Mice heterozygous for this transgenic insertion carry one wild-type netrin allele and one mutant (*netrin-1* ^{β geo/+}) and have no dramatic CNS phenotype (Serafini et al., 1996).

This baseline expression is compared to post pilocarpine induced seizure expression levels in the rat at various time points following treatment. We observe expression of netrin in normal adult animals in the hippocampus and cortex, as well as in several basal ganglia structures and cerebellum, and observe an increase in both protein levels and mRNA expression level in subsets of these regions following seizure. The netrin receptor DCC (deleted in colon carcinoma) is also demonstrated to be upregulated in these regions. Intracellular localization of netrin protein suggests an association with vesicles and putative synaptic structures. Results suggest a strong correlation with regions of dopaminergic innervation, as well as with regions of neurogenesis and sprouting. A role for netrin during injury recovery in the adult is hypothesized.

4.3) **Methods**

4.3.1) *In situ* hybridization

DCC *in situ* hybridization was performed using digoxigenin (DIG) labelled RNA probes (Braissant and Wahli, 1998), which were then detected chromatically using alkaline phosphatase immunochemistry. Netrin *in situ* hybridization was additionally amplified by

the NEN Tyramide Signal Amplification (New England Nuclear) procedure, detected using peroxidase (POD) immunohistochemistry and chromatically reacted with diaminobenzidine (DAB).

1) *Probe preparation* - A rat netrin-1 cDNA fragment was supplied by Mark Tessier-Lavigne. A region of this clone consisting of a 196 bp Not I - Pst I fragment, corresponding to bases 222 - 427 in the chick netrin-1 sequence (Kennedy et al., 1994) was sub-cloned into pBluescript-KS vector (Stratagene). This plasmid (pMC11) was used to make both sense (T3) and anti-sense (T7) digoxigenin netrin-1 RNA probes. For template preparation 10 µg of plasmid was digested with either Bam HI(T7) or Eco RI(T3), run on a 1% agarose gel, the linearized plasmid cut out of the gel and purified using the Quigen T150 DNA purification kit. For DCC *in situ* hybridization, the rat DCC cDNA clone n78 (Keino-Masu et al., 1996) was cut with XhoI, similarly processed and anti-sense probe was transcribed with T7 RNA polymerase. For both netrin and DCC probes, 1 µg of linearized plasmid was used per probe reaction, which synthesised approximately 5 µg of RNA probe. Probe reaction volume was then increased to 100 µl and separated from nucleotides by two precipitations (100 µl NH₄-acetate 4 M and 500 µl EtOH 100%, -70°C 30 minutes, and centrifugation at 4°C in a microfuge). Pellets were resuspended in 40 µl of H₂O and quantified by visual comparison to known concentrations on a formaldehyde gel. Probes were stored at -20°C until use.

3) *Tissue preparation for Netrin in situ hybridization* - Rats (250-350g Sprague-Dawley

males) were anaesthetized with sodium pentobarbital. After animals failed to respond to tail and foot pinch, they were transcardially perfused with 100 ml of 37°C saline with 1 unit/ml heparin. The brain was immediately dissected out and placed in ice cold PBS. The brain was cut into 3 major regions to minimize freeze fracturing. Prior to the dissection iso-pentane (2-methyl butane) was chilled to -145°C in liquid nitrogen. Excess PBS was blotted from the tissue and then blocks were loosely wrapped in foil and submerged in the iso-pentane. Freezing was complete within minutes, and the maximum time from time of death to freezing is approximately 5 minutes for no signal degradation to occur. Once frozen, tissue was stored at -70°C until needed (maximum several weeks). Tissue to be cut was mounted on a cryostat chuck seated in a bed of dry ice. Chilled OCT was slowly applied to the surface of the brain so as not to allow any thawing of the tissue to occur. 5 micron sections were cut on a Micron freezing cryostat and mounted on SuperFrost Plus Slides (Fisher). Slides were allowed to air dry until the tissue became opaque (approximately 30 seconds). Longer drying times resulted in a decrease in signal intensity. Slides were placed directly into 4% paraformaldehyde, 15% picric acid in phosphate-buffered saline (PBS) and fixed for 1.5 to 2 hours. Except where indicated slides were processed vertically in a 5 slide staining jar, with approximately 50 mls of solution per step.

4) Tissue preparation for DCC in situ hybridization - Rats (250-350g Sprague-Dawley males) were anaesthetized with sodium pentobarbital. After animals failed to respond to tail and foot pinch, they were transcardially perfused with 100 ml of 37°C saline with 1

unit/ml heparin. This was followed by perfusion with 150 ml of 37°C freshly prepared fixative [4% paraformaldehyde, 15% picric acid in phosphate-buffered saline (PBS), pH 8.5]. Brains from naive, sham injured and injured animals were removed and equilibrated in the fixative containing 30% sucrose at 4°C for 2 days. Fixed brains were then mounted in O.C.T. (Optimal cutting temperature, Miles Inc., Elkhart, IN) cryostat embedding medium. 40-micron thick coronal sections, spanning the entire hippocampus were cut from each brain on a cryostat. Sections were placed in PBS in 24-well tissue culture plates, washed once with PBS, and stored at 4°C until use.

4) *Netrin-1 Hybridization* - Fixed slides were rinsed twice with 2X SSC (20X - 3.0 M NaCl, 0.5 M Na Citrate, pH 7.0), and then equilibrated in 10mM triethanolamine for 5 minutes. Slides were then transferred to a horizontal rack and treated with 1 ml per slide 0.25% acetic anhydride in 10mM triethanolamine for 10 minutes at room temperature. The solution was then drained from the slides and replaced with pre-hybridization solution (50% formamide, 5X SSC, 5X Denhardt's (50X - 1g BSA (bovine serum albumin), 1g PVP (polyvinylpyrrolidone), 1g Ficoll in 100mls H₂O), 1% SDS, 100 µg/ml yeast tRNA, 100 µg/ml Heparin). Slides were incubated at room temperature for 1 hour. Hybridization was performed in buffer (50% formamide, 5X SSC, 40 µg/ml single stranded salmon sperm DNA) with approximately 200 ng of digoxigenin labelled probe in 100 µl buffer. Probe was denatured by heating to 90°C for 10 minutes in the hybridization solution. Probe was applied by quickly pouring off the pre-hybridization solution, and then applying the warm hybridization solution to the section. Tissue should remain clear

during this step. Slides were then coverslipped with #1 22x40mm coverslips, excess solution aspirated off, and the coverslips sealed with nail polish. The hybridization was performed over-night, the temperature regulated by placing the slides in glass petri dishes and floating them in a 48°C waterbath.

5) *Detection* - Upon completion of the hybridization, slides were removed from the water bath and immersed in 20X SSC. A razor was used to cut off the nail polish and the coverslips removed. Slides were transferred to the staining jar containing 2X SSC. The buffer was changed once and then the stringent wash was done at 48°C for one hour. Upon completion of the wash slides were rinsed with room temperature 2X SSC once and then placed into block (2% BSA, 2% heat inactivated lamb serum, 0.05% TWEEN-20) for 30 minutes. DIG probe was detected by first incubation in POD-coupled anti-digoxigenin antibody (Boehringer Mannheim), followed by washing 3 x 10 minutes with PBS with 0.05% TWEEN-20. Slides were then reacted with the NEN biotinyl tyramide substrate diluted 1:100 in the dilution buffer provided for 10 minutes. Slides were then washed 3 x 10 minutes in PBS. A second blocking step was then performed in the NEN provided blocking agent, and the slides then incubated in a 1:200 dilution of streptavidin horse-radish peroxidase (SA-HRP) in blocking agent for 30 minutes. Slides were washed in PBS 5 x 10 minutes and reacted with DAB (Vector labs). Reactions were taken to completion (approximately 7 minutes). Slides were washed in PBS, rinsed in H₂O and mounted in Aquamount for photomicrography.

5) *DCC hybridization* - DCC *in situ* hybridization was done with free-floating tissue sections, processed in 24-well culture trays. Sections were rinsed once in 2X SSC, then placed in pre-hybridization solution (50% formamide, 5X SSC, 5X Denhardt's (50X - 1g BSA, 1g PVP, 1g Ficoll in 100mls H₂O), 1% SDS, 100 µg/ml yeast tRNA, 100 µg/ml Heprin). Slides were incubated at room temperature for 1 hour. Hybridization was performed in the same buffer by the addition of approximately 200 ng of denatured digoxigenin labelled probe. Trays were sealed with parafilm and place in a shaking water bath overnight at 50°C. The following day the sections were transferred to 2X SSC, then stringently washed in 0.2X SSC at 50°C for 1 hour. Sections were rinsed twice in 2X SSC and placed into blocking solution (2% BSA, 0.2% Triton-X100 in PBS) for 1 hour. DIG labelled probe was detected with anti-DIG alkaline phosphatase linked antibody (Boehringer Mannheim 1093 274, diluted 1:200 in blocking solution) for one hour at room temperature. Sections were washed 3 x 30 minutes in PBS and colormetrically detected over night with BM purple substrate in the dark at 4°C. Sections were mounted on glass slides, coverslipped with Aquamount for photomicrography.

4.3.2) **Immunohistochemistry**

Immunohistochemical analysis was performed on both rat and mouse brain tissue, utilizing an anti-beta-galactosidase polyclonal antibody (5'->3', IC196A) and the anti pan-netrin polyclonal antibody 11760 (Kennedy et al., 1996b; Deiner et al., 1997). Tissue was prepared as follows. Animals were anaesthetized with sodium pentobarbital. After animals failed to respond to tail and foot pinch, they were transcidentally perfused with

37°C saline with 1 unit/ml heparin (approximately 100 mls for rats, 20 mls for mice). This was followed by perfusion with 37°C freshly prepared fixative [4% paraformaldehyde, 15% picric acid in phosphate-buffered saline (PBS)], using approximately 150 mls for rats, 50 mls for mice. Brains from naive and injured animals were removed and equilibrated in the fixative containing 30% sucrose at 4°C for 2 days. Fixed brains were then mounted in O.C.T. (Optimal cutting temperature, Miles Inc., Elkhart, IN) cryostat embedding medium. 40-micron thick coronal sections, spanning the entire brain were cut on a cryostat at -16°C. Sections were placed in PBS in 24-well tissue culture plates, washed once with PBS, and stored at 4°C until use. Immunohistochemistry was performed on free-floating sections in 24 well plates. Sections to be stained were washed twice in PBS, and then transferred to block (PBS, 2% BSA, 0.2% Triton X-100) for 60 minutes. Sections were incubated in antibody (11760 diluted 1:50, anti beta-galactosidase diluted 1:1000 in block) overnight at 4°C. Sections were then washed 3 times for 10 minutes each in PBS at room temperature and incubated with anti rabbit POD conjugated secondary antibody for 30 minutes at room temperature. Sections were washed 3 times 10 minutes in PBS and reacted with DAB (Vector Labs). Sections were mounted on glass slides, coverslipped with Aquamount for photomicrography.

4.3.3) Pilocarpine induction of seizure

Seizures were induced with pilocarpine as described by Starr and Starr (1993). Briefly, male Sprague Dawley rats were injected I.P. with methyl scopolamine (1mg/kg) to

prevent the peripheral autonomic effects of pilocarpine. Fifteen minutes later, they received an injection I.P. of 375 mg/kg pilocarpine hydrochloride. One hour later the seizure was terminated with an I.P. injection of 10 mg/kg diazepam. The animals were hand fed glucose solution and rat chow slurry until they recovered and were able to feed independently, typically 1-2 days.

4.4) Results

4.4.1) Netrin expression in the normal adult rat brain

The polyclonal sera 11760 was raised against a peptide corresponding to sequence highly conserved in vertebrate netrins (RFN MEL YKL SGR KSG GVC). This includes 100 % amino acid identity in chick netrin-1 and chick netrin-2 (Serafini et al., 1994), zebrafish netrin-1a and netrin-2 (de la Torre et al., 1997), mouse netrin-1 (Serafini et al., 1996), human netrin-1 (Swimmer et al., 1998). In immunoblot analysis of lysates of embryonic, post-natal, and adult rat brain, affinity purified anti-netrin 11760 recognizes a band of ~75 KDa corresponding to full length netrin protein (Kennedy et al., 1996). We used antibody 11760 to visualize the distribution of netrin protein in adult rat. Immunohistochemical specificity of the antibody in this system for netrin protein was first confirmed by pre-incubation of the antibody with 293 cell-expressed protein from a clone containing the peptide sequence originally used to make the antibody. Figure 1a shows the effect of pre-incubation (insert) on 11760 signal in the hippocampus. Netrin immunoreactivity was detected outside the cell bodies, in the cytoplasm and on the cell surface, consistent with netrin being a secreted component of the extracellular matrix. To identify netrin

expressing cells, *in situ* hybridization was performed. Figure 1c shows the netrin mRNA distribution in a region corresponding to the protein expression in Figure 1a. Netrin message was detected in the principal cells of the hippocampal gyrus, the dentate gyrus granule cells and the hilar interneurons. Figure 1b and 1d illustrate the cortical expression of netrin. In Figure 1b, 11760 immunohistochemistry of neocortex demonstrates a strong signal in layer 1 cells. Less intense immunoreactivity was also detected in the pyramidal cells of layer 2 and 3. Figure 1d illustrates *in situ* hybridization of a corresponding region with anti-sense netrin-1 probe, demonstrating that cells in both neo-cortical layers express netrin-1. Control hybridization with a sense probe (Figure 1d, insert) did not detect any hybridization signal.

4.4.2) Netrin induction following seizure

Immediately following seizure we observed a dramatic decrease in the level of netrin immunoreactivity in brain regions associated with seizure activity. This can be seen in Figure 2 which shows a comparison between the overall protein level in a coronal section transecting the hippocampus in the normal (Figure 2a) and 24 hours post seizure (Figure 2b). This effect was most dramatic in regions where visible tissue damage occurred following the seizure activity, such as the entorhinal cortex (Figure 2c). By 3 days post seizure this effect was no longer observed (not shown). At 7 days post seizure, overall netrin immunoreactivity increased (Figure 2d). Netrin immunoreactivity in the hippocampus was also induced following seizure, as illustrated in Figure 3. Netrin immunoreactivity in the normal rat (Figure 3a), compared to corresponding tissue from a

rat 7 days post-seizure (Figure 3c), indicates primarily an increase in the level of expression in the granule cells of the dentate gyrus, and the polymorphic cell layer (CA4). The cells of the hilar region, which are strongly netrin immunopositive in the normal rat, continue to show high levels of detectable protein. The induction in this region appeared to be a change in the amount of protein expressed rather than the appearance of new positive cells. In order to compare the level of netrin expression in normal and post seizure brain, both brain samples were cryostat sectioned onto the same slide and *in situ* hybridization analysis carried out simultaneously on both tissues.

This observation was confirmed by both *in situ* hybridization and northern blot analysis. Figure 3b,d shows *in situ* hybridization of same-slide co-processed normal and 3 day post-seizure tissue with the netrin-1 probe, suggesting an increase in netrin-1 message begins in these cells at the 3-days post-seizure time-point. Induction of netrin-1 was also demonstrated using northern blots of RNA from 7 day post injury sham and seized animals (Figure 4). Densitometric analysis indicated an increase of approximately 2 fold over normal total hippocampal mRNA levels occurs following seizure, consistent with the *in situ* hybridization and immunohistochemical analysis.

The increase observed in the entorhinal cortex protein levels 7 days post seizure (Figure 2d) was accompanied by an increase in the detectable level of netrin-1 mRNA 7 days post seizure. Figure 5a shows netrin-1 mRNA levels in the entorhinal cortex of a normal rat. Figure 5b shows the corresponding tissue in a 7 day post-seizure rat. Higher magnification micrographs can be seen in Figure 5c,d. Insert in 5d shows a high magnification micrograph of corresponding cortical neurons in the layer 2/3 region of 7 -

day post-seizure entorhinal cortex stained for netrin protein. High levels and a punctate staining pattern can be seen.

4.4.3) Netrin-1 expression in the netrin-1^{βgeo/+} mouse brain

In order to assist in cataloguing the spatial distribution of netrin expression in normal mammalian brain, expression of netrin was assessed using a transgenic mouse in which the netrin-1 promoter drives the expression of lacZ, netrin-1^{βgeo/+} (provided by Marc Tessier-Lavigne, described in Serafini et al., 1997). This provided an accurate and specific method of characterizing the spatial gene expression profile in the normal mouse. Figure 6 summarizes the location of the netrin-1 producing cells. In the forebrain (illustrated in Figure 6a) high levels of netrin expression can be seen in the piriform cortex, tenia tecta, the nucleus accumbens core and the olfactory tubercle. Moving caudally, Figure 6b illustrates the parietal cortex, cingulate cortex, caudate and putamen, lateral septal nucleus (intermediate region), nucleus accumbens shell, the cell bridges of the ventral striatum and the ventral palladium. Figure 6c, at approximately 1 mm rostral to bregma, indicates expression in the parietal cortex, caudate putamen, bed nuclei of the stria terminalis, ventral palladium and the cell bridges of the ventral striatum. Figure 6d includes the paraventricular hypothalamic nucleus, the subthalamic nuclei, premammillary nuclei, basolateral amygdaloid nucleus and piriform cortex. Figure 6e shows entorhinal cortex, the interfascicular nucleus, paranigral nucleus and substantia nigra pars compacta. Figure 6f shows the cerebellum at the level of the paraflocculus, the region of highest netrin expression detected, although stellate and basket cells showed

expression throughout the cerebellum. Also observed to express netrin-1 but not listed in Figure 6 is the supramammillary nucleus and scattered cells in the medial septal nucleus. Figure 7a-f shows closeup photomicrographs of 6 major beta-galactosidase positive cell regions in striatum and forebrain. Figure 8a-f shows closeup photomicrographs of 6 major striato-nigal regions expressing netrin-1, as well as expression in the cerebellum. Table 1 summarizes the regions of netrin expression by structure.

4.4.4) Netrin receptor DCC induction following seizure in rats

To determine if there was also an alteration of netrin receptor levels in response to seizure, DCC *in situ* hybridization and immunohistochemistry was performed on normal and seized tissue. There is a dramatic localization of DCC protein in layer 3 of the entorhinal cortex (Figure 9e) and in cells of the thalamus (Figure 9f) 3 days following seizure. This is also reflected in the DCC mRNA levels. Figure 9a and c show a comparison between normal and 3 day post-seizure entorhinal cortex. A clear line of DCC positive cells can be detected detected in the entorhinal cortex 3 days post-seizure. Figure 9b and d show a comparison between DCC mRNA levels in the thalamus in normal and 3 day post seizure tissue. A dramatic increase in the cellular labelling can be seen, and this increase in mRNA is complimented by the corresponding immunohistochemical detection of DCC protein (Figure 9f).

Surrounding the region of the damaged entorhinal cortex, many cells were observed to express high levels of DDC or netrin, but it was uncommon to find expression of both molecules in one neuron. This was taken advantage of to investigate

possible sub-cellular interactions between netrin positive and DCC positive neurons.

4.4.5) Subcellular localization of netrin protein

Figure 10a shows a high resolution fluorescent confocal micrograph of a cortical neuron from the region of the entorhinal cortex from a 7 day post injury animal, counterstained with anti-netrin receptor DCC antibody. DCC expression is detected in an approaching neurite (green) which has contacted and is travelling along the netrin positive neurite (red). Co-localization at bead-like structures is suggested at the points of yellow co-labelling. Both proteins appear concentrated at varicosities, suggesting an association with synapses. The high levels of netrin at the varicosities was an interesting observation considering *in situ* hybridization suggested that netrin-1 mRNA might be present in the processes of neurons (Figure 10b).

4.5) Discussion

4.5.1) Netrin expression in basal ganglia

Constitutive netrin expression in the basal ganglia can be overlaid on three main regions, the striatum, the striatopallidal system and the extended amygdala region. Regions of the ventral striatum that express netrin include the nucleus accumbens (Figure 7a,b), the caudate-putamen (Figure 7c,d), the cell bridges of the striatum that connect the tubercle with the overlying caudatoputamen and nucleus accumbens (Figure 7f), and the tenia tecta (Figure 7e). Neurons of the caudate-putamen (Figure 7d) can be seen to have the distinctive morphology and distribution of the large aspiny or sparsely spiny cholinergic

basal forebrain neurons. These cholinergic neurons are distributed as approximately 2% of the total neurons in the dorsal and ventral striatum, and receive both thalamic and dopaminergic afferents (Shepherd, 1990b). Netrin expression in the nucleus accumbens occurs at the highest level in the core, but substantial expression can also be observed in the shell (Figure 7b). Principal connections from the accumbens are to the septum and substantia nigra, but efferents also extend to the bed nucleus of the stria terminalis, pre-optic and lateral hypothalamic regions. Extending from the ventral striatum is the ventral striatopallidal system, in which the ventral pallidum (Figure 8b) can be seen to contain a large number of netrin expressing neurons. Netrin expression in the extended amygdala occurs in the bed nuclei of the stria terminalis (Figure 8a). The basal ganglia structures listed here primarily function in voluntary motor planning and control, and include motor learning pathways (for review see Hikosawa, 1998).

4.5.2) Netrin expression in dopamine related structures

One of the most prominent netrin positive regions is the substantia nigra pars compacta (SNC) (Figure 8e). The multipolar A9 cells of this region comprise the principal region of dopamine production in the rodent (Paxinos, 1995a). This cell group extends posteriorly to the retrorubro field as the A8 dopaminergic neurons. Associated with the SNC is the ventral tegmental area (VTA), which contains approximately 80% dopaminergic A10 neurons which project to striatal areas (Paxinos 1995a). Seven major areas receive dopaminergic innervation from the SNC and VTA, and each of these areas express netrin at high levels. These areas are as follows: 1) Dense outputs from the

ventral and intermediate sheets of the SNC and ventrolateral VTA innervate the caudate-putamen (Paxinos 1995a). Netrin expression in this region is illustrated in Figure 7c. 2) The nucleus accumbens (Figure 7a) and 3) olfactory tubercle (included in Figure 7e) receive inputs from the dorsal and middorsal VTA. 4) The lateral septum is innervated by ventral VTA neurons and medial SNC neurons, and is illustrated in Figure 8d. (Paxinos 1995a) 5) Cingulate cortex, 6) perirhinal cortex, and 7) prefrontal cortex all receive input from the dorsal SNC tier and are netrin positive (exemplified in Figure 1b) (Paxinos 1995a). Inputs to the SNC include axons from the matrix compartment of the striatum (indirect limbic) arriving at the ventral tier of dopaminergic neurons (Paxinos, 1995a), and the dorsal tier of the SNC receives its inputs primarily from frontal and cingulate cortex (direct limbic), hypothalamic, and amygdaloid regions and the patch compartment of the striatum (Paxinos, 1995a).

These findings demonstrate the presence of netrin in the SNC and its efferent targets, and its overlap with the basal ganglia and dopaminergic systems, however the role of netrin in these structures is unclear. These structures are a convergence point for various cortical inputs. It has been suggested that after the formation of a temporary association of these cortical signals, their behavioural significance is evaluated by the limbic system, giving the basal ganglia their role in behavioural procedural memory (Hikosawa, 1998). These structures are also responsive to seizure activity. It has been observed that dopamine utilization increase in the nucleus accumbens, olfactory tubercle and cingulate cortex, and decrease in the hippocampus post-seizure (Alam and Starr, 1996). As with the hippocampus, the basal ganglia are also a highly regenerative region

of the CNS, with well documented examples of post-injury sprouting (Mitsumoto et al., 1998, Ho and Blum., 1998). Induction of such events could be triggered by neurotrophic factors such as BDNF (Cellerino et al., 1998). While finer delineation of the cell types expressing netrin will allow for a more specific investigation of the role of netrin in these structures, the correspondence between regions of regeneration and the presence of netrin is maintained.

4.5.3) Netrin expression in cortical structures

Evidence is presented demonstrating netrin-1 expression in both allocortical and isocortical structures. In the hippocampus the highest level of protein detected was in cells with the distribution of basket cells and hilar interneurons and, however both pyramidal and granule cells were also netrin immunopositive, but at lower intensity. The presence and induction of netrin post-seizure in this hippocampal cell population was of interest, as post-seizure mossy fiber sprouting is a very well characterized example of axon sprouting in the adult brain. The granule neurons and CA3 neurons are both targets of sprouting mossy fibers following seizure. Recent evidence suggests that netrin also functions as a short-range target recognition molecule for synapse formation (Winberg et al., 1998). As such, the regulated expression of netrin by these targets demonstrated here may play a role in promoting mossy fiber outgrowth and reactive synaptogenesis following seizure.

In cortical structures such as cingulate and entorhinal cortex, netrin is seen in the layer 2 pyramidal cell layer, as well as throughout the deeper regions. High protein levels

in isolated layer 1 cells which are morphologically similar to interneurons was also observed. A substantial level of tissue damage was observed in the entorhinal cortex post-seizure. We demonstrated an increase in the level of netrin expression in the layer 2 pyramidal cells of this region, as well as a high level of induction in scattered cells in layers 3-4. Although post-seizure axonal sprouting in the entorhinal cortex has not been documented, it is a region of post-seizure cell death (Du et al., 1995). It is possible that, in a manner similar to the hippocampus, the presence of increased netrin levels in the pyramidal cells could also promote sprouting in this region. This could contribute to altered electrophysiological responsiveness of circuits involving this region (Nagao et al., 1996; Nagao et al., 1994), and consequently the recurrent seizure activity observed post seizure.

4.5.4) Conclusions

The expression of the embryonic chemotropic molecule netrin continues in the normal adult rodent, and is primarily associated with cortical, cerebellar and basal ganglia structures. Localization of increased netrin expression post-seizure is consistent with regions of post-seizure sprouting and altered electrophysiological responses. Acting as an axon guidance molecule and/or a short-range target recognition molecule for synapse formation, netrin could play a role in these events. Netrin is also present in many brain structures demonstrated to exhibit activity-dependent plasticity. It has been suggested that structural changes at the synapse, such as the growth of new synaptic connections, may be a component of activity dependent plasticity (for review see Bailey and Kandel, 1993).

Visualization of netrin associated with structures having the morphological characteristics of vesicles and synapses suggests that it may also be the case that constitutive expression of netrin by neurons, like hippocampal interneurons, may play a role in non-pathological synapse maintenance or plasticity.

Figure 1) Netrin protein and mRNA expression in the normal adult rat hippocampus and cortex, coronal sections. A) 11760 immunoreactivity in the hippocampal dentate gyrus and hilar regions. Insert illustrates the effect of pre-incubation of the antibody with netrin protein peptide. B) 11760 immunohistochemistry, cingulate cortex. Layer 1 sparse, darkly stained interneurons, and lighter staining in pyramidal cells of layer 2 and 3 can be seen. C) *In situ* hybridization for netrin-1 mRNA, hippocampus dentate gyrus and hilar region. Corresponds to protein detection in panel A. Hilar interneurons and the granule cells both express netrin mRNA. D) *In situ* hybridization for netrin-1 mRNA, cortical layers 1-3. Netrin-1 mRNA can be detected in both the layer 1 cells and the pyramidal cells, as was detected in the immunohistochemistry in panel B. Insert shows background hybridization signal with sense probe. Scale bar 100 microns.



Figure 2) Netrin protein induction following seizure activity, 11760

immunohistochemistry A) Normal adult rat, whole brain coronal section showing global distribution of netrin protein. B) 24 hours following pilocarpine induce seizure. C) Comparison of piriform cortex, normal and 1 day post-seizure, showing clearing of signal in inner cortical layers. D) 7 days post-seizure, showing overall increase in protein staining. Scale bar 100 microns.

A

B

C

D



Figure 3) Netrin protein and mRNA induction in the hippocampus. *In situ* hybridizations were co-mounted and repeated in triplicate for comparison. A, B) 11760 immunohistochemistry and netrin-1 *in situ* hybridization, respectively, of the dentate gyrus and hilar hippocampal region in the normal adult rat. C) 11760 immunohistochemistry of 7 day post seizure tissue. General increase in protein staining in the granule and pyramidal cells can be seen. D) netrin-1 *in situ* hybridization of 3 day post seizure tissue. showing a corresponding increase in signal intensity. Labels: CA4 - CA4/polymorphic cell layer; h - hilus; g - granule cell layer. Scale bar 100 microns.

B



D

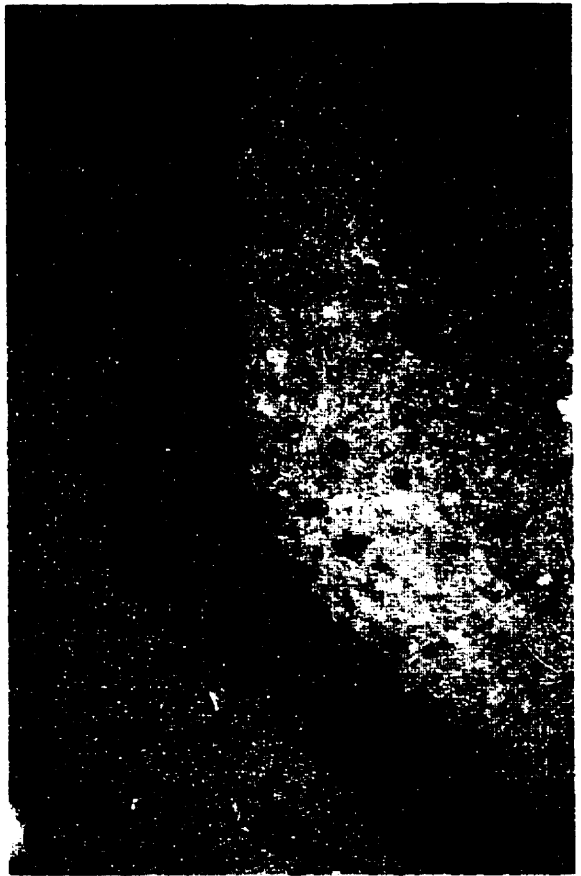


Figure 4) Northern Blot analysis of normal and post-seizure hippocampal mRNA. 5 μ g of total RNA was run on a 1% formaldehyde vertical gel, transferred to nitrocellulose and probed with the same probe used for the *in situ* hybridization. Identical hybridization and detection procedures were also used. The probe detected a single band of approximately 6.0 kb, the reported size of rat netrin-1. Densitometric analysis was performed by reflectance scanning of the blot, and subsequent analysis with NIH Image. M - marker (band sizes in kb: 9.49, 7.49, 4.40, 2.37, 1.35); C - Sham injured control hippocampus; S - 7 day post-seizure hippocampus.

M

C

S



Figure 5) Induction of netrin-1 mRNA in the entorhinal cortex following seizure activity. A, C) *In situ* hybridization of netrin-1 probe with normal rat entorhinal cortex tissue. B, D) *In situ* hybridization of netrin-1 probe with rat entorhinal cortex tissue, 7 days post-seizure, co-processed with the normal tissue in A) and B). A dramatic increase in the amount of signal can be observed. This increase is also reflected in the intensity of 11760 staining (insert) in which very darkly stained neurons in layer 3/4 of the entorhinal cortex can be observed.

A



B



C



D



Figure 6) Spatial localization of netrin-1 expression. Six representative coronal sections from immunohistochemical analysis of the netrin-1^{βgeo/+} mouse brain, in which the netrin-1 promoter drives the expression of lacZ illustrates the over-all distribution of netrin-1 in the brain. Major netrin expressing structures are indicated.

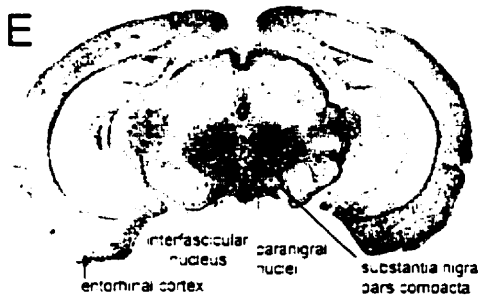
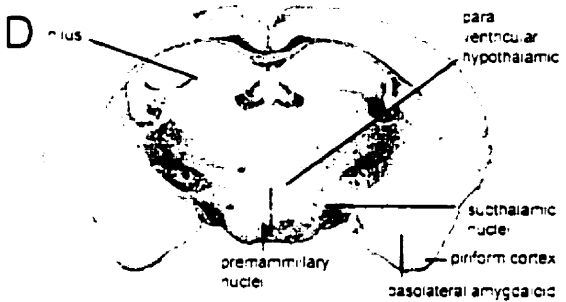
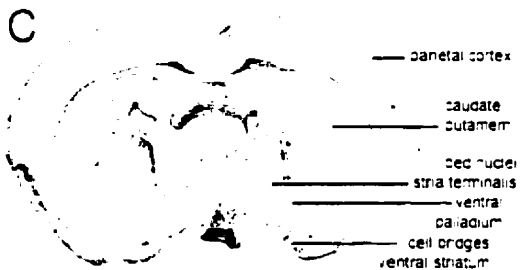
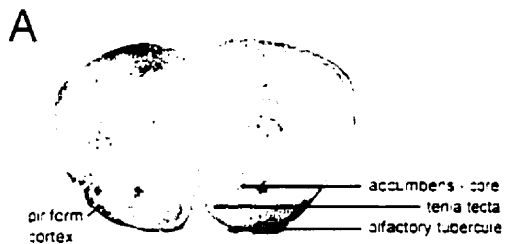
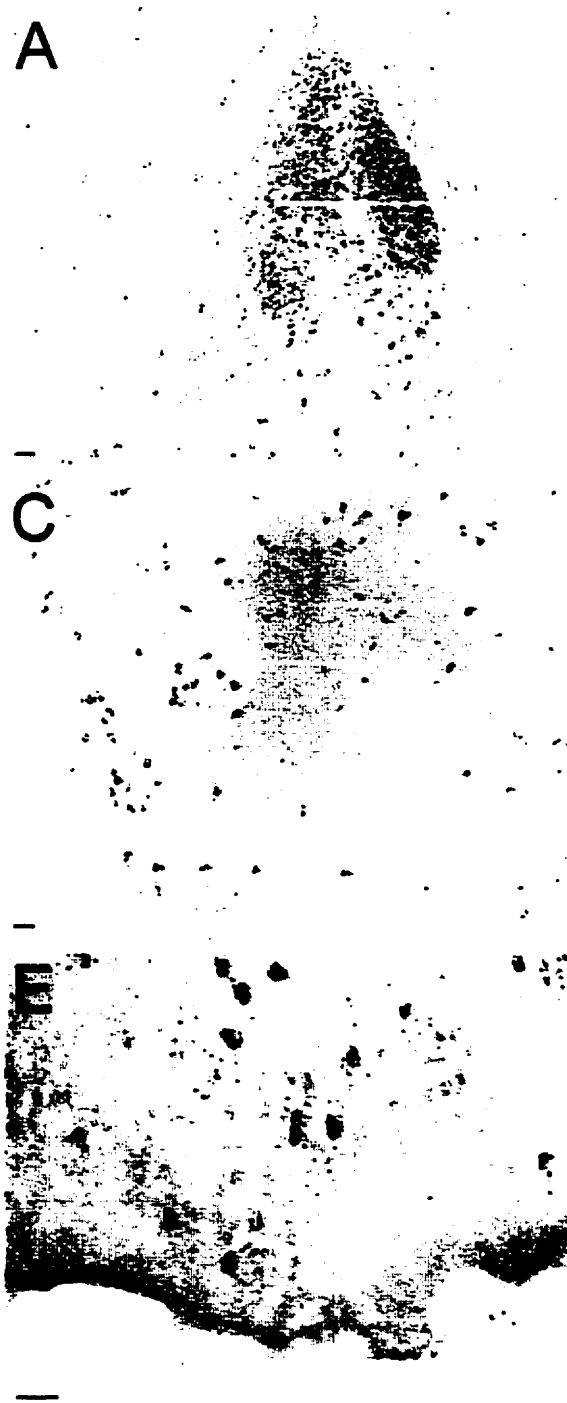


Figure 7) Netrin expression in forebrain and striatal structures. Detected by immunohistochemical analysis of netrin-1^{β_{gal}+/+} lacZ expression in the mouse. A) nucleus accumbens, B) accumbens shell, C) caudate putamen D) higher magnification showing morphology of the striatal labelling E) cell bridges of the striatum, F) tenia tecta. Scale bar A,B,C,E,F) 100 microns, D) 50 microns.

A



B



C



D



Figure 8) Striato-nigral netrin expressing structures. Detected by immunohistochemical analysis of netrin-1^{β_{geo}+} lacZ expression in the mouse. A) bed nucleus, stria terminalis, B) ventral palladium, C) basolateral amygdaloid, D) lateral septal, E) substantia nigra pars compacta, F) cerebellum, stellate and basket cells. Scale bar 100 microns.

A

C

E

B

D

F

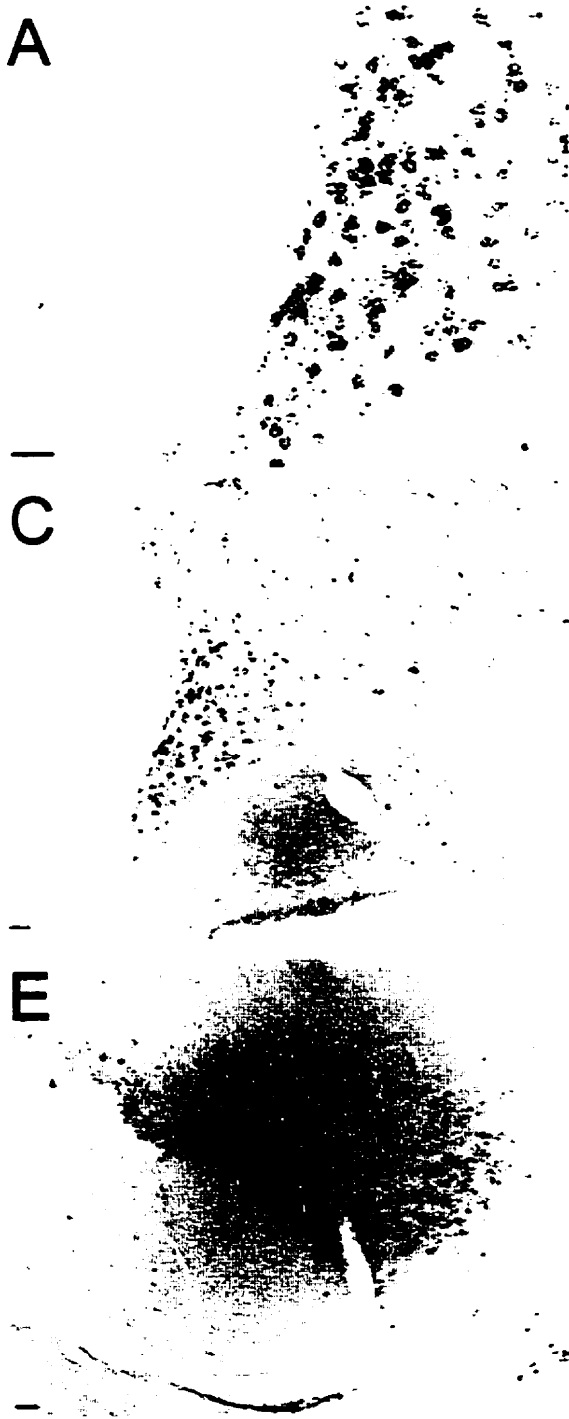


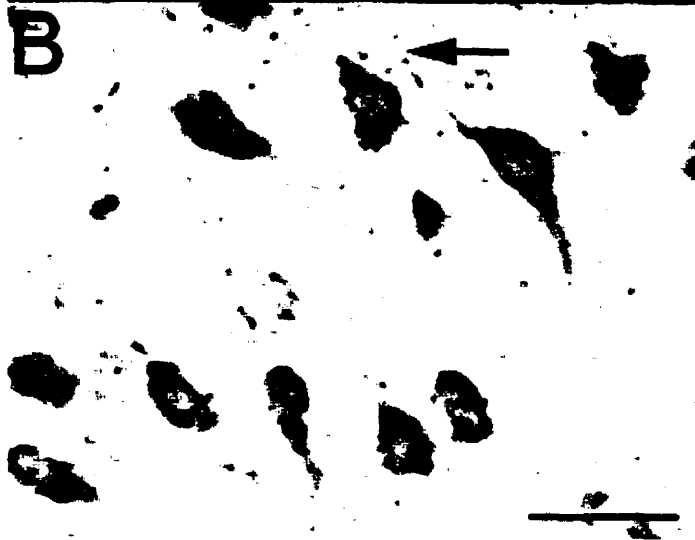
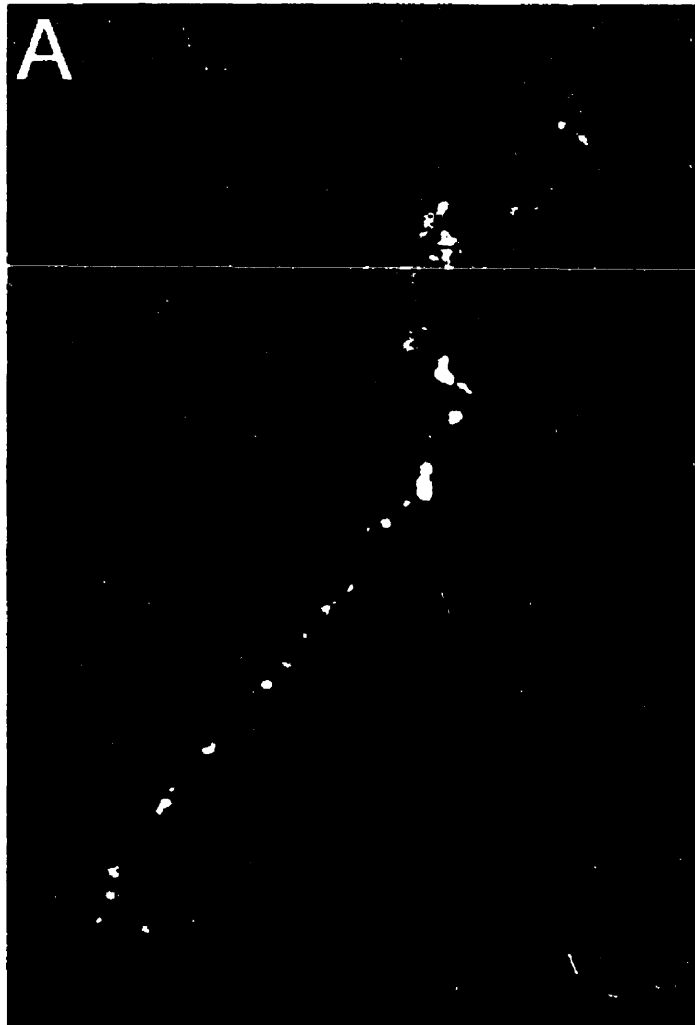
Table 1

Structure	Area
Basal Ganglia	caudate-putamen
	subthalamic nucleus
	accumbens core
	accumbens shell
	substantia nigra compacta
	cell bridges
	ventral palladium
Striatial/Cortical	olfactory tubercule
Cortical	taenia tecta
	piriform
	parietal
	entorhinal
	cingulate
amygdaloid	basolateral amygdaloid
	bed nucleus stria terminalis
limbic	hilus
	lateral septal intermediate
hypothalamic	dorsal hypothalamic
	supramammillary

Figure 9) Netrin receptor DCC induction following seizure in rats, demonstrated with low sensitivity DCC *in situ* hybridization and anti-DCC antibodies . A) DCC *in situ* hybridization of normal rat tissue, entorhinal cortex. C) mRNA detected 3 days following seizure. A faint increase can be seen along the boarder of layer 2 and 3 (arrow), E) DCC protein induction 3 days post seizure. A dramatic staining can be seen in this region, not present at this level in the normal adult (not shown). B) DCC *in situ* hybridization in the normal thalamus, D) thalamus 3 days post seizure. This dramatic increase in the level of DCC mRNA is reflected in the protein staining in F). Scale bar in A) 200 microns, in B) 50 microns.



Figure 10) Subcellular localization of netrin protein and netrin receptor DCC protein. A) Confocal microscopy of double labelled tissue, DCC in green, netrin in red. Tissue from a 7 day post-seizure rat, entorhinal cortex, layer 2-3. DCC positive cells produce DCC positive processes, figure shows one which contacted a netrin positive cell. The processes appear fasciculated, and demonstrated co-localization at varicosities. B) the presence of netrin RNA at varicosities is suggested in some netrin *in situ* hybridization results, such as these hilar interneurons (arrow).



5) Conclusions

Understanding the implications of neuronal injury and the process of regeneration has been a long-standing goal of neurobiology. Elucidating the mechanisms that underlie these aspects of brain function is of practical importance since the knowledge gained in this pursuit has the potential to be applied to the clinical treatment of human pathological conditions. This is also the foundation for the work presented here. This study first addresses the issue of neuronal cell death following traumatic brain injury. I demonstrated that the extent of neuronal cell death expands spatially and temporally from the initial insult. This was followed by a demonstration that the delayed cell death observed occurred by apoptosis. Finally, a possible mechanism that may contribute to CNS regeneration in the adult was investigated by identifying the presence and regulation of the chemotropic factor netrin following pilocarpine-induced seizure in the adult.

5.1) Delayed apoptotic cell death following TBI

5.1.1) TBI

Several animal injury models have been developed for study of traumatic brain injury. Currently the two most widely used are fluid percussion and cortical impact rodent models of TBI. These models each reproduce various aspects of human TBI, but most importantly, they produce cell loss and axonal injury (Dixon and Hayes, 1996; Gennarelli, 1994). For example, death of hilar neurons has been observed in the context of a lateral fluid percussion model of TBI (Hicks et al., 1993; Lowenstein et al., 1992). Loss of CA1 and CA3 cells has been reported following a cortical impact injury with

unilateral craniectomy (Goodman et al., 1994). Several variations of the cortical impact injury model exist, focussing on the nature of the impact device and the method of exposing the cortex. Impact device modifications have generally been a function of available technology, and developments have been aimed toward greater reproducibility and monitoring capabilities. The surgical procedure has had two main approaches, single craniectomy or two bilateral craniectomies. The second cranial opening allows reciprocal movement during impact which alters the nature of the pressure transients that are transmitted during the impact. This is of relevance as cortical impact injury with bilateral craniectomies has been reported to cause diffuse axonal injury which is a hallmark of human TBI (Meany et al., 1994). The axon shearing is thought to be caused by lateral movement of the brain in response to the impact (Povlishock et al., 1992; Povlishock et al., 1983). The wide distribution of dystrophic cells that we detected following cortical impact injury may be accounted for, at least in part, by the use of the bilateral craniectomy employed in this study. In addition, we consistently observed a qualitative correlation between the exact location of the impact in a specific animal and the dystrophic cell staining pattern. For example, the patch of dystrophic cells in the dentate gyrus would shift in position in accordance with impact angle, suggesting perhaps a corticotopic representation in the hippocampus. Future experiments systematically utilizing different impact angles may help verify this hypothesis.

Work at the University of Texas Department of Neurosurgery had previously reported that cortical impact injury with bilateral craniectomy causes deficits in spatial learning and memory using a Morris water maze task (Dash et al., 1995; Long et al.,

1996). It had also been previously proposed that hippocampal cell death may contribute to these deficits (Goodman et al., 1994; Kotapka et al., 1991), due to the functional role of the hippocampus in the memory process (Squire, 1986). Performance in the water maze task is thought to require both hippocampal and entorhinal cortical function (Morris et al., 1982). In this TBI study, marked cell loss was detected in the dentate gyrus, CA1 and CA3 regions. It is therefore possible that the cell loss in these regions could alter neuronal signalling and may contribute to the observed spatial memory deficits. It is difficult to ascertain from this study which of these three hippocampal regions are more important with respect to post-traumatic memory dysfunction. It has been suggested that loss of cells in any subfield of the hippocampus would contribute to spatial memory dysfunction (Amaral and Witter., 1989). Moreover, since the hippocampus receives inputs from various parts of the brain and is involved in integration of information, loss of these cells could also contribute to other cognitive impairments. Furthermore, the identification in this study of cell loss in the amygdala, piriform cortex, thalamus and hypothalamus following cortical impact injury suggests other behavioural deficits might occur following TBI. These deficits would not be detectable by the Morris water maze test, and consequently would require alternative behavioural assays to quantify their extent.

5.1.2) Cell death

This work reported the first description of apoptotic cell loss as a result of experimental cortical impact injury. Several techniques were used to accomplish this.

Modified silver staining demonstrated a large number of argyrophilic cells in the dentate gyrus, CA1 and CA3 subfields of the hippocampus of injured animals. The nature of the detection mechanism utilized by this procedure has not been conclusively demonstrated, however, two theories for its mechanism have been proposed: first, that the membrane of a dystrophic cell is "leaky" and the silver, while in solution, selectively penetrates the cell and upon precipitation forms a black stain in the dying neuron. An alternate hypothesis, presented by Gallyas himself (Gallyas, 1980) suggests that there is an alteration in the microtubule conformation that changes the silver binding efficacy. This second hypothesis is further substantiated by the fact that the production of argyrophilic neurons can occur post-mortem, suggesting that cellular metabolism is unnecessary for the specificity of the stain. This hypothesis is also interesting in terms of the strong labelling seen in the nucleus of the apoptotic cells in this study. Nuclear condensation and compartmentalization of the cell would potentially require microtubule-related machinery to execute this process. A detectable conformational change during this process would be consistent with the increased argyrophilic staining observed. A second issue regarding the significance of the argyrophilic stain was whether or not the neurons eventually die, and if so how long does this process take. Silver stain positive cells were detected for up to two weeks postinjury. However, the argyrophilic neurons visualized at early time points following injury may persist before being cleared and possibly contribute to the signal observed at later time points. The fact that a significant proportion of argyrophilic neurons are dystrophic and eventually die has been established (Crain et al., 1988; Gruenthal et al., 1986; Sloviter et al., 1993a; Sloviter et al., 1993b; Warner et al., 1991).

In agreement with this, we qualitatively observed marked cell loss in the dentate gyrus, CA1 and CA3 subfields of the hippocampus, regions which contained dystrophic neurons.

In addition to these regions, this study also shows the presence of dystrophic cells in the hilar region of the hippocampus, the amygdala, the entorhinal and piriform cortices, the thalamic and hypothalamic regions, and the cortex near the site of impact. The spectrum of brain regions affected can be attributed to the many neuropathological paradigms associated with TBI. Seizure activity, ischemia and mechanical trauma are all components of TBI, and their interaction during the injury will result in the profile observed.

Three forms of neuronal loss following TBI are observed. Cell death due to physical damage as a result of trauma occurs immediately upon impact. While perhaps trivialized due to its simplistic mechanism, it is the response to this event that results in the signals that lead to the processes under investigation. For example, the mechanical cell loss that immediately occurs can include neurons involved in regulatory and inhibitory pathways, and the result could be the hyper-excitation of certain brain regions. This can lead to the second form of cell death observed, necrosis, which is most likely due to depletion of the cell's ATP stores as a result of the release of excessive excitatory neurotransmitters such as glutamate. Several hippocampal regions such as CA3 and CA1 are hyper-susceptible to this effect. Another form of necrotic cell death occurs shortly following injury due to ischemic loss of blood flow as a result of broken vessels and similar tissue damage. The third form of cell death is the delayed cell death reported in detail in this study. Its relationship to the immediate cell loss could be through

mechanisms such as growth factor withdrawal due to lost connectivity in the system. Several studies have shown that the apoptotic death of CNS neurons can result from the loss of target-derived trophic factors or by prolonged exposure to low levels of excitatory neurotransmitters (Ankarcrona et al., 1995; Deckwerth and Johnson, 1993). While the first two types of cell death occur soon after trauma and may not provide an adequate time window for clinical intervention, delayed cell death offers more opportunity in this regard. It has been emphasized in this work that apoptosis is a morphologically defined term. It was the morphological examination of the post injury tissue that led to the further characterization of the mechanism of cell death in the second chapter. For example, some of these cells contained apoptotic bodies and vacuoles, where as some appeared shrunken with condensed chromatin. These cells may represent different stages of apoptosis, and were subsequently investigated in further detail.

5.1.3) Apoptosis

In this study, we examined morphological and biochemical properties of dentate gyrus granule cells following controlled cortical impact brain injury. The dystrophic cells, as identified by silver impregnation, cresyl violet, and Hoechst staining, appear shrunken and have condensed nuclei and chromatin. These cells were predominantly localized to the inner blade of the dentate gyrus. When semi-thin sections of this region were examined, the dystrophic cells were found to be hyperchromatic and shrunken. At the interface between the normal and the dystrophic granule cells, both a quantitative and a qualitative gradient of apoptotic morphology was observed. In this transition region, by

definition, the number of argyrophilic neurons is decreasing, but in addition to this the morphological characteristics also became less distinct. This was interpreted from the observation of the presence of many argyrophilic neurons with a high degree of membrane integrity. However, these cells also contained clearly visible apoptotic bodies and vacuoles. This was an initial indication that the neurons within the heavily dystrophic region exhibited characteristics of necrotic cells as well. This observation necessitated the detailed examination of these cells, to accurately determine the nature of the cell death.

Electron microscopic analysis revealed that the cells did indeed show morphological determinants of apoptosis, including the presence of condensed chromatin associated with the nuclear membrane, and segmentation of the nucleus. The nuclear events of apoptosis begin with the chromatin condensing into large clumps (Duvall and Wyllie, 1986; Earnshaw, 1986; Kerr et al., 1972; Wyllie et al., 1981). These clumps are localized to the nuclear envelope (Earnshaw, 1986). The nuclear pores then redistribute by sliding away from the attachment points of the condensed chromatin and accumulating between them (Lazebnik et al., 1993). Subsequently, nuclear segmentation occurs. Granule cells undergoing apoptosis following TBI had their condensed chromatin appended to the nuclear periphery and showed nuclear segmentation. As previously mentioned, neurons at the core of the dystrophic region appeared to possess some necrotic characteristics as well. Under EM examination, discontinuities in the nuclear membrane can be seen in these cells. This could be due to necrotic membrane breakdown; however, an alternate hypothesis would be the accumulation of nuclear pores. Other characteristic features of apoptosis such as vacuole formation, intact rough endoplasmic reticulum, and

normal mitochondria were detected in these apoptotic granule cells. This conclusively demonstrated the presence of the critical morphological features that define apoptosis. However, the number of mitochondria also appeared to be less than in normal cells. In addition, several mitochondria appeared swollen, again suggesting some loss of membrane integrity. A possible resolution to these parallel observations is that the apoptotic machinery has been activated, but some necrotic features can be observed since the cells are under duress from a multitude of deleterious stresses.

The detection of DNA laddering by gel electrophoresis and *in situ* TUNEL staining were used to examine a biochemical correlate of apoptosis (Batistaton and Greene, 1991; Wyllie et al., 1984). During the process of nuclear breakdown, the cleavage of the DNA into ~180 bp fragments has been a hallmark of apoptosis (Cain et al., 1994). Using hippocampal cytoplasmic DNA extracts, the characteristic DNA ladder was observed in samples obtained from injured animals. The intensity of this ladder was maximal at 24 hours postinjury in the ipsilateral hippocampal sample, consistent with the finding that dystrophic neurons are more abundant in the ipsilateral as compared to the contralateral hippocampus at this time point. There are several endonucleases functioning during apoptosis, one producing 50 and 300 kb fragments (Walker et al., 1994), and a second producing the 180-200 bp internucleosomal fragments (Cain et al., 1994). Although no direct activity measurements were made, the presence of a 180 bp ladder suggests that at least one nuclease is present (Brown et al., 1993; Earnshaw, 1986). In this study, close examination of the TUNEL positive cells suggests that the nucleosome fragments generated are small enough to leak out of the nucleus. TUNEL staining can

also potentially label necrotic nuclei, in that the non-specific degradation of the chromatin would produce a similar increase in 3'-OH groups. However, degradation of the DNA during necrosis is rapid and is not likely to contribute to the labelling reactions at the delayed time points we examined (Bonfoco et al., 1995; Gerschenson and Rotello, 1992). Further evidence for this comes from the fact that the necrotic cells at the site of injury in the cortex did not show strong positive TUNEL staining.

The combination of morphological and biochemical markers for apoptosis demonstrate that activation of apoptotic mechanisms did occur. The contribution of necrosis, however, to the cell death is still uncertain. Apoptosis occurs in two physiological stages. First, a signal, which may be either intrinsic or extrinsic to the cell, causes the cell to enter a committed phase (Earnshaw, 1986). This is then followed by an execution phase, which is autonomously carried out by the cell. The known morphological features of apoptosis were observed following TBI would arise during this phase. Depending on the cell type and the surrounding environment, the duration of the commitment and execution phases may vary. The potential for necrotic injury to overcome an apoptotic cell would always be present during this time. This can be further complicated by the coexistence of cells, some with necrotic and others with apoptotic features, making it difficult to determine the mechanism most significantly contributing to cell death. As previously noted, the potential for the coexistence of both morphologies in the same cell also exists. There are several explanations for this. First, it has been reported that the same insult can elicit either necrosis or apoptosis (Ankarcrona et al., 1995; Choi, 1995). This phenomenon has been observed in several cell types including

neurons. For example, cultured neurons exposed to glutamate or NMDA can show the morphological features of both apoptosis and necrosis (Ankarcrona et al., 1995; Bonfoco et al., 1995). Therefore, it is possible that a single insult, depending on the intensity and duration, may trigger apoptosis and necrosis simultaneously. Second, it is possible that following TBI some cells receive a signal to enter the committed phase of apoptosis and begin the execution phase as observed by cell shrinkage and condensed chromatin. However, subsequent to this, a secondary insult may result in the necrotic morphologies we observed. This is consistent with the reports that following TBI calcium continues to accumulate for up to 48 hrs after the injury (Fineman et al., 1993). Thus, cells may initially begin an apoptotic process, but as calcium continues to accumulate, become necrotic. Finally, it is possible that the duration of the execution phase was too long, allowing secondary necrosis to eliminate the cell (Catchpoole and Stewart, 1993).

5.2) Netrin expression and induction in the adult mammalian brain

5.2.1) Potential mechanisms of regeneration in the CNS

Following brain injury, there are often immediate observable behavioural deficits. Fortunately, there often is also some degree of recovery from these deficits. A potential mechanism for this recovery is the re-initiation of the neuronal growth processes that function during normal development of the nervous system. This has prompted many investigations into the post-injury state of growth factors, transcription factors and other developmental effectors. To investigate a new candidate contributing to the functional mechanisms of post-injury neuronal remodelling, this study examined the expression of a

recently identified chemotrophic factor, netrin. Constitutive expression of netrin in the adult mammalian brain was demonstrated in cortex, hippocampus, cerebellum, basal ganglia, amygdaliod and hypothalamic regions. The presence of this developmentally critical molecule suggested that it could be playing a continuing role during the life of the individual. Induction of netrin following seizure in brain regions shown to undergo post-seizure sprouting was also demonstrated. As there is evidence that netrin can also function as a short-range target recognition molecule (Winberg et al., 1998), this suggests netrin may play a role in in post-seizure neuronal reorganization.

5.2.2) Netrin expression in the normal adult brain

During nervous system development, axons navigate successfully to their targets by responding to guidance cues in the environment (Tessier-Lavigne and Goodman, 1996). A role for netrin in long distance axonal guidance has been established in the case of the development of spinal cord dorsal commissural neurons (Kennedy et al., 1994, Serafini et al 1994) and trochlear motor neurons (Colamarino and Tessier-Lavigne, 1995a). Netrin has also been implicated in the guidance of axons in the dorsal hindbrain and cerebellum (Shirasaki et al., 1995; Tamada et al., 1995; Ackerman et al., 1997) and of retinal ganglion cell growth cones (Diener et al., 1997, Delatorre et al., 1997). Continued expression of netrin in the adult has been reported (Kennedy et al., 1994) and regions of high expression have been identified in an *in situ* analysis of netrin-1 expression in the adult rat brain (Livesey and Hunt, 1997). Here, as a foundation for investigating the role of netrin in the adult, a complete analysis of the netrin-1 mRNA and

the distribution of netrin protein was carried out. Immunohistochemical analysis demonstrated the presence of netrin protein in many brain regions, with a high degree of specificity for distinct cell types. The global distribution of netrin immunoreactivity identified specific brain structures having enhanced netrin expression. To identify the specific cellular sources of the protein, two techniques were employed: *in situ* hybridization and analysis of a transgenic netrin-1 ^{β gal⁺} mouse. *In situ* hybridization analysis provided direct identification of netrin mRNA positive cells, and was also instrumental in identifying the regions in which netrin was transcriptionally induced post-seizure. The complimentary approach of utilizing a transgenic mouse that expressed beta-galactosidase under the control of the netrin-1 promoter provided a simple way to perform a whole-brain analysis of the spatial expression profile. Using these techniques, normal netrin expression was established in components of the basal ganglia, cortex, hippocampus, cerebellar, amygdaloid and hypothalamic regions.

5.2.3) Netrin induction following pilocarpine induced seizure

One week following pilocarpine induced seizure, netrin expression was induced in the hippocampus and entorhinal cortex. Many previous studies have established the presence of robust mossy fiber sprouting in the hippocampus following seizure activity (for review see Holtzman and Lowenstein, 1995). Netrin induction was observed in both hippocampal granule cells and pyramidal cells, the targets of sprouting mossy fibers. In studies of neural development, two potential roles for netrin have been described, acting as a long range target derived axon guidance cue (Kennedy et al., 1994) and as a short-

range target recognition cue (Winberg et al., 1998). As such, it is possible that netrin plays a role in directing or promoting mossy fiber axon outgrowth in the hippocampus post-seizure.

This study also replicated the documented damage suffered by the entorhinal cortex following seizure (Du et al., 1995). While sprouting in this region has not been previously reported, alteration in the electrophysiological response of the circuits involving this region has been documented (Nagao et al., 1996; Nagao et al., 1994). The enhanced expression of netrin and one of its chemoattractant receptors DDC, in the neurons of this region suggests that if netrin contributes to directing neuronal remodeling, in a manner similar to that seen in the hippocampal dentate gyrus, the regulated expression of netrin in this region may be of functional significance as well.

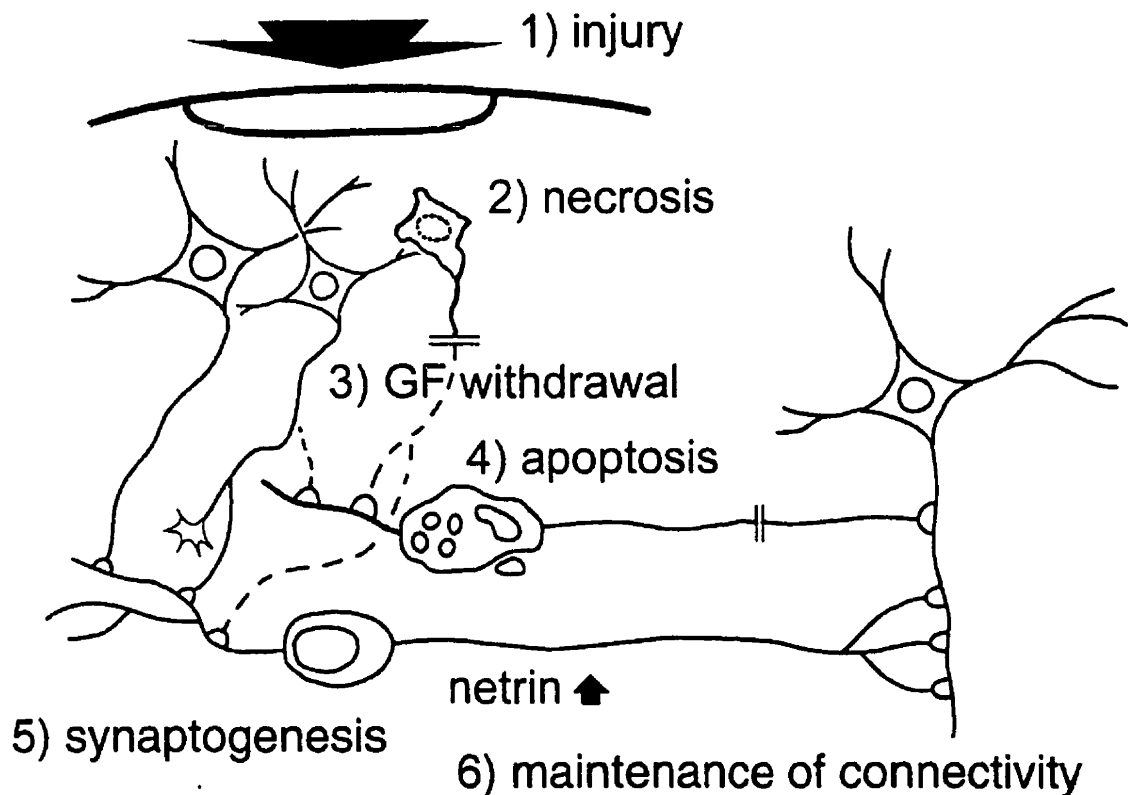
Prior to the induction of netrin expression observed at 3 days and 1 week post-seizure, an initial overall decrease in the level of netrin immunoreactivity is detected one day post-seizure. This change in immunoreactivity could reflect either a direct change in netrin levels, or could result from a post-injury increase in proteolytic processing of pre-existing netrin. This is currently being investigated (Kennedy, personal communication). Experimentally induced seizure activity in rats has often been used to isolate and study neuronal activity-dependent genes (Qian et al., 1993) and a large body of information describing the gene induction events regulating these processes has been collected. While the gene expression cascade regulating the induction of netrin is unknown, candidate signalling molecules known to be regulated by seizure are being investigated (Kennedy personal communication).

5.2.4) **Physiological function of netrin in the adult**

The expression of the embryonic chemotropic molecule netrin continues in the normal adult mammal, and is localized post-seizure to regions of post-seizure sprouting and altered electrophysiological response. Acting as an axon guidance molecule and/or a short-range target recognition molecule for synapse formation, netrin could play a role in these events. In addition to its possible role in post-injury neuronal remodelling, netrin is also present in many brain structures demonstrated to exhibit activity-dependent plasticity. Growth of new synaptic connections and structural synaptic changes may be a component of activity dependent plasticity (for review see Bailey and Kandel, 1993). This study demonstrates co-localization of netrin immunoreactivity with neuronal structures having the morphological characteristics of synapses. In recent studies, the association of netrin with the synapse has been further substantiated by cell fractionation, which has localized netrin to synaptic E.R./golgi and synaptic plasmalemma fractions, and DCC to synapse associated vesicles, synaptosomal organelles and synaptic plasmalemma (Kennedy and Fawcett, personal communication). It is an intriguing possibility that netrin may also play a role in non-pathological synapse maintenance or plasticity.

5.3) The neuronal response to injury

The following diagram summarizes the aspects of the neuronal response to injury addressed in this thesis, and proposes a model describing how they may interact.



Immediately following injury there is both direct neuronal loss (1) and necrosis (2). A consequence of this neuronal cell death is that cells that received either anterograde or retrograde trophic support from these dead cells will now be deprived of trophic support (3) [loss of anterograde trophic support illustrated]. This loss of trophic support may lead to a delayed induction of apoptosis in the deprived neurons (4). This persistent apoptosis will result in further denervation and may contribute to a continued long term cascade of apoptotic cell death. In response to cell death, denervation, and/or changes in activity,

regenerative sprouting activity is triggered in some neurons. This regenerative activity may be promoted by an increase in tropic cues such as netrins and netrin receptors and promote synaptogenesis (5) in affected brain regions. As a consequence of the activation of this regenerative program, connectivity may be maintained (6) or modified in ways that both benefit and/or are deleterious for brain function in the affected individual.

6) Bibliography

Ackerman, S.L., Kozak, L.P., Przyborski, S.A., Rund, L.A., Boyer, B.B., Knowles, B.B. (1997) The mouse rostral cerebellar malformation gene encodes an UNC-5-like protein. *Nature* 386(6627):838-42.

Alam, A.M., Starr, M.S. (1996) Regional changes in brain dopamine utilization during status epilepticus in the rat induced by systemic pilocarpine and intrahippocampal carbachol. *Neuropharmacology* Feb;35(2):159-67.

Alnemri, E.S., and Litwack, G. (1993) Glucocorticoid-induced programmed cell death (apoptosis) in leukemia and pre-b cells. In *Programmed Cell Death*, Lavin, M. and Watters, D. eds., Harwood Academic Publishers, Switzerland., pp 99.

Amaral, D. and Witter, M.P. (1989) The three dimensional organization of the hippocampal formation: a review of anatomical data. *Neurosci*, 31 571-591.

Amaral, D.G. (1978) A Golgi study of cell types in the hilar region of the hippocampus in the rat. *J Comp Neurol* 182(4 Pt 2):851-914.

Amati, B., Alevizopoulos, K., Vlach, J. (1998) Myc and the cell cycle. *Front Biosci* Feb 15;3:D250-68.

Ankarcrona, M., Dybukt, J.M., Bonfoco, E., Zhivotovsky, B., Orrenius, S., Lipton, S.A. and Nicotera, P. (1995) Glutamate-induced neuronal death: A succession of necrosis or apoptosis depending on mitochondrial function. *Neuron*, 15 961-973.

Arends, M.J. and Wyllie, A.H. (1991) Apoptosis: mechanisms and role in pathology, *Int. Rev. Exp. Pathol.*, 32 223-254.

Ashkenazi, A., Dixit, V.M. (1998) Death receptors: signaling and modulation. *Science* ;281(5381):1305-8

Auer, R.N. and Siesjo, B.K. (1988) Biological differences between ischemia, hypoglycemia, and epilepsy. *Annals Neurol*, 24 699-707.

Babb, L. and Brown, W.J. (1991) Neuronal, dendritic and vascular profiles of human temporal lobe epilepsy correlated with cellular physiology *in vivo*. In *Basic Mechanisms of Epilepsies: Advances in Neurology*, vol 44, 949-966.

Babb, T.L., Pretorius, J.K., Kupfer, W.R., Crandal, P.H. (1989) Glutamate decarboxylase-immunoreactive neurons are preserved in human epileptic hippocampus. *J Neurosci* 9(7):2562-74.

Bailey, C.H., Kandel, E.R. (1993) Structural changes accompanying memory storage. *Annu Rev Physiol* 55:397-426.

Barnes, C.A. (1979) Memory deficits associated with senescence: a neurophysiological and behavioral study, *J. Comp. Physiol. Psychol.*, 93:74-104.

Barker, P.A (1998) p75^{NTR}: A study in contrasts. *Cell Death and Differentiation* 5, 346-356.

Barinaga, M. (1998) Stroke-damaged neurons may commit cellular suicide. *Science* Aug 28;281(5381):1302-3.

Batistatou, A. and Greene, L.A. (1991) Aurintricarboxylic acid rescues PC12 and sympathetic neurons from cell death caused by nerve growth factor deprivation: correlation with suppression of endonuclease activity. *J. Cell Biol.*, 115:461-471.

Baudry, M., Lynch, G., Gall, C. (1986) Induction of ornithine decarboxylase as a possible mediator of seizure-elicited changes in genomic expression in rat hippocampus. *J Neurosci* 6(12):3430-5.

Bengzon, J., Kokaia, Z., Elmer, E., Nanobashvili, A., Kokaia, M., Lindvall, O. (1997) Apoptosis and proliferation of dentate gyrus neurons after single and intermittent limbic seizures. *Proc Natl Acad Sci U S A* Sep 16;94(19):10432-7.

Boll, T.J., in *Head Injury*. Paul R Cooper, Ed. Behavioral Sequelae of Head Injury. Williams and Wilkins. (1982) 363-375.

Bonfoco, E., Krainc, D., Ankarcrona, M., Nicotera, P. and Lipton, S.A. (1995) Apoptosis and necrosis: two distinct events induced respectively by mild and intense insults with N-methyl-D-aspartate or nitric oxide/superoxide in cortical cell cultures. *Proc. Natl. Acad. Sci.*, 92:7162-7166.

Braissant, O. and Wahli, W. (1998) A simplified *in situ* hybridization protocol using non-radioactively labeled probes to detect abundant and rare mRNAs on tissue sections. *Biochemica*, 1:10-16.

Brown, D.G., Sun, X.,-M and Cohen, G.M. (1993) Dexamethasone-induced apoptosis involves cleavage of DNA to large fragments prior to internucleosomal fragmentation. *J. Biol. Chem* 268:3037-3039.

Bryan, R.M. Jr., Cherian, L., Robertson, C. (1995) Regional cerebral blood flow after controlled cortical impact injury in rats. *Anesthesia & Analgesia*. 80(4):687-95.

Cain, K., Inayat-Hussain, S.H., Wolfe, J.T. and Cohen, G.M. (1994) DNA fragmentation into 200-250 and/or 30-50 kilobase pair fragments in rat liver nuclei is stimulated by Mg^{2+} alone and Ca^{2+}/Mg^{2+} but not by Ca^{2+} alone, *FEBS Lett.*, 349:385-91.

Cajal, Santiago Ramón y, (1909-1911) Histologie du système nerveux de l'homme et des vertébrés, Paris: Maloine.

Catchpole, D.R. and Stewart, B.W. (1993) Etoposide-induced cytotoxicity in two human T-cell leukemic lines: delayed loss of membrane permeability rather than DNA fragmentation as an indicator of programmed cell death. *Cancer Res.* 53:4287-96.

Cavalheiro, E.A., Leite, J.P., Bortolotto, Z.A., Turski, W.A., Ikonomidou, C., Turski, L. (1991) Long-term effects of pilocarpine in rats: structural damage of the brain triggers kindling and spontaneous recurrent seizures. *Epilepsia Nov-Dec*;32(6):778-82.

Chan, S.S., Zheng, H., Su, M.W., Wilk, R., Killeen, M.T., Hedgecock, E.M., Culotti, J.G. (1996) UNC-40, a *C. elegans* homolog of DCC (Deleted in Colorectal Cancer), is required in motile cells responding to UNC-6 netrin cues. *Cell* 87(2):187-95.

Charriaut-Marlangue, C., Aggoun-Zouaoui D., Represa A. and Ben-Ari Y. (1996) Apoptotic features of selective neuronal death in ischemia, epilepsy and gp120 toxicity, *Trends Neurosci.*, 19:109-114.

Charriaut-Marlangue C., Margaill, I., Plotkine, M. and Ben-Ari, Y. (1995) Early endonuclease activation following reversible focal ischemia in the rat brain. *J. Cereb. Blood Flow Metab.*, 15 385-388.

Choi, D.W. (1995) Calcium: still center-stage in hypoxic-ischemic neuronal death, *TINS*, 18:58-60.

Colamarino, S.A., Tessier-Lavigne, M. (1995a) The axonal chemoattractant netrin-1 is also a chemorepellent for trochlear motor axons. *Cell* 81(4):621-9.

Colamarino, S.A., Tessier-Lavigne, M. (1995b) The role of the floor plate in axon guidance. *Annu Rev Neurosci* 18:497-529.

Colicos, M.A., Baranes, D., Aznar, S., Shatzmiller, R., Manitt, C., Swedlow, P., Kelly, M.E., McIntyre, D.C., Tessier-Lavigne, M., Lowenstein, D.H., Kennedy, T.E. (1997) Netrin expression in the adult mammalian brain. *Soc. Neurosci. Abstr.*

Colicos, M.A., Dash, P.K. (1996) Apoptotic morphology of dentate gyrus granule cells following cortical impact injury: Possible role in spatial memory deficits. *Brain Research* 739:111-119.

Colicos, M.A., Dixon, C.E., Dash, P.K. (1996) Selective neuronal death following cortical impact injury in rats: A silver impregnation study. *Brain Research* 739:120-131.

Coulter, D.A., Rafiq, A., Shumate, M., Gong, Q.Z., DeLorenzo, R.J., Lyeth, B.G. (1996) Brain injury-induced enhanced limbic epileptogenesis: anatomical and physiological parallels to an animal model of temporal lobe epilepsy. *Epilepsy Res* Dec;26(1):81-91

Cossarizza, A., Kalashnikova, G., Grassilli, E., Chiappelli, F., Salvioli, S., Capri, M., Barbieri, D., Troiano, L., Monti, D. and Franceschi, C. (1994) Mitochondrial modification during rat thymocyte apoptosis: a study at the single cell level. *Exptl. Cell Res.*, 214:323-330.

Crain, B.J., Westerkam, W.D., Harrison, A.H. and Nadler, J.V. (1988) Selective neuronal death after transient forebrain ischemia in the Mongolian gerbil: a silver impregnation study. *J. Neuroscience* 27:387-402.

Dash, P.K., Moore, A.N. and Dixon, C.E. (1995) Spatial memory deficits, increased phosphorylation of the transcription factor CREB, and induction of AP-1 complex following experimental brain injury. *J. Neurosci.*, 15:2030-2039.

Deckwerth, T.L. and Johnson, E.M. Jr. (1993) Neurotrophic factor deprivation-induced death. *Ann. N.Y. Acad. Sci.*, 679:121-131.

Deiner, M.S., Kennedy, T.E., Fazeli, A., Serafini, T., Skarnes, W.C., Tessier-Lavigne, M., Sretavan, D.W. (1997). Netrin-1 and DCC mediate axon guidance at the optic disc: loss of function leads to optic nerve hypoplasia. *Neuron* 19, 575-589.

de la Torre, J.R., Hopker, V.H., Ming, G.L., Poo, M.M., Tessier-Lavigne, M., Hemmati-Brivanlou, A., Holt, C.E. (1997) Turning of retinal growth cones in a netrin-1 gradient mediated by the netrin receptor DCC. *Neuron* 19(6):1211-24.

Dixon, C.E., Lyeth, B.G., Povlishock, J.T., Findling, R.L., Hamm, R.J., Marmarou, A., Young, H.P. and Hayes, R.L. (1987) A fluid-percussion model of experimental brain injury in the rat, *J. Neurosurg.*, 67:110-119.

Dixon, C.E., Clifton, G.L., Lighthall, J.W., Yaghma, A.A. and Hayes, R.L. (1991) A controlled cortical impact model of traumatic brain injury in the rat. *J. Neurosci. Methods*, 39:253-62.

Dixon, C.E. and Hayes, R.L. (1996) Fluid-percussion and cortical impact models of traumatic brain injury. *J. Neurotrauma*, in press.

Du, F., Eid, T., Lothman, E.W., Kohler, C., Schwarcz, R. (1995) Preferential neuronal loss in layer III of the medial entorhinal cortex in rat models of temporal lobe epilepsy. *J Neurosci* Oct;15(10):6301-13.

Duvall, E., Wyllie, A.H., Morris, R.G. (1985) Macrophage recognition of cells undergoing programmed cell death (apoptosis), *Immunology*, 56:351-358.

Duvall, E., and Wyllie, A.H. (1986) Death and the cell. *Immunology Today*, 7:115-119.

Earnshaw, W.C. (1986) Nuclear changes in apoptosis. *Current Opinion in Cell Biology*, 7:115-119.

Enari, M., Sakahira, H., Yokoyama, H., Okawa, K., Iwamatsu, A., Nagata, S. (1998) A caspase-activated DNase that degrades DNA during apoptosis, and its inhibitor ICAD [published erratum appears in *Nature* 1998 May 28;393(6683):396] *Nature*. 391(6662):43-50.

Emfors, P., Bengzon, J., Kokaia, Z., Persson, H., Lindvall, O. (1991) Increased levels of messenger RNAs for neurotrophic factors in the brain during kindling epileptogenesis. *Neuron* 7(1):165-76.

Evan, G. and Littlewood, T. (1998) A matter of life and cell death. *Science*. 281(5381): 1317-22.

Fadok, V.A., Voelker, D.R., Campbell, P.A., Cohen, J.J., Bratton, D.L. and Henson, P.M. (1992) Exposure of phosphatidylserine on the surface of apoptotic lymphocytes triggers specific recognition and removal by macrophages, *J. Immunol.*, 148:2207-16.

Fazeli, A., Dickinson, S.L., Hermiston, M.L., Tighe, R.V., Steen, R.G., Small, C.G., Stoeckli, E.T., Keino-Masu, K., Masu, M., Rayburn, H., Simons, J., Bronson, R.T., Gordon, J.I., Tessier-Lavigne, M., Weinberg, R.A. (1997) Phenotype of mice lacking functional Deleted in colorectal cancer (Dcc) gene. *Nature* 386(6627):796-804.

Fineman, I., Hovda, D., Smith, M., Yoshino and Baker D. (1993) Concussive brain injury is associated with a prolonged accumulation of calcium: A ⁴⁵Ca autoradiograph study, *Brain Res.*, 624:94-102.

Fujikawa, D.G. (1996) The temporal evolution of neuronal damage from pilocarpine-induced status epilepticus. *Brain Res Jun 24;725(1):11-22.*

Gall, C.M., Isackson, P.J. (1989) Limbic seizures increase neuronal production of messenger RNA for nerve growth factor. *Science 245(4919):758-61.*

Gall, C.M. (1993) Seizure-induced changes in neurotrophin expression: implications for epilepsy. *Exp Neurol 124(1):150-66.*

Gallyas, F., Wolff, J.R., Bottcher, H. and Zaborszky, L. (1980) A reliable and sensitive method to localize terminal degeneration and lysosomes in the central nervous system, *Stain Technol.*, 55:299-306.

Gallyas, F. and Zoltay, G. (1992) An immediate light microscopic response of neuronal somata, dendrites, and axons to non-contusing concussive head injury in the rat. *Acta Neuropathol.*, 83:386-393.

Gennarelli, T.A. (1994) Animate models of human head injury. *J. Neurotrauma.*, 11:357-368.

George, B., Kulkarni, S.K. (1997) Dopaminergic modulation of lithium/pilocarpine-induced status epilepticus in rats. *Methods Find Exp Clin Pharmacol Sep;19(7):481-8.*

Gerschenson, L.E. and Rotello, R.J. (1992) Apoptosis: a different type of cell death, *The FASEB Journal*, 6 2450-2455.

Gwag, B.J., Lobner, D., Koh, J., Wie, M.B. and Choi, D.W. (1994) Blockade of glutamate receptors during oxygen or glucose deprivation unmasks apoptosis in cultured cortical neurons. *Society for Neurosci.*, Abs 20:248.

Goodman, J.C., Cherian, L., Bryan, R.M. Jr. and Robertson, C.S. (1994) Lateral cortical impact injury in rats: pathological effects of varying cortical compression and impact velocity. *J. Neurotrauma*, 11:587-597.

Gruenthal, M., Armstrong, D.R., Ault, B. and Nadler, J.V. (1986) Comparison of seizures and brain lesions produced by intracerebroventricular kainic acid bicuculline methiodide, *Expl. Neurol.*, 93:621-630.

Gruss, H.J., Dower, S.K. (1995) The TNF ligand superfamily and its relevance for human diseases. *Cytokines & Molecular Therapy*, 1(2):75-105.

Hamani, C., Mello, L.E. (1997) Status epilepticus induced by pilocarpine and picrotoxin. *Epilepsy Res* Jul; 28(1):73-82.

Hamburger, V. and Oppenheim, R.W. (1982) Naturally occurring neuronal death in vertebrates. *Neurosci. Comm.*, 1:39-55.

Hamm, R.J., Dixon, C.E., Gbadebo, D.M., Singha, A.K., Jenkins, L.W., Lyeth, B.G. and Hayes, R.L. (1992) Cognitive deficits following traumatic brain injury produced by controlled cortical impact. *J. Neurotrauma*, 9:11-20.

Harrington, E.A., Fanidi, A., Evan, G.I. (1994) Oncogenes and cell death. *Current Opinion in Genetics & Development*, 4(1):120-9.

Harris, W.A. (1989) Local positional cues in the neuroepithelium guide retinal axons in embryonic *Xenopus* brain. *Nature* 339(6221):218-21.

Hedgecock, E.M., Culotti, J.G., Hall, D.H. (1990) The *unc-5*, *unc-6*, and *unc-40* genes guide circumferential migrations of pioneer axons and mesodermal cells on the epidermis in *C. elegans*. *Neuron* 4(1):61-85.

Hicks, R.R., Smith, D.H., Lowenstein, D.H., Saint-Marie, R. and McIntosh, T.K. (1993) Mild experimental brain injury in the rat induces cognitive deficits associated with regional neuronal loss in the hippocampus. *J. Neurotrauma*, 4 405-414.

Hikosaka, O. (1998) Neural systems for control of voluntary action--a hypothesis. *Adv Biophys* 35:81-102 .

Hofmann, K., Tschopp, J. (1995) The death domain motif found in Fas (Apo-1) and TNF receptor is present in proteins involved in apoptosis and axonal guidance. *FEBS Lett* Sep 11;371(3):321-3.

Holtzman, D.M., Lowenstein, D.H. (1995) Selective inhibition of axon outgrowth by antibodies to NGF in a model of temporal lobe epilepsy. *J Neurosci* Nov;15(11):7062-70.

Hynes, R.O., Lander, A.D. (1992) Contact and adhesive specificities in the associations, migrations, and targeting of cells and axons. *Cell* 68(2):303-22.

Isackson, P.J., Huntsman, M.M., Murray, K.D., Gall, C.M. (1991) BDNF mRNA expression is increased in adult rat forebrain after limbic seizures: temporal patterns of induction distinct from NGF. *Neuron*, Jun;6(6):937-48.

Ishii, N., Wadsworth, W.G., Stern, B.D., Culotti, J.G., Hedgecock, E.M. (1992) UNC-6, a laminin-related protein, guides cell and pioneer axon migrations in *C. elegans*. *Neuron* 9(5):873-81.

Jarrard, L.E. (1993) On the role of the hippocampus in learning and memory in the rat. *Behav Neural Biol* Jul;60(1):9-26.

Jessell, T.M. (1988) Adhesion molecules and the hierarchy of neural development. *Neuron* 1(1):3-13.

Keino-Masu, K., Masu, M., Hinck, L., Leonardo, E.D., Chan, S.S., Culotti, J.G., Tessier-Lavigne, M. (1996) Deleted in Colorectal Cancer (DCC) encodes a netrin receptor. *Cell* Oct 18;87(2):175-85.

Kennedy, T.E., Colicos, M.A., Swedlow, P., Shatzmiller, R., Liebowitz, R., Kelly, M.E., Serafini, T., Skarnes, W., McIntyre, D.C., Tessier-Lavigne, M., Lowenstein, D.H. (1996a) Evidence for constitutive expression of netrin in the adult rodent hippocampus. *Annual Meeting of the American Epilepsy Society*.

Kennedy, T.E., Hinck, L., Colamarino, S., Mirzayan, C., Faynboym, S., Marshall, W., Tessier-Lavigne, M. (1996b) Graded expression of netrin protein in the embryonic spinal cord. *Soc. Neurosci. Abstr.*

Kennedy, T.E., Serafini, T., de la Torre, J.R., Tessier-Lavigne, M. (1994) Netrins are diffusible chemotropic factors for commissural axons in the embryonic spinal cord. *Cell* 78(3):425-35.

Kerr, J.F.R. (1993) Introduction: Definition of apoptosis and overview of its incidence. In *Programmed Cell Death*, Lavin, M. and Watters, D. eds., Harwood Academic Publishers, Switzerland., pp 99.

Kerr, J.F.R., Searle, J., Harmon, B.V. and Bishop, C.J. (1987) *Apoptosis. In Perspectives on Mammalian Cell Death* (Potten CS ed) pp 93-128, Oxford University Press, Oxford, England.

Kerr, J.F., Wyllie, A.H. and Currie, A.R. (1972) Apoptosis: a basic biological phenomenon with wide-ranging implications in tissue kinetics, *Br. J. Cancer*, 26 239-57.

Kolodziej, P.A., Timpe, L.C., Mitchell, K.J., Fried, S.R., Goodman, C.S., Jan, L.Y., Jan, Y.N. (1996) frazzled encodes a Drosophila member of the DCC immunoglobulin subfamily and is required for CNS and motor axon guidance. *Cell* 87(2):197-204.

Kotapka, M.J., Gennarelli, T.A., Graham, D.I., Adams, J.H., Thibault, L.E., Ross, D.T. and Ford, I. (1991) Selective vulnerability of hippocampal neurons in acceleration-induced experimental head injury. *J. Neurotrauma*, 8:247-258.

Lance-Jones, C., Landmesser, L. (1981) Pathway selection by embryonic chick motoneurons in an experimentally altered environment. *Proc R Soc Lond B Biol Sci* 214(1194):19-52.

Lance-Jones, C., Landmesser, L. (1980) Motoneurone projection patterns in embryonic chick limbs following partial deletions of the spinal cord. *J Physiol (Lond)* 302:559-80.

de Lanerolle, N.C., Kim, J.H., Robbins, R.J., Spencer, D.D. (1989) Hippocampal interneuron loss and plasticity in human temporal lobe epilepsy. *Brain Res* 495(2):387-95.

Lazebnik, Y.A., Cole, S., Cooke, C.A., Nelson, W.G. and Earnshaw, W.C. (1993) Nuclear events in apoptosis *in vitro* in cell-free mitotic extracts: a model system for analysis of the active phase of apoptosis. *J. Cell Biol.*, 123:7-22.

Leonardo, E.D., Hinck, L., Masu, M., Keino-Masu, K., Ackerman, S.L., Tessier-Lavigne, M. (1997) Vertebrate homologues of *C. elegans* UNC-5 are candidate netrin receptors *Nature*, Apr 24;386(6627):833-8.

Leung-Hagesteijn, C., Spence, A.M., Stern, B.D., Zhou, Y., Su, M.W., Hedgecock, E.M., Culotti, J.G. (1992) UNC-5, a transmembrane protein with immunoglobulin and thrombospondin type 1 domains, guides cell and pioneer axon migrations in *C. elegans*. *Cell* 71(2):289-99.

Levin, H.S. (1992) Neurobehavioral recovery Central nervous system trauma status report. *J. Neurotrauma*, S359-S373.

Li, Y., Chopp, M., Jiang, N., Zhang, Z.G. and Zaloga, C. (1995) Induction of DNA fragmentation after 10 to 120 minutes of focal cerebral ischemia in rats, *Stroke*, 26:1257-1258.

Liu, X., Zou, H., Slaughter, C., Wang, X (1997) DFF, a heterodimeric protein that functions downstream of caspase-3 to trigger DNA fragmentation during apoptosis. *Cell*. 89(2):175-84.

Livesey, F.J., Hunt, S.P. (1997) Netrin and netrin receptor expression in the embryonic mammalian nervous system suggests roles in retinal, striatal, nigral, and cerebellar development. *Mol Cell Neurosci* 8(6):417-29.

Long, D.A., Ghosh, K., Moore, A.N., Dixon, C.E. and Dash, P.K. (1996) Deferoxamine improves spatial memory performance following experimental brain injury in rats. *Brain Res Apr* 22;717(1-2):109-17.

Loo, D.T., Copani, A., Pike, C.J., Whittmore, E.R., Warncewicz, A.J. and Cotman, C.W. (1993) Apoptosis is induced by β -amyloid in cultured central nervous system neuron. *Proc. Natl. Acad. Sci.* 90 7951-7955.

Lowenstein, D.H., Thomas, M.J., Smith, D.H. and McIntosh, T.K. (1992) Selective vulnerability of dentate hilar neurons following traumatic brain injury: a potential mechanistic link between head trauma and disorders of the hippocampus. *J. Neurosci.*, 12 4846-53.

Lumsden, A.G., Davies, A.M. (1983) Earliest sensory nerve fibres are guided to peripheral targets by attractants other than nerve growth factor. *Nature* 306(5945):786-8

Lumsden, A.G., Davies, A.M. (1986) Chemotropic effect of specific target epithelium in the developing mammalian nervous system. *Nature* 323(6088):538-9.

Lyeth, B.G., Jenkins, L.W. and Hamm, R.J. (1990) Prolonged memory impairment in the absence of hippocampal cell death following traumatic brain injury in the rat. *Brain Res* 256:249-258.

Ma, J., Endres, M., Moskowitz, M.A. (1998) Synergistic effects of caspase inhibitors and MK-801 in brain injury after transient focal cerebral ischaemia in mice. *British Journal of Pharmacology*. 124(4):756-62. 1998 Jun.

MacManus, J.P., Buchan, A.M., Hill, I.E., Rasquinha, I. and Preston, E. (1993) Global ischemia can cause DNA fragmentation indicative of apoptosis in rat brain, *Neurosci. Lett.*, 164:89-92.

Marcinkiewicz M, Nagao T, Day R, Seidah NG, Chretien M, Avoli M (1997) Pilocarpine-induced seizures are accompanied by a transient elevation in the messenger RNA expression of the prohormone convertase PC1 in rat hippocampus: comparison with nerve growth factor and brain-derived neurotrophic factor expression. *Neuroscience*, Jan;76(2):425-39.

McIntosh, T., Vink, R., Noble, L., Yamakami, S., Soares, H. and Faden, A. (1989) Traumatic brain injury in the rat: characterization of a lateral fluid percussion model, *Neurosci.*, 28:233-244.

Meaney, D.F., Ross, D.T., Winkelsteon, B.A., Brasko, J., Goldstein, D., Bliston, L.B., Thibault, L.E. and Gennarelli, T.A. (1994) Modification of the cortical impact model to produce axonal injury in the rat cerebral cortex, *J. Neurotrauma*, 11:599-612.

Mello, L.E., Covolan, L. (1996) Spontaneous seizures preferentially injure interneurons in the pilocarpine model of chronic spontaneous seizures. *Epilepsy Res* Dec;26(1):123-9

Mello, L.E., Cavalheiro, E.A., Tan, A.M., Kupfer, W.R., Pretorius, J.K., Babb, T.L., Finch, D.M. (1993) Circuit mechanisms of seizures in the pilocarpine model of chronic epilepsy: cell loss and mossy fiber sprouting. *Epilepsia* Nov-Dec;34(6):985-95.

Meunier, M., Bachevalier, J., Mishkin, M. and Murray, E.A. (1993) Effects of visual recognition of combined and separate ablation of the entorhinal and perirhinal cortex in Rhesus monkeys, *J. Neurosci.*, 13:5418-5432.

Miller, F.D., Kaplan, D.R. (1998) Life and death decisions: a biological role for the p75 neurotrophin receptor. *Cell Death and Differentiation* 5, 343-345.

Morgan, J.I., Curran, T. (1991) Proto-oncogene transcription factors and epilepsy. *Trends Pharmacol Sci Sep*;12(9):343-9.

Morris, R.G.M., Garrud, P., Rawlins, J.N.P. and O'Keefe J. (1982) Place navigation impaired in rats with hippocampal lesions, *Nature*, 297:681-683.

Moser, E., Moser, M.B., Andersen, P. (1993) Spatial learning impairment parallels the magnitude of dorsal hippocampal lesions, but is hardly present following ventral lesions. *J. Neurosci.* 13(9):3.

Nagao T, Alonso A, Avoli M (1996) Epileptiform activity induced by pilocarpine in the rat hippocampal-entorhinal slice preparation. *Neuroscience*, May;72(2):399-408.

Nagao, T., Avoli, M., Gloor, P. (1994) Interictal discharges in the hippocampus of rats with long-term pilocarpine seizures. *Neurosci Lett Jun 20*;174(2):160-4

Nagata, S (1997) Apoptosis by death factor. *Cell.* 88(3):355-65.

Namura S, Zhu J, Fink K, Endres M, Srinivasan A, Tomaselli KJ, Yuan J, Moskowitz MA (1998) Activation and cleavage of caspase-3 in apoptosis induced by experimental cerebral ischemia. *Journal of Neuroscience.* 18(10):3659-68.

Nevander, G., Ingvar, M., Auer, R.N. and Siesjo, B.K. (1985) Status epilepticus in well oxygenated rats causes neuronal necrosis. *Ann. Neurol.*, 18:281-290.

Newmeyer, D., Farschon, D.M. and Reed, J.C. (1994) Cell free apoptosis in *Xenopus* egg extracts: inhibition by Bcl-2 and requirement for an organelle fraction enriched in mitochondria, *Cell* 79:353-364.

Nilsson, P., Ronne-Engstrom, E., Flink, R., Ungerstedt, U., Carlson, H., Hillered, L. (1994) Epileptic seizure activity in the acute phase following cortical impact trauma in rat. *Brain Research*. 637(1-2):227-32.

Nitatori, T., Sato, N., Waguri, S., Karasawa, Y., Araki, H., Shibana, K., Kominami, E. and Uchiyama Y. (1995) Delayed neuronal death in the CA1 pyramidal cell layer of the gerbil hippocampus following transient ischemia is apoptosis, *J Neurosci.*, 15:1001-1011.

Okazaki, M.M., Nadler, J.V. (1995) Protective effects of mossy fiber lesions against kainic acid-induced seizures and neuronal degeneration. *Neuroscience*. 26(3):763-81.

Olney, J.W., de Gubareff, T. and Sloviter, R.S. (1983) Epileptic brain damage in rats induced by sustained electrical stimulation of perforant path: II. Ultrastructural analysis of acute hippocampal pathology. *Brain Res. Bull.*, 10:699-712.

Orth, K., Chinnaiyan, AM., Garg, M., Froelich, CJ., Dixit, VM (1996) The CED-3/ICE-like protease Mch2 is activated during apoptosis and cleaves the death substrate lamin A. *Journal of Biological Chemistry* 271(28):16443-6.

Parent, J.M., Yu, T.W., Leibowitz, R.T., Geschwind, D.H., Sloviter, R.S., Lowenstein, D.H. (1997) Dentate granule cell neurogenesis is increased by seizures and contributes to aberrant network reorganization in the adult rat hippocampus. *J Neurosci* 17(10):3727-38.

Pesold, C., Liu, W.S., Guidotti, A., Costa, E., Caruncho, H.J. (1999) Cortical bitufted, horizontal, and Martinotti cells preferentially express and secrete reelin into perineuronal nets, nonsynaptically modulating gene expression. *Proc Natl Acad Sci USA* 16;96(6): 3217-3222.

Petito, C.K., Feldmann, E., Pulsinelli, W.A. and Plum, F. (1987) Delayed hippocampal change in humans following cardiorespiratory arrest. *Neurology*, 37:1281-1286.

Pini, A. (1993) Chemorepulsion of axons in the developing mammalian central nervous system. *Science* 261(5117):95-8.

Pollard, H., Charriaut-Marlangue, C., Cantagrel, S., Represa, A., Robain, O., Moreau, J. and Ben-Ari, Y. (1994) Kainate-induced apoptotic cell death in hippocampal neurons. *Neurosci.* 63:7-18.

Povlishock, J.T., Becker, D.P., Cheng, C.L., Vaughan, G.W. (1983) Axonal change in minor head injury. *J Neuropathol Exp Neurol* 42(3):225-42.

Povlishock, J.T., Erb, D.B. and Astruc, J. (1992) Axonal response to traumatic brain injury: reactive axonal change, deafferentation and neuroplasticity. *J. Neurotrauma*, 9: S189-S200.

Pulsinelli, W.A., Brierley, J.B. and Plum, F. (1982) Temporal profile of neuronal damage in a model of transient forebrain ischemia, *Ann. Neurol.* 11:491-498.

Qian, Z., Gilbert, M.E., Colicos, M.A., Kandel, E.R., Kuhl, D. (1993) Tissue-plasminogen activator is induced as an immediate-early gene during seizure, kindling and long-term potentiation. *Nature* 361(6411):453-7.

Qiao, X., Noebels, J.L. (1993) Developmental analysis of hippocampal mossy fiber outgrowth in a mutant mouse with inherited spike-wave seizures. *J Neurosci* 13(11):4622-35.

Reichardt, L.F., Bixby, J.L., Hall, D.E., Ignatius, M.J., Neugebauer, K.M., Tomaselli, K.J. (1989) Integrins and cell adhesion molecules: neuronal receptors that regulate axon growth on extracellular matrices and cell surfaces. *Dev Neurosci* 11(4-5):332-47.

Represa, A., Niquet, J., Pollard, H., Khrestchatisky, M., Ben-Ari, Y. (1994) From seizures to neo-synaptogenesis: intrinsic and extrinsic determinants of mossy fiber sprouting in the adult hippocampus. *Hippocampus* Jun;4(3):270-4.

Rudelli, R., Strom, J.O., Welch, P.T., Ambler, M.W. (1982) Posttraumatic premature Alzheimer's disease. Neuropathologic findings and pathogenetic considerations. *Arch. Neurol.* 39(9) 570-5.

Ratan, R.R., Murphy, T.H. and Baraban, J.M. (1994) Macromolecular synthesis inhibitors prevents oxidative stress-induced apoptosis in embryonic cortical neurons by shunting cysteine from protein synthesis to glutathione, *J. Neurosci.*, 14 4385-4392.

Rice, A.C., Floyd, C.L., Lyeth, B.G., Hamm, R.J., DeLorenzo, R.J. (1998) Status epilepticus causes long-term NMDA receptor-dependent behavioral changes and cognitive deficits. *Epilepsia* Nov;39(11):1148-57

Riggott, M.J., Moody, S.A. (1987) Distribution of laminin and fibronectin along peripheral trigeminal axon pathways in the developing chick. *J Comp Neurol* 258(4):580-96.

Robbins, R.J., Brines, M.L., Kim, J.H., Adrian, T., de Lanerolle, N., Welsh, S., Spencer, D.D. (1991) A selective loss of somatostatin in the hippocampus of patients with temporal lobe epilepsy. *Ann Neurol* 29(3):325-32.

Schmidt-Kastner, R., Wetmore, C., Olson, L. (1996) Comparative study of brain-derived neurotrophic factor messenger RNA and protein at the cellular level suggests multiple roles in hippocampus, striatum and cortex. *Neuroscience*, Sep;74(1):161-83.

Scoville, W., Milner, B. (1957) Loss of recent memory after bilateral hippocampal lesions. *Journal of Neurology, Neurosurgery and Psychiatry* 20: 11-21.

Serafini, T., Colamarino, S.A., Leonardo, E.D., Wang, H., Beddington, R., Skarnes, W.C., Tessier-Lavigne, M. (1996) Netrin-1 is required for commissural axon guidance in the developing vertebrate nervous system. *Cell* 87(6):1001-14.

Serafini, T., Kennedy, T.E., Galko, M.J., Mirzayan, C., Jessell, T.M., Tessier-Lavigne, M. (1994) The netrins define a family of axon outgrowth-promoting proteins homologous to *C. elegans* UNC-6. *Cell* Aug 12;78(3):409-24

Shepherd, G.M. (1990a) *The Synaptic Organization of the Brain*. Oxford University Press, pp. 359-364.

Shepherd, G.M. (1990b) *The Synaptic Organization of the Brain*. Oxford University Press, pp. 290.

Shirasaki, R., Tamada, A., Katsumata, R., Murakami, F. (1995) Guidance of cerebellofugal axons in the rat embryo: directed growth toward the floor plate and subsequent elongation along the longitudinal axis. *Neuron* 14(5):961-72.

Skarnes, W.C., Moss, J.E., Hurlley, S.M., Beddington, R.S.P. (1995) Capturing genes encoding membrane and secreted proteins important for mouse development. *PNAS* 92, 6592-6596.

Sloviter, R.S. (1994a) The functional organization of the hippocampal dentate gyrus and its relevance to the pathogenesis of temporal lobe epilepsy. *Ann Neurol* 1994 Jun 35(6):640-54.

Sloviter, R.S. (1994b) On the relationship between neuropathology and pathophysiology in the epileptic hippocampus of humans and experimental animals. *Hippocampus* Jun 4(3):250-3.

Sloviter, R.S., Dean, E. and Neubort, S. (1993a) Electron microscopic analysis of adrenalectomy-induced hippocampal granule cell degeneration in the rat: apoptosis in the adult central nervous system. *J. Comp. Neurol.*, 30: 337-51.

Sloviter, R.S., Sollas, A.L., Dean, E. and Neubort, S. (1993b) Adrenalectomy-induced granule cell degeneration in the rat hippocampal dentate gyrus: characterization of an *in vivo* model of controlled neuronal death. *J. Comp. Neurol.*, 30:324-36.

Smith, CA., Farrah, T., Goodwin, RG (1994) The TNF receptor superfamily of cellular and viral proteins: activation, costimulation, and death. *Cell*. 76(6):959-62.

Smith, D.H., Okiyama, K., Thomas, M.J., Claussen, B. and McIntosh, T.K. (1991) Evaluation of memory dysfunction following experimental brain injury using the Morris Water Maze. *J. Neurotrauma*, 8:259-269.

Squire, L.R. and Zola-Morgan, S. (1991) The medial temporal lobe memory system. *Science* 253 1380-1386.

Squire, L.R. (1992) Memory and the hippocampus: a synthesis from findings with rats, monkeys, and humans, *Psychological Rev.* 99:195-231.

Squire, L.R. and Alvarez, P. (1995) Retrograde amnesia and memory consolidation: a neurobiological perspective, *Current Opinion in Neurobiology*, 5:169-177.

Stanfield, B.B. (1989) Excessive intra- and supragranular mossy fibers in the dentate gyrus of tottering (tg/tg) mice. *Brain Res* 480(1-2):294-9.

Stoeckli, E.T., Sonderegger, P., Pollerberg, G.E., Landmesser, L.T. (1997) Interference with axonin-1 and NrCAM interactions unmasks a floor-plate activity inhibitory for commissural axons. *Neuron* 18(2):209-21.

Stoeckli, E.T., Landmesser, L.T. (1995) Axonin-1, Nr-CAM, and Ng-CAM play different roles in the in vivo guidance of chick commissural neurons. *Neuron* 14(6):1165-79.

Sutton, R.L., Hovda, D.A., Adelson, P.D., Benzel, E.C., Becker, D.P. (1994) Metabolic changes following cortical contusion: relationships to edema and morphological changes. *Acta Neurochirurgica - Supplementum.* 60:446-8

Sutton, R.L., Lescaudron L. and Stein D.G. (1993) Unilateral cortical contusion injury in the rat vascular disruption and temporal development of cortical necrosis, *J. Neurotrauma* 10:135-159.

Sutula, T., He, X.X., Cavazos, J., Scott, G. (1988) Synaptic reorganization in the hippocampus induced by abnormal functional activity. *Science* 239(4844):1147-50.

Suzuki, W.A., Zola-Morgan, S., Squire, L.R. and Amaral, D.G. (1993) Lesions of the perirhinal and parahippocampal cortices in the monkey produce long-lasting memory impairment in the visual and tactual modalities, *J. Neurosci.*, 13:2430-2451.

Swanson, L.W. (1983) The hippocampus and the concept of the limbic system. In: *Neurobiology of the Hippocampus* (Seifert, W., ed.) London: Academic Press, pp. 3-19.

Swimmer, C., Shyjan, A., Leonardo, D., Zhang, Y., Kennedy, T., Serafini, T., Tessier Lavigne., M. (1998) US Patent 5,824,775 Oct 20,1998. "HUAMN NETRIN-1".

Takahashi, A., Alnemri, ES., Lazebnik, YA., Fernandes-Alnemri, T., Litwack, G., Moir, RD., Goldman, RD., Poirier, GG., Kaufmann, SH., Earnshaw, WC (1996) Cleavage of lamin A by Mch2 alpha but not CPP32: multiple interleukin 1 beta-converting enzyme -related proteases with distinct substrate recognition properties are active in apoptosis. *PNAS USA*. 93(16):8395-8400.

Takeichi, M. (1988) The cadherins: cell-cell adhesion molecules controlling animal morphogenesis. *Development* 102(4):639-55.

Tamada, A., Shirasaki, R., Murakami, F. (1995) Floor plate chemoattracts crossed axons and chemorepels uncrossed axons in the vertebrate brain. *Neuron* 14(5):1083-93.

Tauck, D.L., Nadler, J.V. (1985) Evidence of functional mossy fiber sprouting in hippocampal formation of kainic acid-treated rats. *J Neurosci* Apr;5(4):1016-22.

Tartaglia, L.A., Ayres, T.M., Wong, G.H., Goeddel, D.V. (1993) A novel domain within the 55 kd TNF receptor signals cell death. *Cell*. 74(5):845-53.

Thornberry, N.A., Lazebnik, Y (1998) Caspases: enemies within. *Science*. 281(5381): 1312-6.

Tessier-Lavigne, M., Goodman, C.S. (1996) The molecular biology of axon guidance. *Science* 274(5290):1123-33.

Tessier-Lavigne M, Placzek M, Lumsden AG, Dodd J, Jessell TM (1988) Chemotropic guidance of developing axons in the mammalian central nervous system. *Nature* 22-29; 336(6201):775-8

Turski, L., Ikonomidou, C., Turski, W.A., Bortolotto, Z.A., Cavalheiro, E.A. (1989) Review: cholinergic mechanisms and epileptogenesis. The seizures induced by pilocarpine: a novel experimental model of intractable epilepsy. *Synapse* 3(2):154-71.

Uno, H., Lohmiller, L., Thieme, C., Kemnitz, J.W., Engle, M.J., Roecker, E.B., Farrell, P.M. (1990) Brain damage induced by prenatal exposure to dexamethasone in fetal rhesus macaques. I. Hippocampus. *Brain Research. Developmental Brain Research*. 53(2): 157-67.

Volenec, A., Bhogal, R.K., Moorman, J.M., Leslie, R.A., Flanigan, T.P. (1997) Differential expression of DCC mRNA in adult rat forebrain. *Neuroreport* 8(13):2913-7.

Walker, P.R., Weaver, V.M., Lach, B., LeBlanc, J. and Sikorska, M. (1994) Endonuclease activities associated with high molecular weight and internucleosomal DNA fragmentation in apoptosis, *Exp. Cell Res*. 213:100-106.

Warner, M.A., Neill, K.H., Nadler, J.V. and Crain, B.J. (1991) *J. Cerebral Blood flow and Metabol.*, 11 600-610.

Watt, J.A., Pike, C.J., Walencewicz-Wasserman, A.J. and Cotman, C.W. (1994) Ultrastructural analysis of beta-amyloid-induced apoptosis in cultured hippocampal neurons. *Brain Res.*, 661:147-156.

Weis, M., Schlegel, J., Kass, G.E., Holmstrom, T.H., Peters, I., Eriksson, J., Orrenius, S. and Chow, S.C. (1995) Cellular events in Fas/APO-1-mediated apoptosis in JURKAT T lymphocytes, *Exptl. Cell Res.*, 219:699-708.

Winberg, M.L., Mitchell, K.J., Goodman, C.S. (1998) Genetic analysis of the mechanisms controlling target selection: complementary and combinatorial functions of netrins, semaphorins, and IgCAMs. *Cell* 93(4):581-91.

Wood, K.A., Dipasquale, B. and Youle, R.J. (1993) *In situ* labeling of granule cells for apoptosis-associated DNA fragmentation reveals different mechanisms of cell loss in developing cerebellum. *Neuron*, 11:621-32.

Wyllie, A.H., Beattie, G.J. and Hargreaves, A.D. (1981) Chromatin changes in apoptosis, *Histochem.*, 13:681-92.

Wyllie, A.H. (1980) Glucocorticoid-induced thymocyte apoptosis is associated with endogenous endonuclease activation. *Nature*, 284:555-6.

Wyllie, A.H., Morris, R.G., Smith, A.L. and Dunlop, D. (1984) Chromatin cleavage in apoptosis: association with condensed chromatin morphology and dependence on macromolecular synthesis. *J. Pathol.*, 142:67-77.

Yakovlev, A.G., Knobloch, S.M., Fan, L., Fox, G.B., Goodnight, R., Faden, A.I. (1997) Activation of CPP32-like caspases contributes to neuronal apoptosis and neurological dysfunction after traumatic brain injury. *Journal of Neuroscience*. 17(19):7415-24.

Yamamoto, T., Lyeth, B.G., Dixon, C.E., Robinson, S.E., Jenkins, L.W., Young, H.F., Stonnington, H.H., Hayes, R.L. (1988) Changes in regional brain acetylcholine content in rats following unilateral and bilateral brainstem lesions. *J. Neurotrauma* 5(1) 69-79.